PARAMETRIC AND NON-PARAMETRIC ANALYSIS OF CAROTID SINUS BAROREFLEX SYSTEM USING ELECTRICALLY INDUCED MUSCLE CONTRACTION

SHEETAL DESHMUKH

Presented to the Faculty of the Graduate School of

The University of Texas at Arlington in Partial Fulfillment

of the Requirements

for the Degree of

MASTER OF SCIENCE IN BIOMEDICAL ENGINEERING

THE UNIVERSITY OF TEXAS AT ARLINGTON

May 2006

ACKNOWLEDGEMENTS

I am indebted to a number of people who have helped me make this thesis possible. First of all, I sincerely thank my supervising professor, Dr. Khosrow Behbehani for his invaluable guidance and constant motivation.

I would like to thank Dr. Jeffrey Potts (Dalton cardiovascular research center, University of Missouri) for his insight and attention in my work. I would like to thank my supervising committee consisting of Dr. Hanli Liu and Dr. Karel Zuzak for their interest in my thesis work and for taking their time to be on the thesis committee.

Above all, I thank my mother Vasanti Deshmukh and my father Deepak Deshmukh for believing in my abilities, constantly providing the support I needed and being the greatest teachers of my life.

Last but not the least; I also would like to thank Piyush Gehalot for his helpful suggestions during my work tenure at Bioinstrumention Laboratory (BME-UTA).

December 5, 2005

ABSTRACT

PARAMETRIC AND NON-PARAMETRIC ANALYSIS OF CAROTID SINUS BAROREFLEX SYSTEM USING ELECTRICALLY INDUCED MUSCLE CONTRACTION

Publication No. _____

Sheetal Deshmukh, M. S.

The University of Texas at Arlington, 2006

Supervising Professor: Khosrow Behbehani, Ph.D., P.E.

The arterial pressure is an important physiological parameter which if not maintained at desired level may lead to fatal disorders or in worst situations even death. The physiological feedback control mechanism in order to regulate the arterial pressure is performed by the arterial baroreflex. In this study the dynamic characteristics of carotid sinus baroreceptor reflex are identified to obtain the open-loop characteristics of the carotid sinus pressure (CSP, mmHg) to the renal sympathetic nerve activity (RSNA, Arbitrary unit), RSNA to systemic arterial pressure (SAP, mmHg), CSP to SAP and CSP to heart rate (HR, bpm).The purpose of this study was to know if resetting of the baroreflex takes place during exercise. The assumption that the baroreflex afferents

interact with the somatic afferents at the level of the nucleus tractus soliterius (NTS) affects the baroreflex functioning was evaluated by studying the baroreflex transfer functions for two different measurement conditions.

Data for this study was recorded from 6 dogs for two experimental conditions, control and the electrically induced muscle contraction (an experimental model of exercise). The control measurement condition was assumed to be the rest condition and the electrical stimulation mimicked exercise. Non-parametric (NP) estimation technique was applied to the measured data and the baroreflex transfer functions were estimated. The gain and the phase was analyzed in the frequency range of 0.1 to 1Hz. Comparison of CSP-RSNA, RSNA-SAP, CSP- SAP and the CSP –HR transfer functions was made between the electrical stimulation and the control measurement conditions to see if the transfer characteristics differ due to stimulation. It was observed that the DC gain for the two measurement conditions, control and electrical stimulation differed. The slope and the coherence were analyzed in the frequency range of 0.2 to 0.4Hz. Parametric models were estimated employing autoregressive model with exogenous input (ARX) and output error modeling (OE) methods for all four transfer functions, for two measurement conditions to obtain a best possible fit of the model output to the measured output. MSE value from the measured and estimated output was used as the criterion for order selection. Higher order models were estimated along with lower order models. The parametric models were also obtained for the shorter ensembles of the data selected by visual inspection from data of 15 min. Comparison of the

nonparametric estimated transfer function and the parametric estimated transfer function was made.

It is seen that the models obtained from the basic linear model structures doesn't fit well to the measured output. The stationarity of the data and the linearity of the system analyzed is an important issue in parametric modeling.

TABLE OF CONTENTS

LIST OF ILLUSTRATIONS

LIST OF TABLES

LIST OF ABREVIATIONS

CSP…….Carotid Sinus Pressure

SAP…….Systemic Arterial Pressure

RSNA……..Renal Sympathetic Nerve Activity

HR……...Heart Rate

NTS…….Nucleus Tractus Solitarius

MSE…….Mean Square Error

FPE……..Final Prediction Error

GABA…….Gamma-amino Butyric Acid

LTI……..Linear time invariant system

CHAPTER 1

INTRODUCTION

1.1 Baroreflex System

The baroreflex system is a physiological system that regulates the changes in the arterial blood pressure in the body. Cardiovascular system provides adequate blood flow to various parts of the body which might change due to any kind physical activity or exercise. If sufficient supply of blood is not provided to the functioning organs, physiological damage may be caused due to scarcity of blood due to changes in its flow. To avoid any kind of damage, blood pressure control is essential in order to stabilize the blood flow. This control mechanism is provided by the arterial and the carotid sinus baroreceptors, which is termed as the baroreflex. The arterial baroreceptors are located inside the wall of the aorta near the heart, while carotid sinus baroreceptors are at the bifurcation of the carotid arteries which are located in the neck region.

Fundamentally the baroreceptors are the nerve endings, sensitive to the tension depending on the local blood pressure and therefore called as the pressoreceptors. The glossopharyngeal nerve(CN IX) coming from the carotid sinus and the vagus nerve (CN

X) carry the afferent signal (electromechanical) from the carotid sinuses and the aortic baroreceptors respectively to the nucleus tractus solitarius (TS) in the medulla oblongata of the brain stem. At NTS the detected blood pressure is compared to the desired pressure (set point) and the discharge rate of CN IX and CN X to the NTS varies depending on the detected level of systemic arterial pressure (SAP).

The SAP is controlled by varying the three physiological parameters as shown in Figure 1.1, the HR, and stroke volume (SV) and the total peripheral resistance (TPR). An increase in mean value of SAP, elevates the carotid sinus pressure (CSP) and hence there is increase in the firing rates of carotid baroreceptors. This increased baroreceptor activity results in fall in the sympathetic nerve activity (SNA) and rise in the parasympathetic nerve activity (PSNA) which is signaled to the cardiovascular centers in the medulla oblongata. Sympathetic and parasympathetic efferent fibers from these centers innervate the heart and the smooth muscles in the walls of arteries and veins leading to lowering of HR and vasodilation of veins and arteries throughout the body in order to decrease the TPR, driving the blood pressure back to its normal value. This proves that there exists a negative feedback in the baroreflex system. The opposite occurs if the blood pressure decreases below set point, increased sympathetic, decreased parasympathetic activity, which results in increased HR, SV and TPR and return of SAP to its normal value. The cardiovascular baroreflex system is one of the well known examples of negative feedback existing in physiology for short term blood pressure regulation.

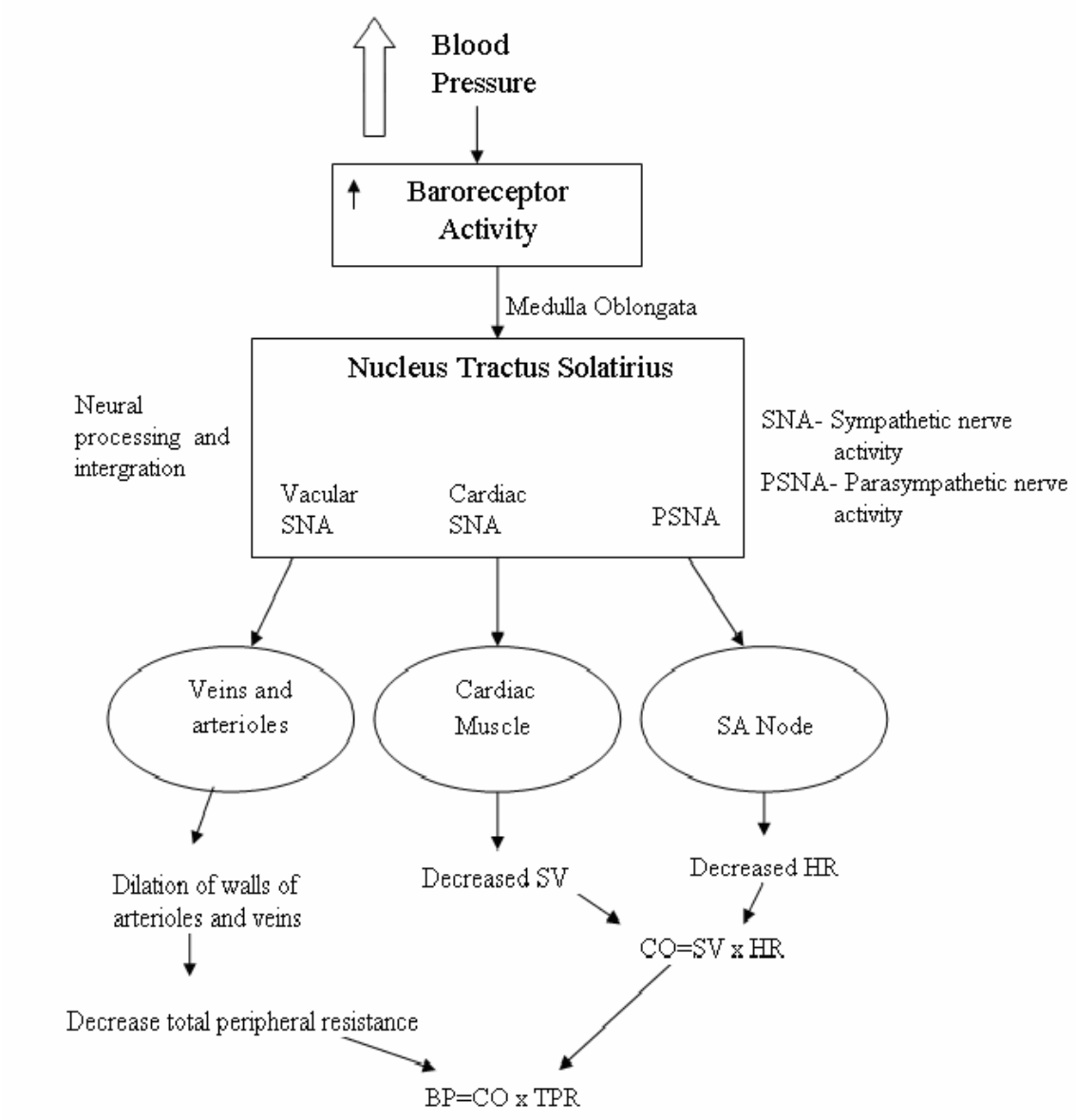

Figure 1.1 Baroreflex mechanism in case of the increased blood pressure

In order to characterize baroreflex system thoroughly it can be divided into two arcs, the neural arc (neuromechanical arc) and the peripheral arc (mechanoneural arc) as shown in Figure 1.2[1]. The neural arc is the afferent path from the baroreceptors afferents to the sympathetic efferents..Peripheral arc is the pathway from the medullary centers to the effector organs through the sympathetic nerves. The signal from the baroreceptor is fast through the neural arc as compared to the peripheral arc and the fast neural arc compensates for the slow peripheral arc.

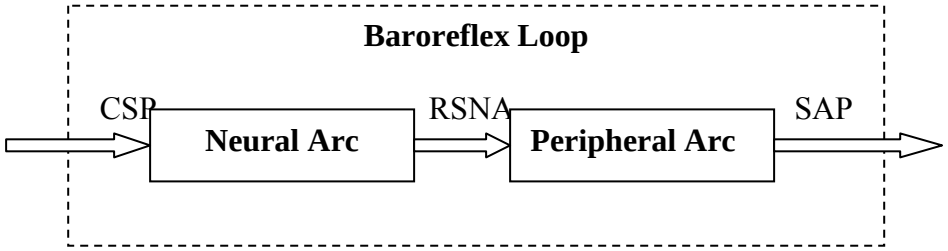

Figure 1.2 Open baroreflex loop

1.2 Role of NTS in inhibition of baroreflex activity during exercise

It has been experimentally shown by Potts *et al* [14] that the operational set-points for the control of the heart rate and blood pressure is reset during physical activity or exercise, maintaining the baroreflex sensitivity same as at rest. The afferent signal from the baroreceptors is carried to the central baroreflex arc located in the medulla oblongata where it is integrated and processed.

The first medullary region in the central arc is the NTS, where the baroreceptor and somatosensory receptor inputs interact. The primary baroreceptor afferent as well as

the spinal dorsal horn neurons (transmitting the somatosensory input) synapse within the NTS to modulate the level of the baroreflex activity. This signal is further passed on to the other central nuclei involved in the baroreceptor transmission. The interaction between excitatory and inhibitory neurons and neurotransmitters takes place in NTS which aids in modulating the sensory signals. Due to the above mentioned reasons researchers [15] anticipate that NTS plays a key role in resetting the set-point. Along with NTS, the caudal ventrolateral medulla (cVLM) and the rostral ventrolateral medulla (rVLM) are also involved in the central interaction.

Figure 1.3, describes the working of the NTS circuit for three different conditions A) at rest the baroreceptor afferents synapse with the NTS neurons from where the signal is carried to the nucleus ambiguus (NA) and the caudal and rostral ventrolateral medulla (cVLM), the outcome of this circuit is to set up the operating point for HR and SNA. The activation of these central circuits due to increased baroreflex activity results in decrease in HR and SNA. This circuit is used to decide the operating point. B) The circuit for no resetting of set-point is shown in this part. Here due to exercise the neural activity to the cVLM and the NA increases due to increase in the baroreflex activity and the HR and RSNA decrease beyond the set-point this is observed from the static baroreflex curve. C) On the other hand Dr Potts [15] has hypothesized in his study that the interaction of somatic afferents and baroreceptor efferents in the NTS leads to resetting of set-point while exercising. While exercising there is activation of an inhibitory circuit in the NTS. Exercise leads to activation of the skeletal muscle afferent fibers due to muscle contraction or stretch [16].The

somatosensory input from the skeletal afferents then limits the excitation of barosensitive neurons via excitation of intrinsic inhibitory GABA mechanism. Due to the resultant inhibitory neurotransmission there is decrease the activity relayed to the NA and cVLM due to which the increased heart rate during exercise does not decrease above the operating point or set-point. This means that additional baroreflex input is needed to decrease heart rate above the set-point which indirectly suggests shift in the set-point towards the right. Also the somatic afferents synapse at the rVLM which leads to increase in the net output nerve activity and hence upward shift in the set-point is anticipated along with the lateral shift.

The above hypothesis is derived from the static study which is used to obtain the sigmoidal relationship between the input-output where the input i.e. CSP is varied in ramp fashion and then HR and RSNA are recorded. Also the operating point lies in the linear region of the sigmoidal curve [9].In this study the dynamic transfer characteristics of CSP-RSNA and CSP-HR was studied and the change in the DC gain obtained from the H_{RSNA} and H_{HR} transfer functions was used as an index for the change in set-point derived from the static study. The DC gain which is the steady state gain could be mapped on the sigmoidal curve, which is also obtained from the steady state analysis.

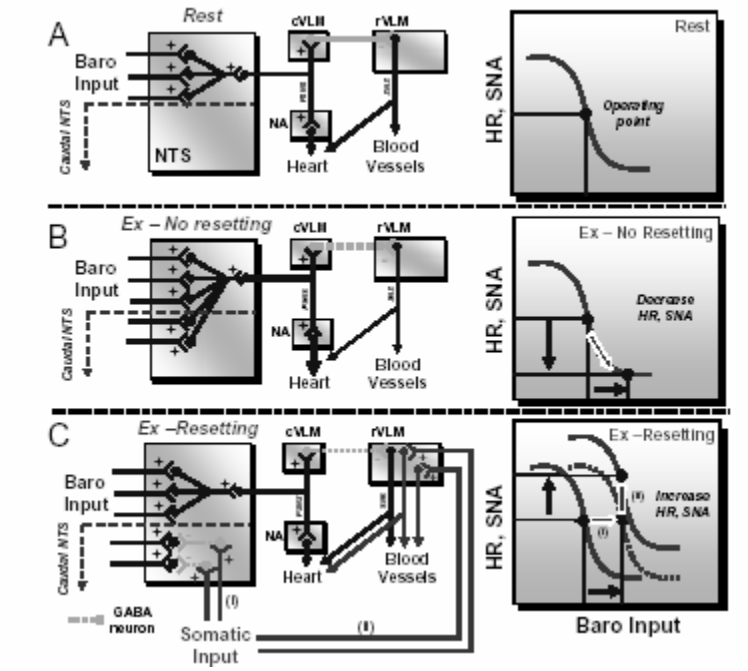

Figure 1.3 Conceptual framework for the central interaction between arterial baroreceptor and somatic afferents in the NTS. (Source: Inhibitory Neurotransmission in the NTS: Implications for the baroreflex resetting during exercise, Jeffrey T. Potts, Ph.D.)

Hence, the anticipated shift in the set-point towards right and upwards would lead to increase in the DC gain. This also explains the need for more input so that the HR or RSNA decreases above the set-point and the DC gain would also decrease in case of CSP-HR and CSP-RSNA transfer functions for exercise condition (electrical stimulation).

Let *H(z)* be the transfer function giving the relation between CSP-HR or CSP-RSNA and *X(z)* and *Y(z)* are the input and output respectively. From Equation 1.9 it can be seen that at low frequency (almost zero), the gain of *H(z)* is b_0 which is nothing but the steady state gain. Hence every point on the sigmoidal curve can be mapped on the

magnitude plot of the *H(z)* at zero frequency (DC gain). Any shift in the sigmoidal curve would lead to change in the DC gain of the transfer function.

$$H(z) = \frac{Y(z)}{X(z)} = \frac{HR / RSNA}{CSP} = \frac{b_0 + b_1 z^{-1} + \cdots b_n z^{-n}}{1 + a_1 z^{-1} + \cdots a_m z^{-m}} \tag{1.9}$$

Figure 1.4 shows pictorially the relationship between the sigmoidal curve and the gain plot. Also the dynamic study is performed under linear system assumption and hence the results may differ due to non-linearities introduced due to the baroreceptors itself.

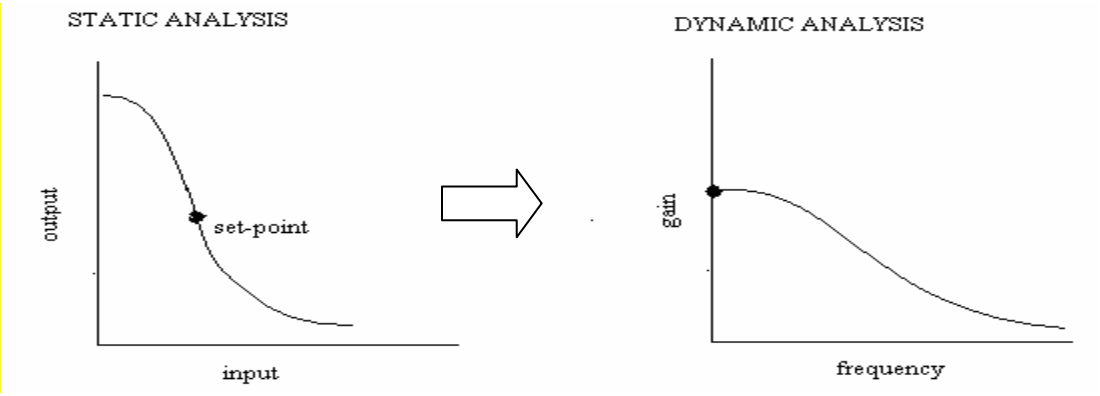

Figure 1.4 Baroreflex curve and gain curve

1.3 Literature overview

The baroreflex control of SNA and the SAP has been characterized in animals by identifying the carotid sinus and arterial baroreceptors. The arterial baroreflex response of cardiac SNA and SAP to variation in CSP was studied in rabbits by Ikeda *et al* [1].These researchers experimentally opened the baroreflex loops and CSP was perturbed over the amplitude range from 25 ± 8 to 117 ± 30 mmHg every 0.5 s by binary white noise process. They dissected the baroreflex loop into the fast neural arc,

CSP as input and SNA as output and slow peripheral arc, SNA as input and SAP as output. By using standard nonparametric LTI analysis the transfer functions of these two arcs were estimated to find that the neural arc behaves as a high pass filter between 0.1 Hz and 1 Hz which contributes to both stability and quickness in regulation of the SAP.

Later Kawada *et al* [3, 7] characterized the CSP and SNA coupling in closed loop rather than opening the baroreflex loops as above researchers. They also utilized the nonparametric estimation along with the white noise perturbation to the aortic depressor nerve in rabbits. It was found that the estimated closed loop transfer function did not significantly differ compared to the open loop transfer function.

All the system identification studies carried out approximated the carotid sinus baroreflex control of SNA and SAP as linear models. Previous experiments showed that the static relationship of SAP to SNA as sigmoidal rather than linear [9].Hence a there exists a dependence on both input amplitude and the operating point (set point). But Sato *et al* [12] limited the range of CSP perturbation to ±10mmHg about the set point to satisfy the linear approximation. The study showed transfer function from CSP to SNA as a high pass filter. The above research was further strengthened by Kawada *el al* [13], they examined that the transfer function of high pass filter of CSP to SNA to show the existence of sigmoidal nature between CSP and SNA. This result also suggested the dominance of nonlinearity in the peripheral arc rather than at the baroreceptors.

The above investigations were carried taking CSNA into consideration to estimate the neural arc transfer function, on the other hand Kawada *et al* [4] considered

the RSNA for this purpose. The CSNA regulates SAP through cardiac output which accounts for only 40-50% of the baroreflex control of blood pressure and the remaining 50% is due to changes in the peripheral resistance offered by the vasoconstriction and vasodilation of arteries and veins. Hence RSNA is taken into consideration instead of CSNA to examine the role of kidney in regulating the SAP. The high pass nature of the neural arc is more pronounced in CSNA than in RSNA. The CSNA response is more sensitive towards the baroreceptor pressure than the RSNA response; this is because systemic pressure regulation is faster via the cardiac output than due to urine excretion. Also it is seen that there is a significant difference between H_{RSNA} and H_{CSNA} but the coherence is sufficiently high for both. Hence both CSNA and RSNA could be used to identify neural arc as along as we are able to recognize the potential difference in their high pass characteristics.

Potts *et al* has experimentally demonstrated that the somatosensory input from the skeletal muscle afferents during exercise or muscle contraction help in resetting the baroreflex set-point while restoring the baroreflex sensitivity of the neurons in NTS [14,15, 16].

1.4 Objectives and Outline of the Thesis

Transfer function analysis of baroreflex system using the parametric model structures like ARX model and OE model are employed in this study. An attempt to extract the dynamic properties from the measured data by estimating the parameters of

the numerator and denominator polynomial of the transfer function was made. Even smaller data length could be utilized for this purpose.

In this study the data is collected from anesthetized dogs for two measurement conditions. The first condition is the control or baseline condition, where the carotid sinus was altered by binary white noise sequence using linear shaker motor and data was measured. The data measured consists of the carotid sinus pressure (CSP, mmHg), SAP (mmHg), RSNA (Arbitrary Unit) and HR (BPM). The second condition is when the L7 and S1 ventral roots were stimulated by electrical pulses and the similar data set was recorded.

The purpose of this study was to determine the effect of electrically induced muscle contraction due to stimulation of sciatic nerve (L7-S1ventral roots) on the carotid sinus baroreflex functioning in controlling the SAP, HR and the RSNA. It has been hypothesized that the baroreflex set-point is reset to a higher pressure value due to the interaction of baroreflex afferents and the somatic afferents in NTS. Following transfer functions were determined from the data by parametric and nonparametric methods:

i) CSP to RSNA [$H(\omega)_{RSNA}$], the transfer function of the neural arc.

ii) CSP to SAP [$H(\omega)_{SAP}$] , the transfer function of the baroreflex loop.

iii) RSNA to SAP [$H(\omega)_{RSNA\text{-}SAP}$] gives the peripheral arc transfer function.

iv) CSP to HR [$H(\omega)_{HR}$] gives the transfer function of carotid sinus to heart rate.

On the whole the objective of the study was to test the hypothesis:

i) $H(\omega)_{RSNA}$ has first order high pass filter characteristics and its DC gain increases after electrical induced muscle contraction .

ii) $H(\omega)_{HR}$ has a first order low pass filter characteristics and its DC gain increases after electrical stimulation.

iii) $H(\omega)_{SAP}$ has a first order low pass characteristics.

iv) $H(\omega)_{RSNA\text{-}SAP}$ has a second order low pass characteristics.

v) To estimate all four transfer functions of the baroreflex loop by ARX and OE method and compare with the non-parametric results.

The rest of the thesis is organized in following manner: Chapter 2 gives the background theory regarding the model structures and modeling techniques applied to the data and the experimental setup and protocol. Chapter 3 gives the results obtained from the parametric and non-parametric estimation of transfer functions. Chapter 4 is about the discussion on the results obtained and the limitations in the study and Chapter 5 concludes the study with scope for the future work.

CHAPTER 2

METHODS

This chapter deals with the theory of white noise method, modeling method, experimental setup and protocol, preparation of the data and the assessment of stationarity of measured data.

2.1 Background theory of white-noise method in system identification

The study of dynamics of any physiological system always initiates with the search for the linear region in the system's operational range. But in reality nonlinearity dominates in the operation of these kinds of systems, without which they would not function well. Hence in order to analyze the stimulus-response(S-R) relation in them, they have to be stimulated in such a way that all the frequencies are activated and this is accomplished by the white-noise stimulus in an efficient manner. The white-noise or the Gaussian white-noise is signal containing all possible frequencies and all amplitudes within the Gaussian distribution of the signal. Now in order to characterize the black box where the S-R relationship is unknown, the aim is to find mathematical

model that responds to the white noise in the same way that the physical system responds to white noise [21].

2.2 Nonparametric (NP) model estimation

Assume a LTI system with input as *x(n), h(n)* as it's impulse response and *y(n)* the output. The output of the system by convolution sum is given by

$$y(n) = h(n) * x(n) = \sum_{k=-\infty}^{\infty} h(k)x(n-k) \tag{2.1}$$

where, *n* is the sample number and *k* represents the time shift.

The input-out relation from cross-correlation is given as follows

$$r_{yx}(l) = h(l) * r_{xx}(l) \tag{2.2}$$

where $r_{yx}(l)$ is the crosscorrelation between the *x(n)* and *y(n)*, $r_{xx}(l)$ is the autocorrelation of the input signal *x(n)* and *l* represents time shift or lag.

By applying properties of convolution to equation (2.2), the relationship between the autocorrelation of input and the autocorrelation output is obtained for *l*=0.

$$r_{yy}(0) = r_{hh}(n) * r_{xx}(n) \tag{2.3}$$

where, $r_{yy}(l)$ is the autocorrelation of the output *y(n)* and $r_{hh}(l)$ is the autocorrelation of the impulse response *h(n)*.

The equation (2.2) can be given in the form of cross power spectrum of *y(n)* as follows:

$$S_{YX}(z) = H(z)S_{XX}(z) \tag{2.4}$$

Here, $S_{yx}(z)$ is the cross power spectrum of the output and the input, H(z) is the transfer function and $S_{xx}(z)$ gives the auto power spectrum of input.

Substituting $z=e^{jw}$, we obtain the above relation in frequency domain, where ω represents the frequency in rad/sec.

$$S_{YX}(\omega) = H(\omega)S_{XX}(\omega) \tag{2.5}$$

$$H(\omega) = \frac{S_{YX}(\omega)}{S_{XX}(\omega)} \tag{2.6}$$

Equation (2.6) implies that the transfer function $H(\omega)$ of a LTI system can be obtained by knowing the cross power spectrum of the output and input (Syx) and the auto power spectrum of the input signal (S_{xx}). Hence, the transfer function can be obtained from the ratio of the cross power spectrum and the auto power spectrum

The gain ($|H(\omega)|$) and the phase ($\theta(\omega)$) of $H(\omega)$ can be computed from its real and imaginary parts respectively.

$$\left|H(\omega)\right| = \sqrt{H_{real}(\omega)^2 + H_{imag}(\omega)^2} \tag{2.7}$$

$$\theta(\omega) = \tan^{-1}\left[\frac{H_{imag}(\omega)}{H_{real}(\omega)}\right] \tag{2.8}$$

The measure of linear dependence between the input and output is given by the coherence function ($Coh(\omega)$)in frequency domain. It is computed using the following equation

$$Coh(\omega) = \frac{\left|S_{YX}(\omega)\right|^2}{S_{XX}(\omega)S_{YY}(\omega)} \tag{2.9}$$

If the system is linear without any measurement noise then $Coh(\omega)$=1,however if the output and the input are contaminated with noise the coherence function is less than

unity. As physiological systems are nonlinear as well contaminated with noise, the coherence function is widely used in this area. Equation (2.9) shows that *Coh(ω)* is always positive value between 0 and 1[20,21]. Figure 2.1 gives the detailed description of the non-parametric analysis carried out in this study. The above discussed nonparametric method is applied in this study so as to identify the dynamic properties of $H(\omega)_{RSNA}$, $H(\omega)_{RSNA\text{-}SAP,}$ $H(\omega)_{SAP}$ and $H(\omega)_{HR}$. In the case of, $H(\omega)_{RSNA}$ CSP was treated as input and RSNA as the output, $H(\omega)_{RSNA\text{-}SAP}$ had RSNA as the input and SAP as the output, while the $H(\omega)_{SAP}$ was identified by CSP as the input and SAP as the output and the $H(\omega)_{HR}$ has CSP as input and HR as the output. The input-output data pairs for all the transfer functions were first low-pass filtered by a Butterworth filter of cutoff frequency 10Hz and then re-sampled at 20Hz. The filter specifications are given later in this chapter. The entire data length of 15 minutes is then segmented into finite number of data sets of 50% overlapping bins/ensembles, each containing 1024 data points. The linear trend was subtracted from each segment and Hanning window was applied to it. Fast Fourier transform was performed on the input and the output to obtain the cross power spectra and the auto power spectra of the input and the output signals of each transfer function. The cross spectra and the auto spectra was then ensemble averaged over 9 ensembles obtained from the 15 minutes of data. Thus, the transfer functions of the carotid sinus baroreflex system were computed from equation (2.6). Following are the transfer functions which are analyzed in this study:

$$H_{RSNA} = \frac{S_{CSP.CSP}(\omega)}{S_{RSNA.CSP}(\omega)} \tag{2.10}$$

$$H_{RSNA-SAP} = \frac{S_{RSNA.RSNA}(\omega)}{S_{SAP.RSNA}(\omega)} \tag{2.11}$$

$$H_{SAP} = \frac{S_{CSP.CSP}(\omega)}{S_{SAP.CSP}(\omega)} \tag{2.12}$$

$$H_{HR} = \frac{S_{CSP.CSP}(\omega)}{S_{HR.CSP}(\omega)} \tag{2.13}$$

where, $S_{CSP\ CSP}$, $S_{SAP\ SAP}$, $S_{RSNA\ RSNA}$,$S_{CSP\ RSNA}$,$S_{RSNA\ SAP}$ and $S_{CSP\ SAP}$ are the auto spectra and the cross spectra of inputs and outputs of transfer functions. The transfer functions estimated by the non-parametric method for control group are defined as H_{NC} for neural arc, H_{PC} for peripheral arc, H_{TC} for total baroreflex arc and H_{HC} for the CSP-HR transfer function. Similarly H_{NS}, H_{PS}, H_{TS} and H_{HS} are the transfer functions for the electrical stimulation group for neural arc, peripheral arc, total arc and the CSP-HR relationship.

2.3 Parametric model estimation

System identification of a linear time invariant (LTI) system is performed by constructing a model in order to describe the properties of the system. The general equation for the model giving relationship between the input, output and the disturbance is given by

$$y(k) = G(q).u(k) + H(q).e(q) \tag{2.14}$$

where, y is the output, u is the input and e is the additive disturbance in the system, k is the instance, q is the shift operator in this case. G is the transfer function which gives relationship between the input and the output and H is the noise model relating the output and the disturbance. In order to identify the properties of the system both G and

H are represented as rational functions and the parameters obtained are the numerator

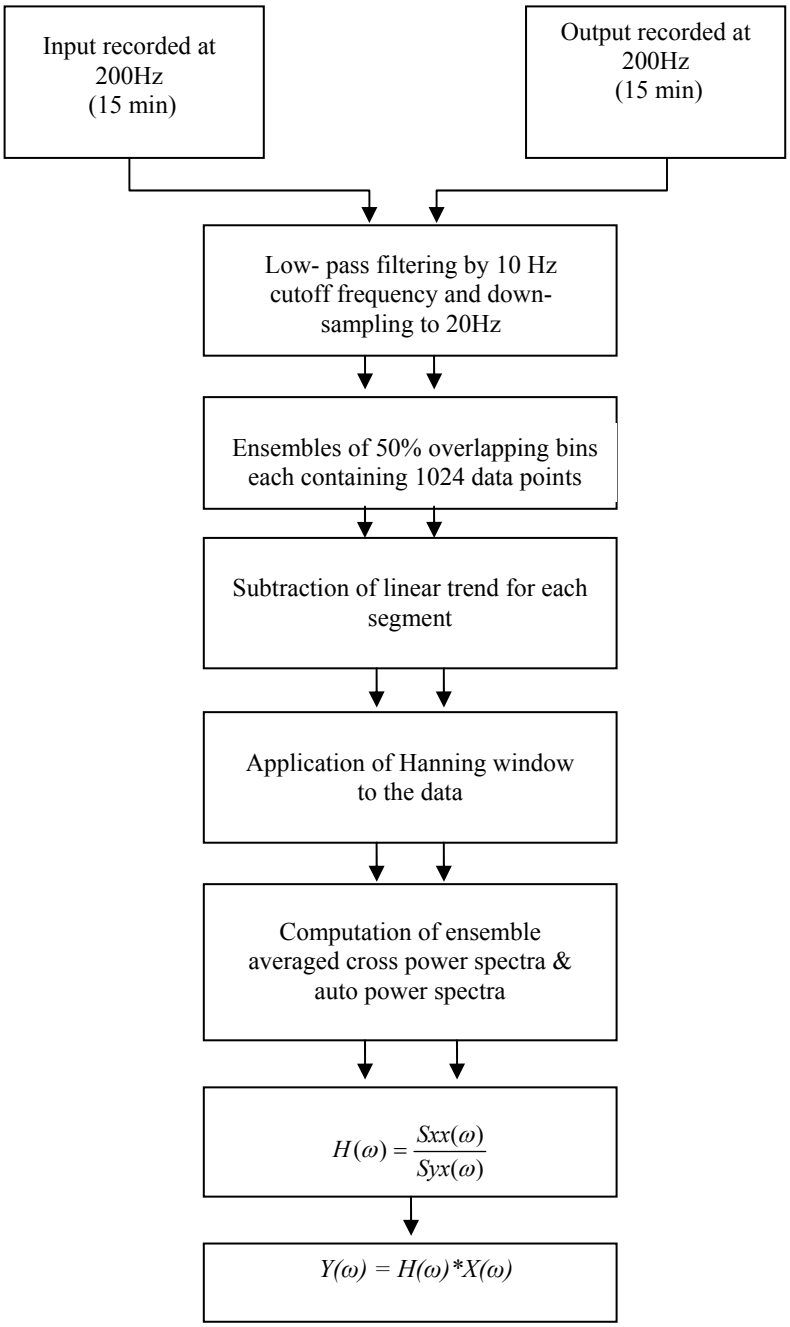

Figure 2.1 Block schematic of the non-parametric method

and denominator coefficients of the function G. Next section gives the description of the two such model structures, the autoregressive model with exogenous input (ARX) and the output error (OE) [17, 18].

2.3.1 Autoregressive model with exogenous input (ARX)

In practice the effect of the disturbance on the output of the model would be insignificant as compared to the input to the model. Hence the ARX model structure can be given by a simple linear equation without the noise model H as below.

$$A(q)y(t) = B(q)u(t) + e(t) \tag{2.15}$$

The Equation (2.14) can also be written in the form of a difference equation.

$$y(t) + a_1 y(t-1) + \cdots + a_{na} y(t-n_a) = b_1 u(t-1) + \cdots + b_{nb} u(t-n_b) \tag{2.16}$$

The above equation relates the current input to the past outputs *y(t-k)* and inputs *u(t-k)* and na, nb and nk gives the number of poles,nb-1 are the number of zeroes and nk is the pure time delay in the system.

Comparing Equation (2.14), Equation (2.15) and Equation (2.16) the transfer function *G (q)* of the system is given by

$$G(q) = \frac{B(q)}{A(q)} = \frac{b_1 q^{-1} + \cdots + b_{nb} q^{-nb}}{1 + a_1 q^{-1} + \cdots + a_{na} q^{-na}} \tag{2.17}$$

The parameters of the estimated model are then the coefficients of the numerator *(b_1, b_2...b_{nb})* and the denominator *(a_1, a_2...a_{na})* polynomial of *G(q)*. The model order *(na, nb)* is obtained such that there is a good fit between the measured and the estimated model output [17].

2.3.2 Output error model

The another model structure is one in which the output is assumed to be the combination of the undisturbed output *w(t)* and white noise *e(t)*.The difference equation is as given below

$$w(t) + f_1 w(t-1) + \cdots + f_{nf} w(t-n_f) = b_1 u(t-1) + \cdots + b_{nb} u(t-n_b) \tag{2.18}$$

$$y(t) = w(t) + e(t) \tag{2.19}$$

$$y(t) = \frac{B(q)}{F(q)} u(t) + e(t) \tag{2.20}$$

Comparing Equation (2.14) and Equation (2.20) in OE model structure H(q)=1 and G(q) is given as

$$G(q) = \frac{B(q)}{F(q)} = \frac{b_1 q^{-1} + \cdots + b_{nb} q^{-nb}}{1 + f_1 q^{-1} + \cdots + f_{nf} q^{-nf}} \tag{2.21}$$

The parameters which need to be estimated for output error model are $b_1, b_2 \ldots b_{nb}$ and $f_1, f_2 \ldots f_{nf}$ where nb represents the the number of zeroes plus one which is the order of the numerator polynomial and nf represents the number poles of the estimated transfer function.

The model order and the model structure is selected using the Akaike's index or the final prediction error (FPE) and or the mean square error (MSE).In this study MSE was used to in selection of the model order [17].MSE value is computed as follows

$$MSE = \sum_{i=0}^{L} \frac{(y_m(i) - y_e(i))^2}{L} \tag{2.22}$$

where, y_m is the measured output and y_e is the estimated output, L is the data length subjected to modeling.

In this study let Mn, Mp, Mt and Mh be four models of the H_{RSNA}, $H_{RSNA\text{-}SAP}$, H_{SAP} and H_{HR} transfer functions respectively, where i) Mn has measured CSP as input and measured RSNA as output ii) Mp has measured RSNA as input and measured SAP as output iii) Mt has measured CSP as input and measured SAP as output iv) Mh has measured CSP as input and measured HR as output. Depending on the order of the models there are two schemes which are employed in this study to estimate the transfer functions.

2.3.3 M-1 modeling scheme

In this scheme of modeling the ARX and OE models are estimated by varying their respective orders from 1 to 20.The best model is selected on the basis of lowest MSE calculated from the measured and estimated output for the ARX as well as the OE model. Figure 2. shows the block schematic for the M-1 modeling scheme. Measured input and measured output is used for the ARX and OE estimation. The order of the models is selected for lowest MSE by varying orders of ARX and OE models from 1 to 20.This scheme was applied on the entire data length of 15 min of control and stimulation and on short ensemble of data of control and stimulation. In this study the M-1 scheme is applied to the CSP, SAP, RSNA and HR data to Mn Mp, Mt and Mh.

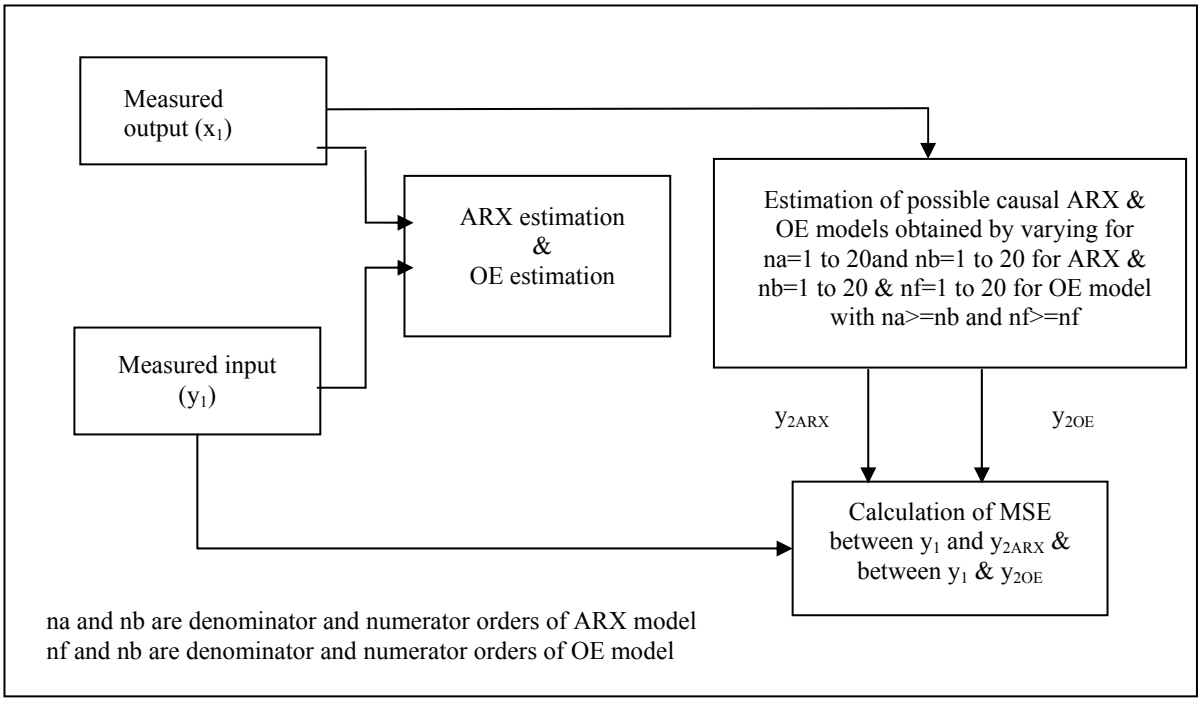

Figure 2.2 Block schematic for M-1 scheme for estimation of ARX and OE models

2.3.4 M-2 modeling scheme

In this scheme of modeling the ARX and OE models are estimated by varying their respective orders from 1 to 3.The order was varied from 1 to 3 The best model is selected on the basis of lowest MSE calculated from the measured and estimated output for the ARX as well as the OE model. Figure 2.3 shows the block schematic for the M-2 modeling scheme. Measured input and measured output is used for the ARX and OE estimation. The order of the models is selected for lowest MSE by varying orders of ARX and OE models from 1 to 3. From earlier studies [2,3,4,5,7,8] it has been seen that the transfer functions H_{RSNA} is a first order high-pass filter, $H_{RSNA-SAP}$ is a second order low-pass filter, H_{SAP} is a first order low-pass filter and H_{HR} is a first order low-pass filter

[22].Hence in this section the order of the Mn,Mp,Mt and Mh models is varied from 1 to 3 so as to see if the linear models could predict actual output by using few parameters compared to high orders. This scheme was applied on the entire data length of 15 min of control and stimulation and on short ensemble of data of control and stimulation. In this study the M-2 scheme is applied to the CSP, SAP, RSNA and HR data to Mn, Mp, Mt and Mh.

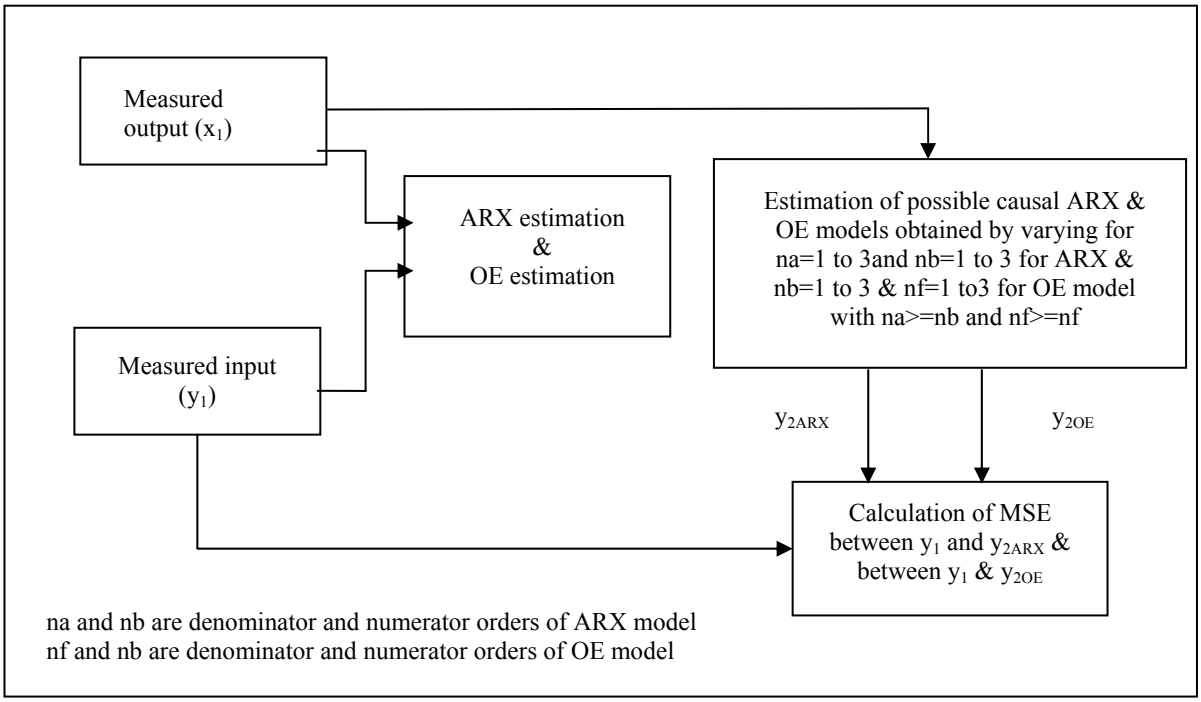

Figure 2.3 Block schematic for M-2 scheme for estimation of ARX and OE models

2.4 Experimental setup and protocol

The data for this study was recorded from 6 dogs for two experimental conditions, the control and the electrically induced muscle contraction. This section

presents the surgical preparation, experimental setup and experimental protocol for this study. All the data is recorded in the linear region of the baroreflex curve [9] in order to satisfy the approximation of linear operation of the carotid sinus baroreflex system.

2.4.1 Surgical preparation

Surgery was performed on six pentobarbital sodium anesthetized dogs. Supplemental dose was given every 60 minutes. The animals were ventilated by 100% of oxygen and ventilation was determined from arterial blood gas measurements (Model ABL5, radiometer, Copenhagen) which were taken every 30 minutes. Arterial PO_2 and PCO_2 were kept in normal limits.

In order to open the closed baroreflex loop the left and right carotid sinuses were vascularly isolated from the remainder of the circulation and were perfused with varied levels of static pressure. The internal and external carotid arteries and any small branches originating from the carotid bifurcation were completely ligated. The blood flow to the carotid chemoreceptor body was ceased by ligating the occipital arteries at the origin. Additional surgery was performed on dogs so as to test them under the condition of electrically induced muscle contraction. Laminectomy was performed to expose the spinal cord at the level of the lower lumber-upper sacral region. The dorsal and ventral spinal rootlets at the L7and S1 levels were carefully exposed by removing the necessary vertebrae. The ventral roots were carefully dissected from the dorsal roots, sectioned, and placed on the bipolar platinum stimulating electrodes. The skin covering the ipsilateral lower limb was removed and the calcaneal bone was sectioned and the Achilles tendon was connected to the force transducer (model F10, Grass

Instruments) to measure the amount of tension generated during electrical induced contraction and mechanical stretch of the gastrocnemius.

2.4.2 Experimental setup

The carotid sinus was connected to the linear shaker motor (Ling Dynamics Inc.) and a servo controlled pump system (Harvard Apparatus Company, Inc., MA), the input to the motor was a computer generated binary white-noise signal which was amplified using a linear power amplifier (PA-119). In this manner the carotid sinus was perturbed by white-noise, which altered the CSP according to the pressure variation of white noise. The input to the shaker motor was varied by the computer program during the experiment so as to produce ±10mmHg change in the CSP about the DC pressure level which is controlled by the linear power amplifier. The CSP was measured using a fluid-filled Statham transducer which was calibrated such that 1 volt equaled 100mmHg. This signal was then amplified by means of a transducer signal conditioner (Model: 13-16615-50, Gould Instrument systems, Inc., Ohio). SAP was recorded using a high fidelity solid-state pressure transducer (Model: TCB – 600 Millar Instruments Inc., Houston, Texas). The solid state pressure transducer was interfaced with the acquisition system via a transducer control unit which was calibrated such that 1volt equaled 100mmHg of output pressure. The HR was obtained using a Gould biotach amplifier. The input to this device is the R wave of the electrocardiogram and HR was computed calculating the beats per min. Sympathetic nerve activity was measured through Teflon coated silver wires wound around the nerves and separated by approximately 1cm.RSNA measured was very low voltage signal which was then

amplified 20,000 to 200,000 times and band-pass filtered (100 – 3000 Hz) using an AC amplifier. The amplified and band-pass filtered RSNA signal was then rectified and integrated using an analog circuitry.

2.4.3 Experimental protocol

For the control condition the CSP, SAP, RSNA and HR were measured 30min after the surgery to ensure that the body conditions have reached the baseline. No electrical stimulation of any kind was given during the experimentation for control condition. In the case of electrically induced contraction the measurements were taken after a 60 minute stabilization period. The contraction-sensitive muscle afferent fibers were activated by electrically stimulating the L7 and S1 ventral roots (3X motor threshold, a stimulus frequency of 30 Hz, and pulse duration of 0.1ms) to contract the gastrocnemius. The measurement were carried under two conditions i) control condition where there was no electrical stimulation given to the L7 and S1 ventral roots and ii) electrical stimulation condition where the L7 and S1 ventral roots were stimulated as described above. Hence there are two sets of CSP, SAP, HR and RSNA signals recorded. The transfer functions H_{RSNA}, $H_{RSNA\text{-}SAP}$, H_{SAP} and H_{HR} for control condition are represented as H_{NC}, H_{PC}, H_{TC} and H_{HC} and that for electrical stimulation are represented as H_{NS}, H_{PS}, H_{TS} and H_{HS} respectively.

The experimental setup for both the experimental conditions is same as mentioned above. The DC pressure level was maintained at the mid-point of the linear portion of the baroreflex curve (set-point) and CSP was varied ±10mmHg around it every 0.5 s for 15-20 minutes and CSP (mmHg), SAP (mmHg), HR (bpm) and RSNA

(Arbitrary unit) were recorded using Labview 5.1 at 200Hz.

2.5 Data Preparation

Previous studies have shown that the response of SAP through the baroreflex system was evident most at frequencies <1Hz [2]. This indicates that the CSP, SAP, RSNA and HR have useful frequencies up to 1Hz and the high frequencies could be eliminated. In this study the time series of the CSP, SAP, RSNA and HR signals are low-pass filtered by a fourth-order Butterworth filter with a corner frequency of 10Hz eliminating the unwanted higher frequencies. The signals were then down-sampled to 20Hz from 200Hz and the Butterworth filter also acts as the anti-aliasing filter. Following are the specifications of the filter:

Table 2.1 Specification of the Butterworth filter used to filter the CSP, SAP, RSNA and the HR signals

Pass band corner frequency in (W_p)	10 Hz
Stop band corner frequency in (W_s)	40 Hz
Pass band ripple in (R_p)	3 dB
Stop band attenuation in (R_s)	50 dB
Order (N)	4

W_n and N of the filter was found by describing the analog prototype of the filter. Wn and N were then used to generate the numerator and denominator polynomials of the filter which were used to filter the signals. The Butterworth filter introduces a finite delay in the filtered signal. This delay in the signal was eliminated by filtering the

reverse signal and was reverted back to obtain the filtered signal without any delay.

For non-parametric estimation of H_{RSNA}, H_{SAP}, H_{HR} and $H_{CSP\text{-}RSNA}$, the CSP, SAP, RSNA and the HR signals were first filtered and re-sampled. The entire 15 minutes input-output data was segmented into finite number of data sets of 50% overlapping bins each containing 1024 data points. Hanning window was applied to each segment after subtracting linear trends from them. Fourier analysis was then carried out on the data to obtain the transfer functions, which is explained in section 2.2.1 in detail.

In order to obtain the parametric models the data should be free from the linear trends and spurious signal present in them to obtain the better fit from estimated output. In this study in order to estimate the parametric models of $H_{RSNA,}$ $H_{RSNA\text{-}SAP}$, H_{SAP} and H_{HR} the input and output signals to the respective models are first low-pass filtered by using a Butterworth filter whose specifications are given in Table 2.1 and then they are freed from the linear trends present in them.

2.6 Stationarity Assessment

Any signal related to a physical process is called stationary if and only if its essential statistical properties (mean, variance and autocorrelation) are independent of time. If the properties change over time then the signal is non-stationary. In any stochastic or random process $\{X_t\}$, if the joint probability distribution of $\{X_{t1}, X_{t2}, \ldots, X_{tn}\}$ and of $\{X_{t1+k}, X_{t2+k}, \ldots, X_{tn+k}\}$ is same then the it is said to be strongly stationary, where t_1 to t_n are the time instants and k is the shift with *t, k* are integers. In

practice the useful form of stationarity is the weak or wide-sense stationarity in which the mean and the autocorrelation does not change with time [19, 21].

2.6.1 Run Test

Run test is a statistical test to check whether the data is stationary. No assumption regarding the probability distribution of the data is made prior to testing. In this test the data $\{x_1,x_{2,\ldots},x_N\}$ is divided into k groups containing M successive samples , such that $N=kM$. A statistic m_i , like the mean or the variance is computed for each one of the k groups using its M samples. In this way the sequence of statistics $\{m_1,m_2,\ldots,m_k\}$ is obtained. The median m_n, of the sequence of statistics is calculated along with the differences

$$d_i=m_i - m_n, \qquad i=1,2,\ldots,k \tag{2.23}$$

where, d_i is the sequence of the difference of the statistics and the median and k is an integer. A sequence of signs of these differences is formed and the number of sign changes occurring in the sequence of signs is counted. This number plus one gives the number of runs in the sequence. This is then compared to the bounds of confidence interval which supports the hypothesis that the time series data is stationarity [19].

CHAPTER 3

RESULTS

3.1 Results of non-parametric analysis for control and electrical stimulation

The transfer characteristics of $H_{RSNA,}$ $H_{RSNA-SAP,}$ H_{SAP} and H_{HR} were analyzed by using the non-parametric method, which is explained in section 2.2 The carotid sinus baroreflex system is identified for two measurement conditions, the control condition (rest) and the electrical stimulation (exercise) condition, Following analysis is carried out to determine if there is any change in the operation of the baroreflex functioning before and after electrically induced muscle contraction i.e. before and after exercise, which is achieved by comparing the magnitude, phase, coherence, slope and DC gain of H_{NC}, H_{PC}, H_{TC} and H_{HC} with H_{NS}, H_{PS}, H_{TS} and H_{HS} respectively (these transfer functions are defined in section 2.2) for all the 6 dogs. The frequency response plots for only one dog is shown due to limitation of space, which are similar to the results from all the other 5 dogs. The plots for remaining 5 dogs out of 6 are shown in appendix A.

3.1.1 Comparison of the magnitude, phase, coherence and DC gain values for control and electrical stimulation

In this section the magnitude and phase responses are plotted for transfer functions of $H_{RSNA,}$$H_{RSNA-SAP,}$$H_{SAP}$ and H_{HR} from 0.01 Hz to 1Hz along with the coherence in the same frequency range. These transfer functions are obtained from dog

5 for the control and the electrical stimulation. The ratio of gains H_{NS} to H_{NC}, H_{PS} to H_{PC}, and H_{TS} to H_{TC} was computed from dog 5 over the frequency range of 0.01Hz to 1Hz. and plotted .Similarly, the difference of the gains H_{NS}-H_{NC}, H_{PS}-H_{PC}, and H_{TS}-H_{TC} H_{NS}-H_{NC}, H_{PS}- H_{PC}, and H_{TS}- H_{TC} is computed and plotted over frequency range of 0.01Hz to 1Hz along with the ratio plot. The ratio and the gain plots shows the relative difference in the gain of control and electrical stimulation over the desired frequency range. Figure **3.** through Figure 3.4 gives the plots for the magnitude, phase, coherence, gain ratio and gain difference for all the four transfer functions.

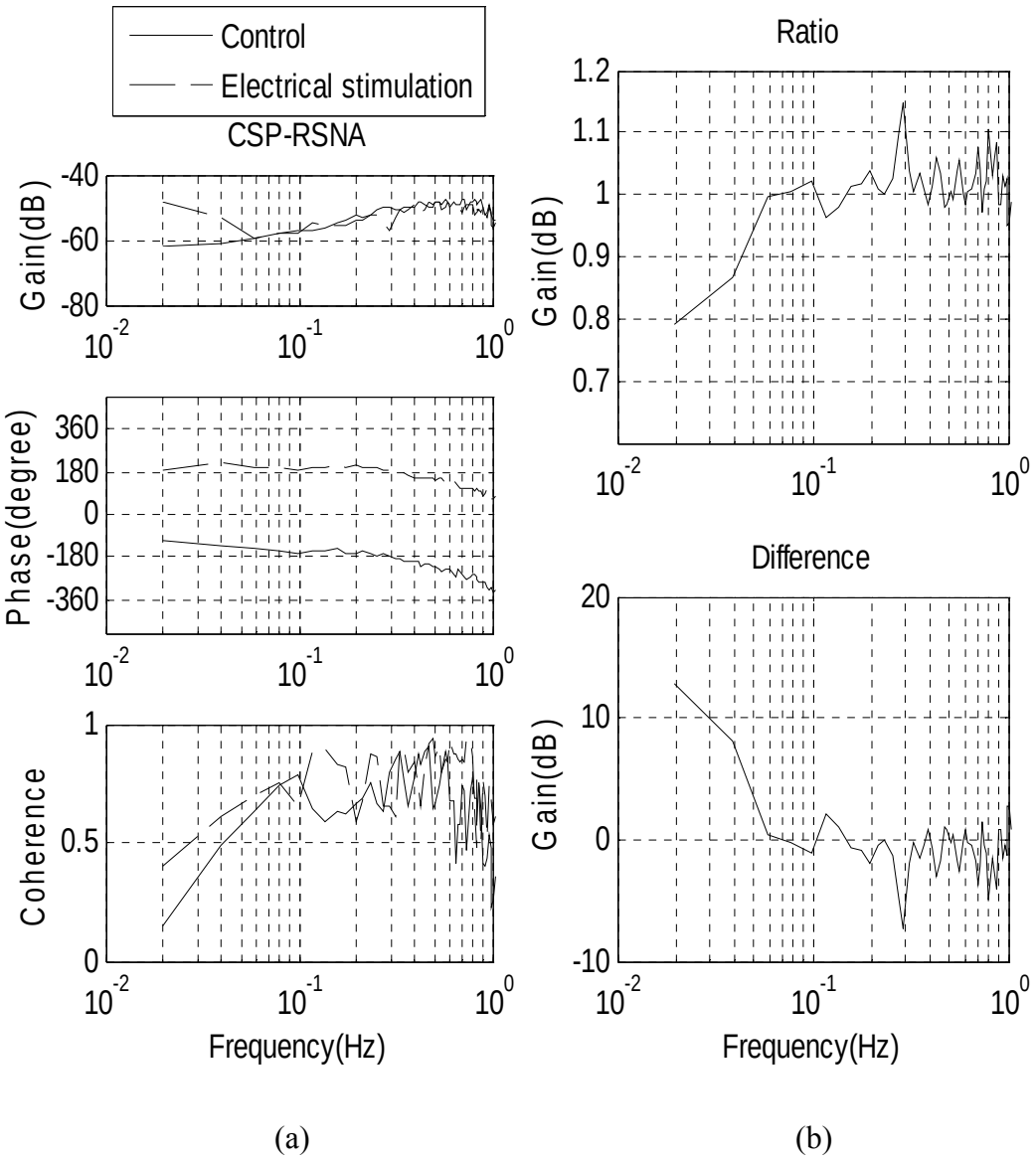

(a) (b)

Figure 3.1 a) Magnitude, phase and coherence plots of H_{NC} and H_{NS} from dog 5, (b) Plots of ratio and difference of gains H_{NC} and H_{NS} from dog 5

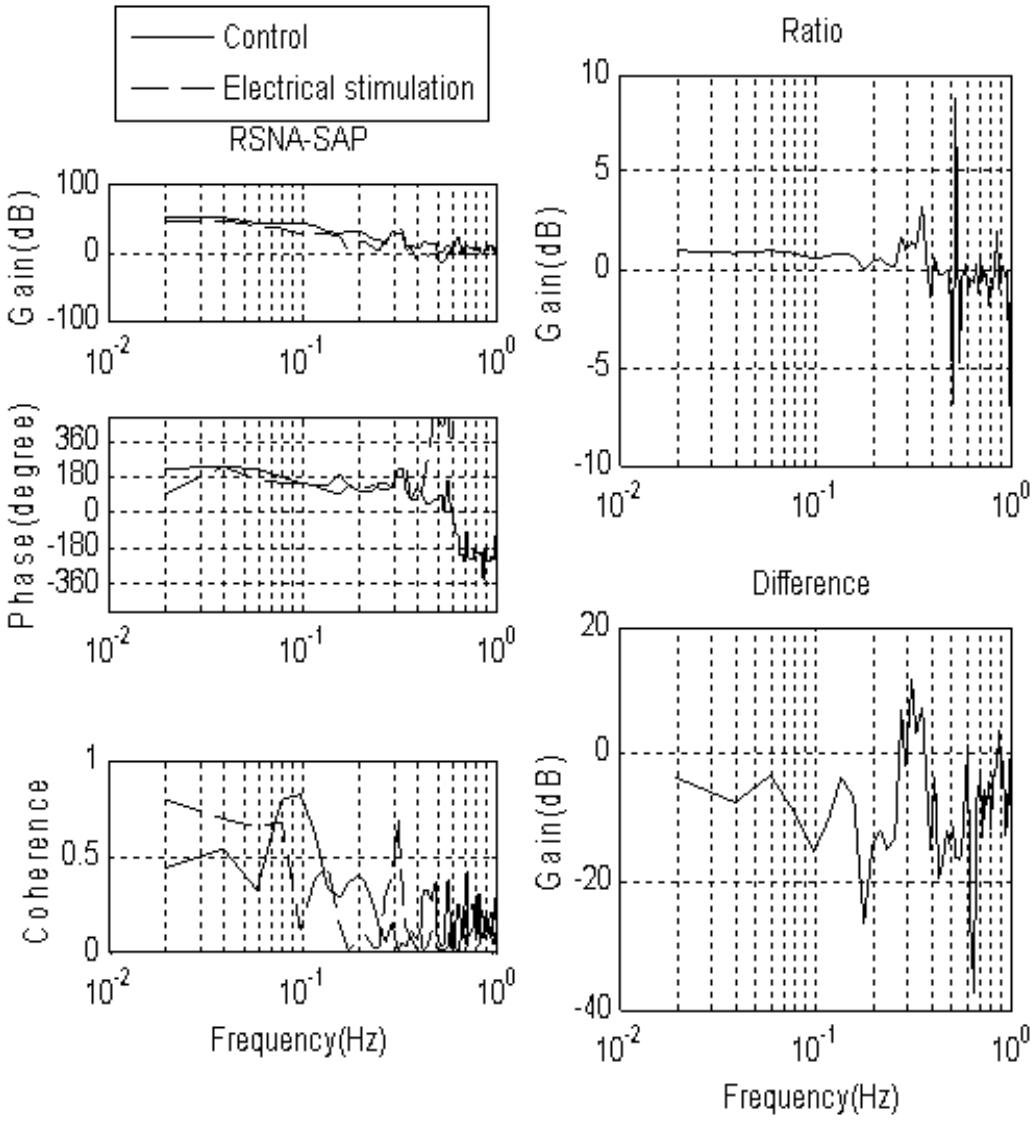

(a) (b)

Figure 3.2 (a) Magnitude, phase and coherence plots of H_{PC} and H_{PS} from dog 5; (b) Plots of ratio and difference of gains H_{PC} and H_{PS} from dog 5

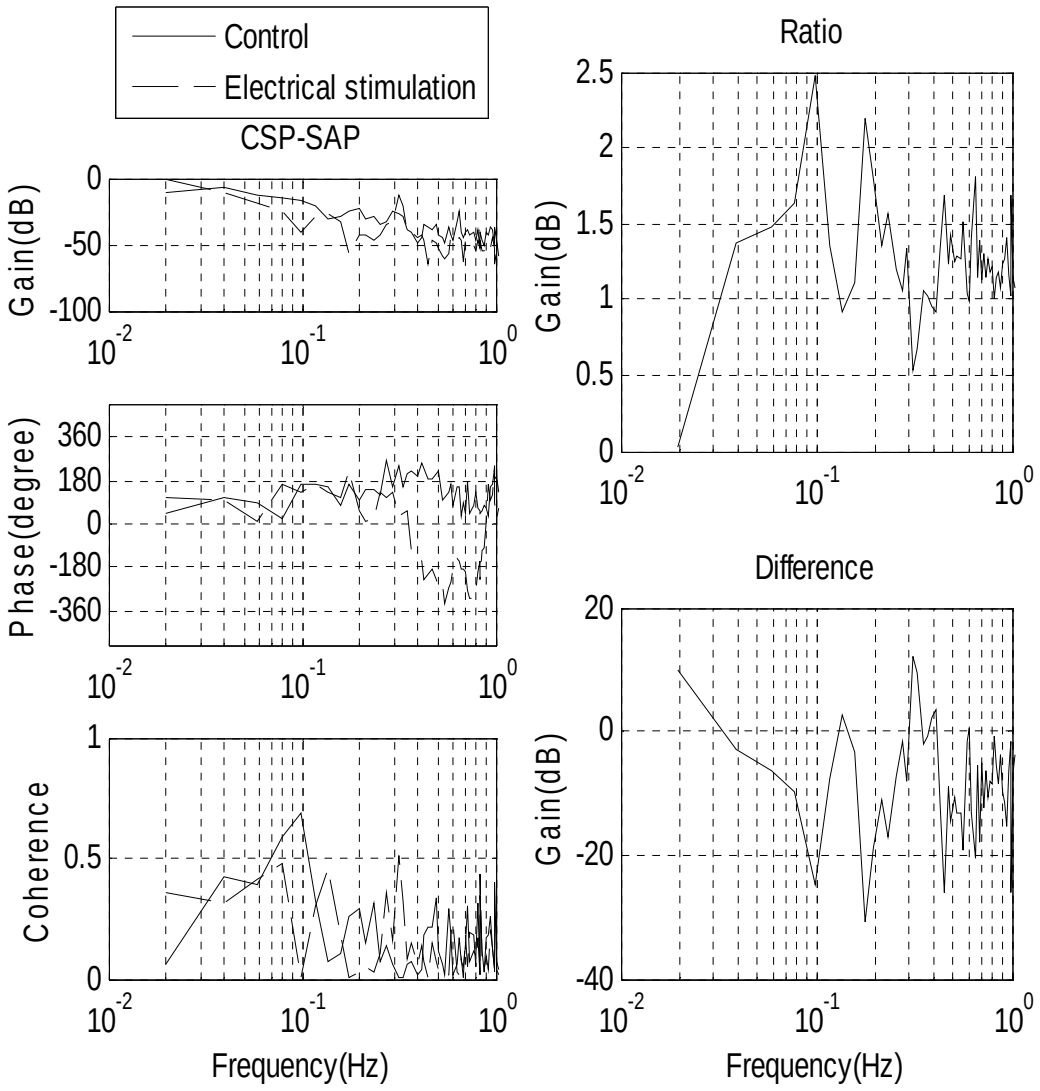

(a) (b)

Figure 3.3 a) Magnitude, phase and coherence plots of H_{TC} and H_{TS} from dog 5; (b) Plots of ratio and difference of gains H_{NC} and H_{NS} from dog 5

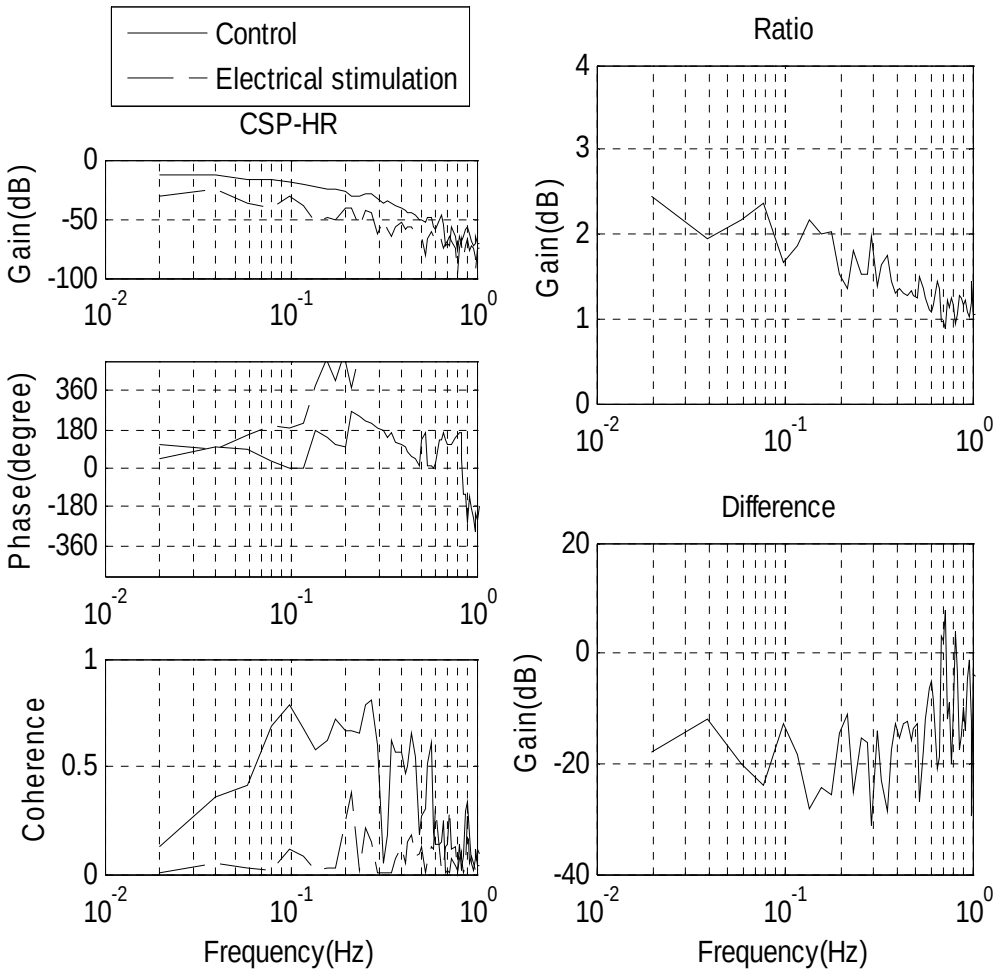

(a) (b)

Figure 3.4 a) Magnitude, phase and coherence plots of H_{HC} and H_{HS} from dog 5, (b) Plots of ratio and difference of gains H_{HC} and H_{HS} from dog 5

Figure 3.5 through Figure 3.6 give the magnitude, phase, coherence, ratio and difference plots obtained from the averaged transfer functions from group average of 6 dogs. All these plots are plotted from a frequency range of 0.01 to 1 Hz

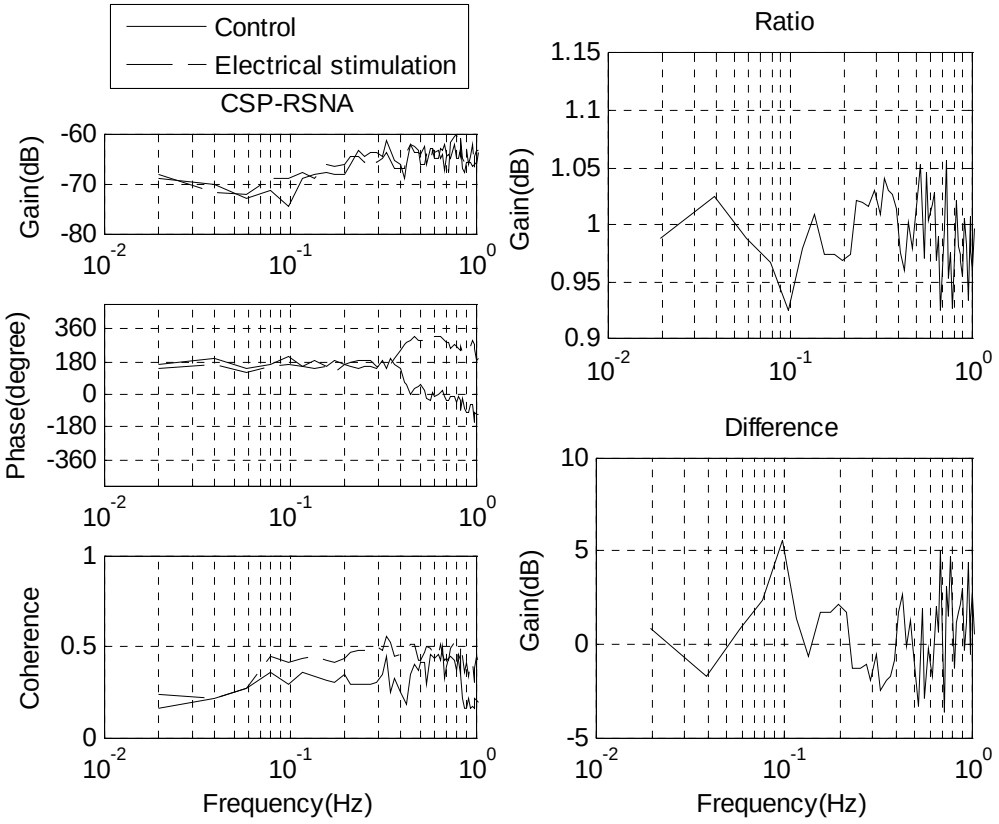

(a) (b)

Figure 3.5 (a) Magnitude, phase and coherence plots of averaged H_{NC} and averaged H_{NS} from 6 dogs; (b) Plots of ratio and difference of averaged gains of H_{NC} and H_{NS} from 6 dogs

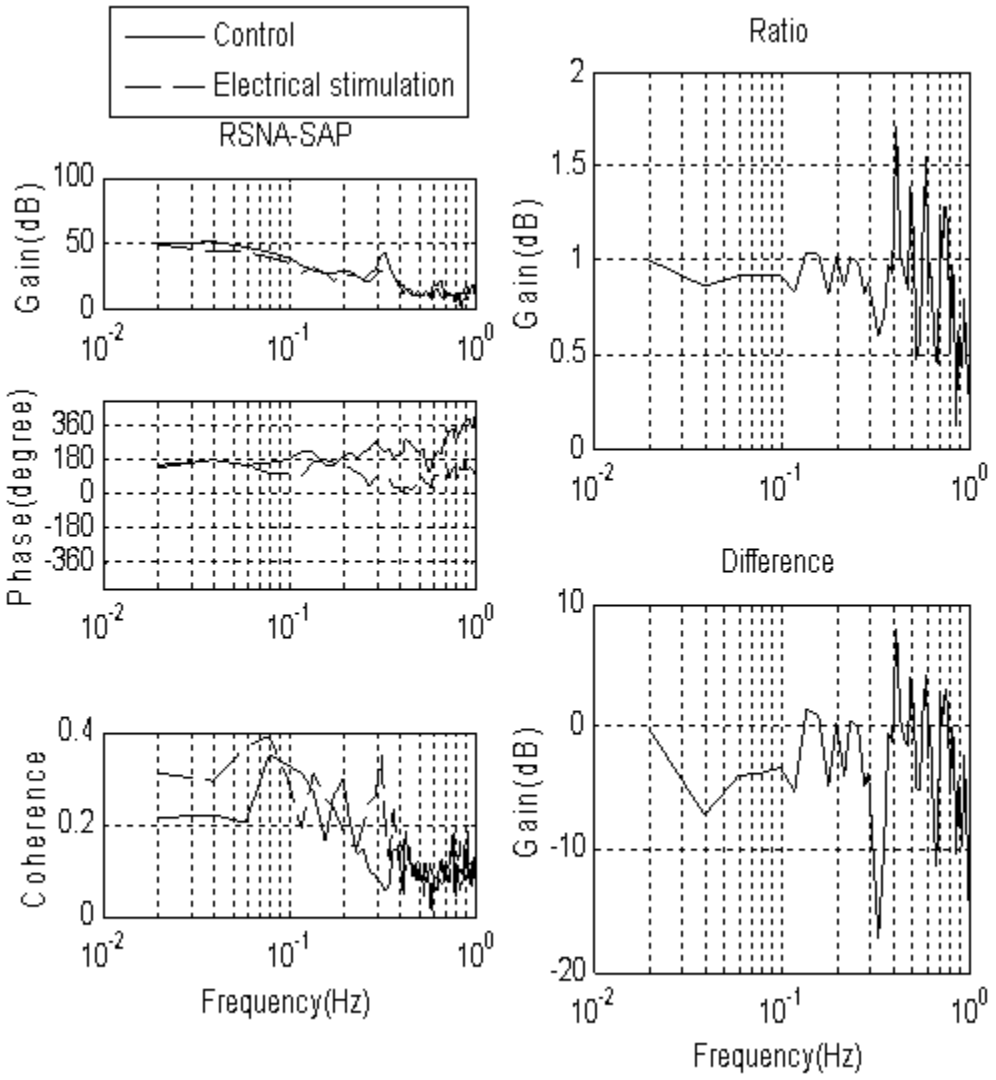

(a) (b)

Figure 3.6 (a) Magnitude, phase and coherence plots of averaged H_{PC} and averaged H_{PS} from 6 dogs; (b) Plots of ratio and difference of averaged gains of H_{PC} and H_{PS} from 6 dogs

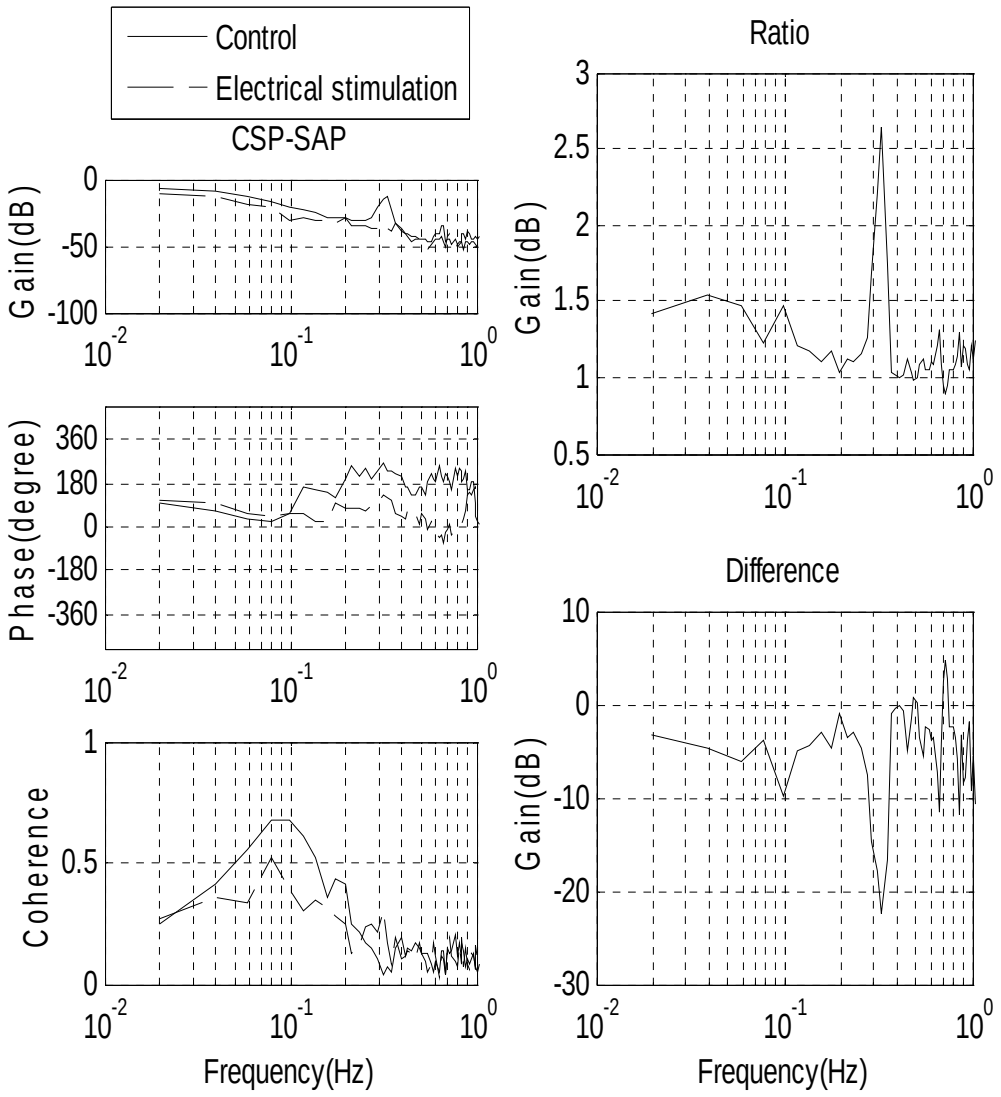

(a) (b)

Figure 3.7 (a) Magnitude, phase and coherence plots of averaged H_{TC} and averaged H_{TS} from 6 dogs; (b) Plots of ratio and difference of averaged gains of H_{TC} and H_{TS} from 6 dogs

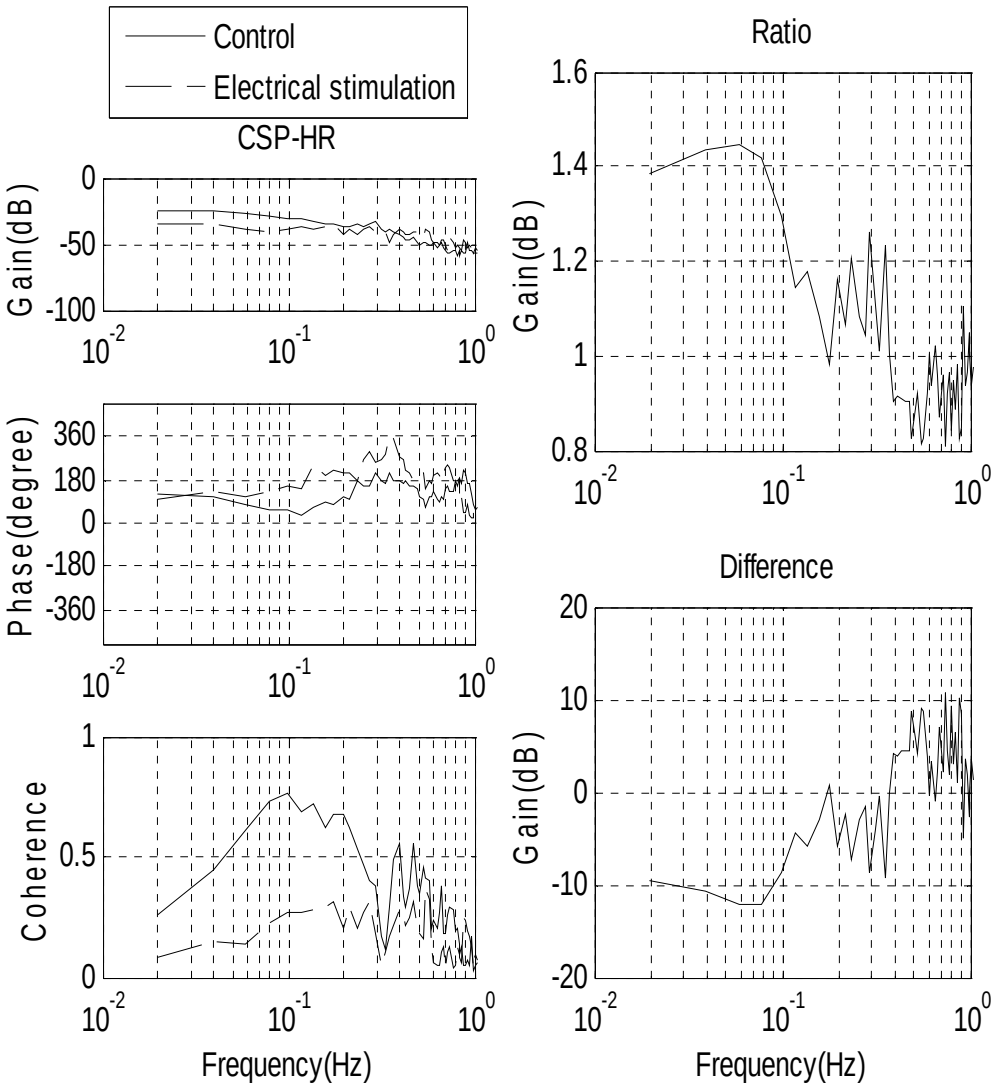

(a) (b)

Figure 3.8 (a) Magnitude, phase and coherence plots of averaged H_{HC} and averaged H_{HS} from 6 dogs; (b) Plots of ratio and difference of averaged gains of H_{HC} and H_{HS} from 4 dogs

3.1.2 Slope, Coherence and DC gain values for control and electrical stimulation

The mean slope and the mean coherence of H_{NC}, H_{PC}, H_{TC}, H_{HC} H_{NS}, H_{PS}, H_{TS} and H_{HS} are computed for a group average of 6 dogs between the frequency range of 0.2Hz to 0.4Hz which are given in Table 3.1**.** The range of 0.2Hz to 0.4Hz was selected because the magnitude of the H_{RSNA} , $H_{RSNA-SAP}$,H_{SAP}, and H_{HR} are flat below 0.1Hz [2]. This can also observed from the magnitude plots in section 3.1.1. The comparison of slope and coherence is done for all the transfer functions between the control and electrical stimulation with the help of t-test, the p-values are given in Table 3..2 and Table 3.3. The t-test is conducted to see if there is any change in the slope and coherence for all the baroreflex transfer function for the control and electrical stimulation conditions.

Table 3.1 Mean values of slope, mean values of coherence for the averaged transfer functions from 6 dogs between 0.2Hz to 0.4Hz for control and electrical stimulation

	Control		Electrical stimulation	
	Slope (dB/octave)	Coherence	Slope (dB/octave)	Coherence
H_{RSNA}	3.91±3.47	0.50±0.24	5.27±3.83	0.30±0.27
$H_{RSNA-SAP}$	-11.32±5.16	0.47±0.14	-9.50±4.39	0.25±0.20
H_{SAP}	-10.12±2.81	0.53±0.24	-11.89±1.97	0.48±0.22
H_{HR}	-4.16±2.47	0.68±0.13	-6.09±9.99	0.07±0.01

Table 3.2 T-test comparison of slopes for four transfer functions from 6 dogs between the control and electrical stimulation

	H_{RSNA}	$H_{RSNA-SAP}$	H_{SAP}	H_{HR}
Pval	0.212084	0.573977	0.158448	0.727186

Table 3.3 T-test comparison of coherence for four transfer functions of 6 dogs between the control and electrical stimulation

	H_{RSNA}	$H_{RSNA-SAP}$	H_{SAP}	H_{HR}
Pval	0.068233	0.018426	0.661058	0.003484

The change in the set-point from control (rest) to electrical stimulation (exercise) condition is associated to change in the DC gain obtained from the gain plots from dynamic analysis of the baroreflex system in this study as explained in section 1.2. The DC gain for H_{NC}, H_{PC}, $H_{TC,}$ H_{HC}, H_{NS}, H_{PS}, H_{TS} and H_{HS} is obtained by taking average of their respective gains below 0.1Hz, the reason being that the magnitude of all the transfer functions is almost flat in this low frequency range. The Table 3.3.4 contains the average DC gain values from 6 dogs for each transfer function. Comparison t-test is done between the Dc gain values for the control and the DC gain values for the electrical stimulation for all the transfer functions, its p-values are tabulated in Table 3.5.

Table 3.4 Mean DC gain values of each transfer function from 6 dogs for control and electrical stimulation

	Dc gain	
	Control	Electrical stimulation
HRSNA	-62.64±5.91	-60.70±8.91
HRSNA-SAP	39.50±6.49	35.81±6.02
HSAP	-11.11±6.27	-14.76±9.33
HHR	-14.48±4.32	-20.54±6.04

Table 3.5 T-test comparison of the Dc gain for each transfer functions from 6 dogs between the control and electrical stimulation measurement conditions

	H_{RSNA}	$H_{RSNA-SAP}$	H_{SAP}	H_{HR}
Pval	0.6053	0.059	0.1122	0.1332

3.2 Parametric estimation of baroreflex transfer functions applied to the control data

This section deals with the results obtained from parametric estimation of the carotid sinus baroreflex transfer functions, H_{RSNA}, $H_{RSNA-SAP}$, H_{SAP} and H_{HR} for the control measurement condition (rest condition). ARX and OE methods were applied to the data using M-1 and M-2 modeling schemes as discussed in section 2.3.2 and section 2.3.3. Section 3.2.1 gives the ARX and OE method for estimation of Mn, Mp, Mt and Mh applied to the 15 min of measured data while section 3.2.2 gives the ARX and OE method for estimation of Mn, Mp, Mt and Mh applied to the short ensembles of data which are selected by visual inspection. The short ensembles were selected on the basis of stationarity from the 15 min data. Run test was performed on the selected ensembles to check if they were stationary. The input-output data to the non-parametric and parametric models, i.e. CSP, SAP, RSNA and HR is filtered, zero mean detrended and down-sampled which is explained in section 2.5. Total of 6 dogs were analyzed in this study but due to constraint of space, results of only dog 5 are shown in this section. The results obtained from dog 5 are similar to that obtained for all the remaining dogs Appendix B also gives results of run test performed on entire 15 min of CSP, SAP, RSNA and HR data for control to check whether the input and output time series was stationary .The run test results for the short data ensembles are also given here.

3.2.1 M-1 and M-2 modeling schemes applied to entire 15 min of control data

Figure 3.9 through Figure 3.2 gives the plots for CSP, RSNA, SAP and HR for entire 15 min data and the run test to check the stationarity of this plotted data is given in appendix B.

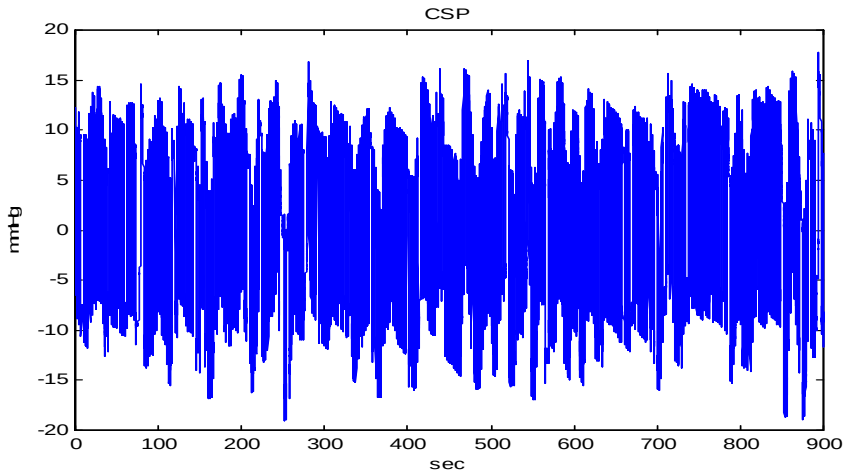

Figure 3.9 Plot of entire 15 minute of measured CSP from Dog 5(control)

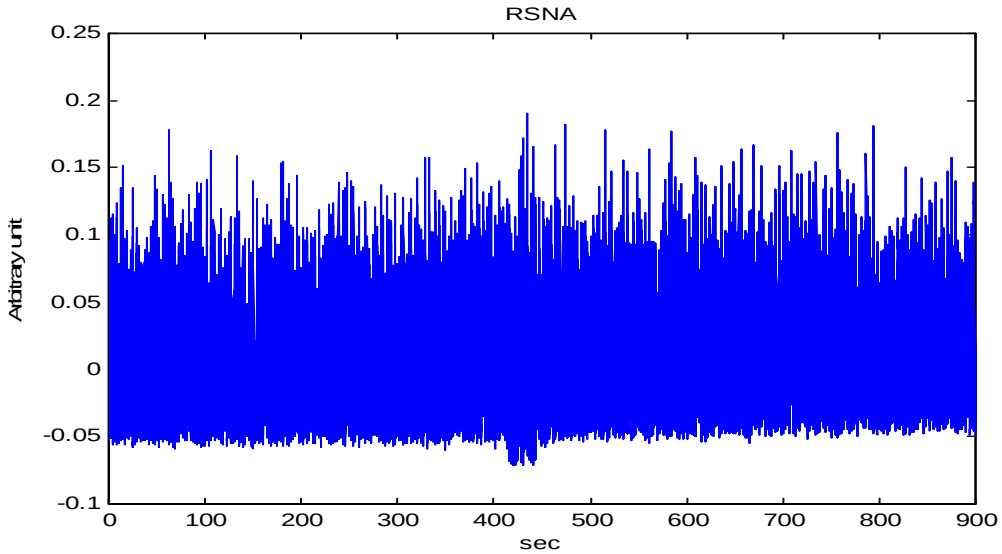

Figure 3.10 Plot of entire 15 minute of measured RSNA from Dog 5(control)

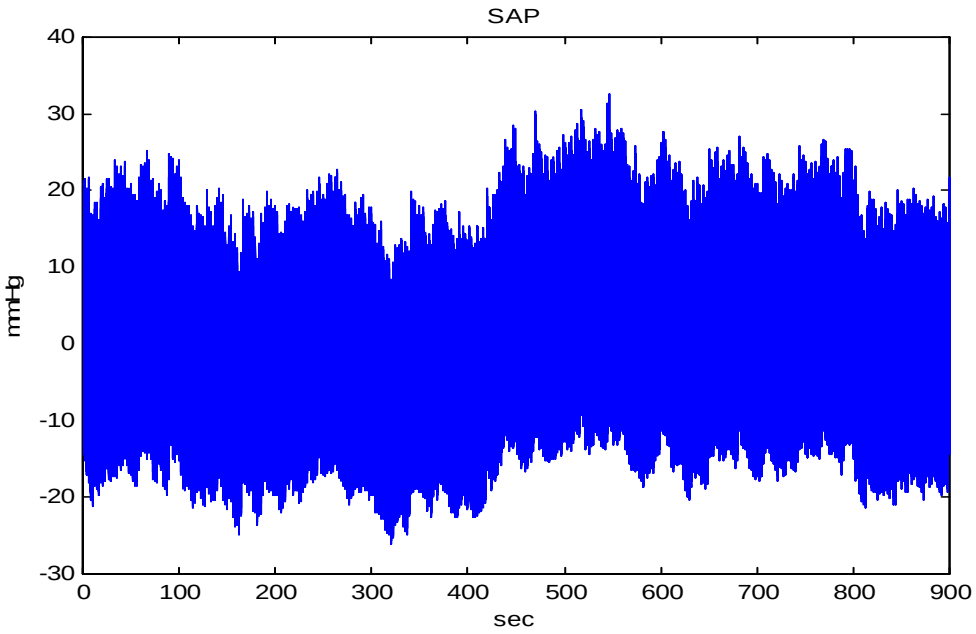

Figure 3.11 Plot of entire 15 minute of measured SAP from Dog 5(control)

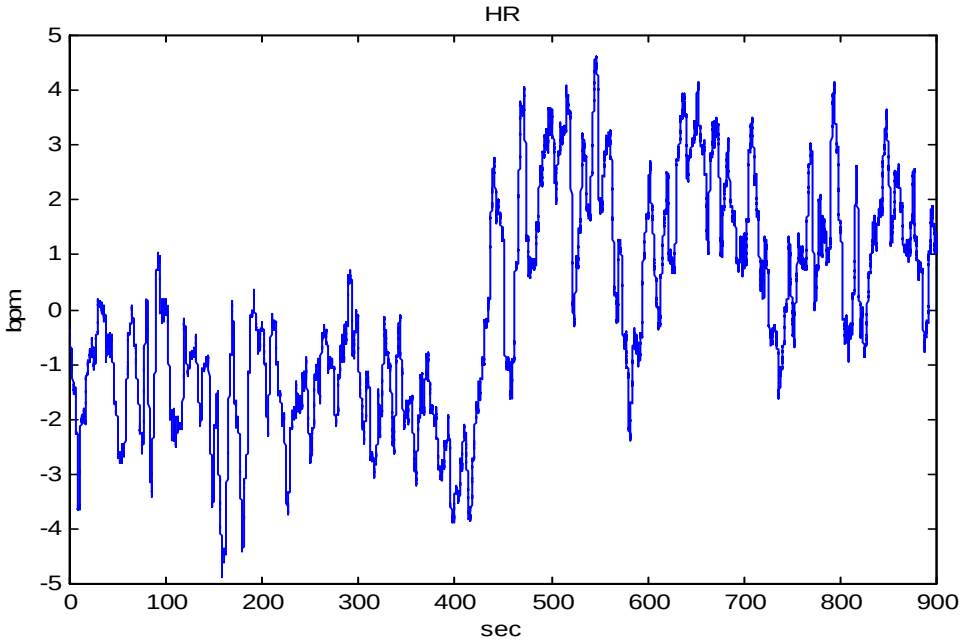

Figure 3.12 Plot of entire 15 minute of measured HR from Dog 5(control)

MSE is used as criterion in selection of the model order in case of both the ARX and OE models. In this section 3-D plots of MSE value are shown, obtained by applying the 15 min measured data to M-1 modeling scheme for ARX and OE method. The MSE value is seen to decrease with increase in the model order for ARX as well as OE models. Figure 3.13 and Figure 3.14 give the sample MSE plots for ARX and OE Mn models.

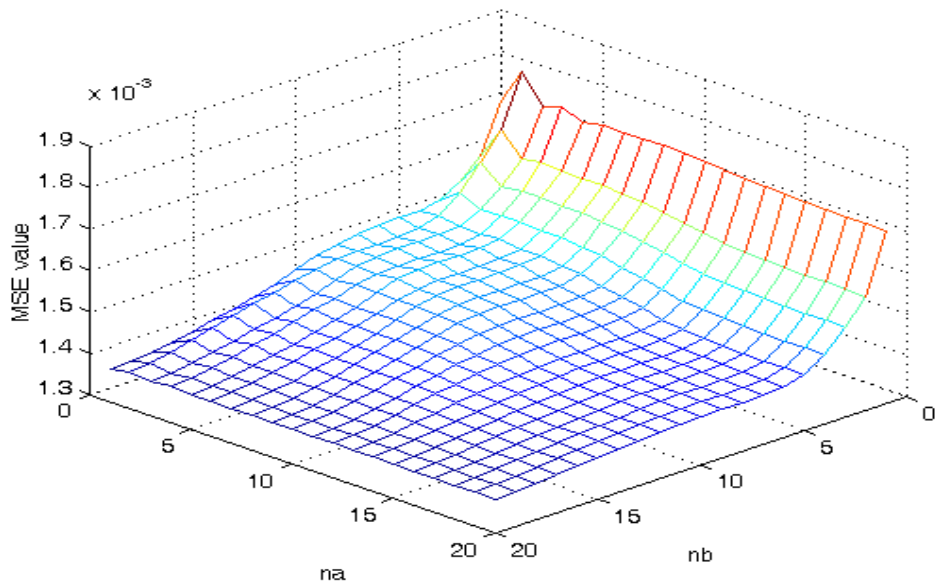

Figure 3.13 Plot of MSE values for ARX model of Mn for 15 min of control data

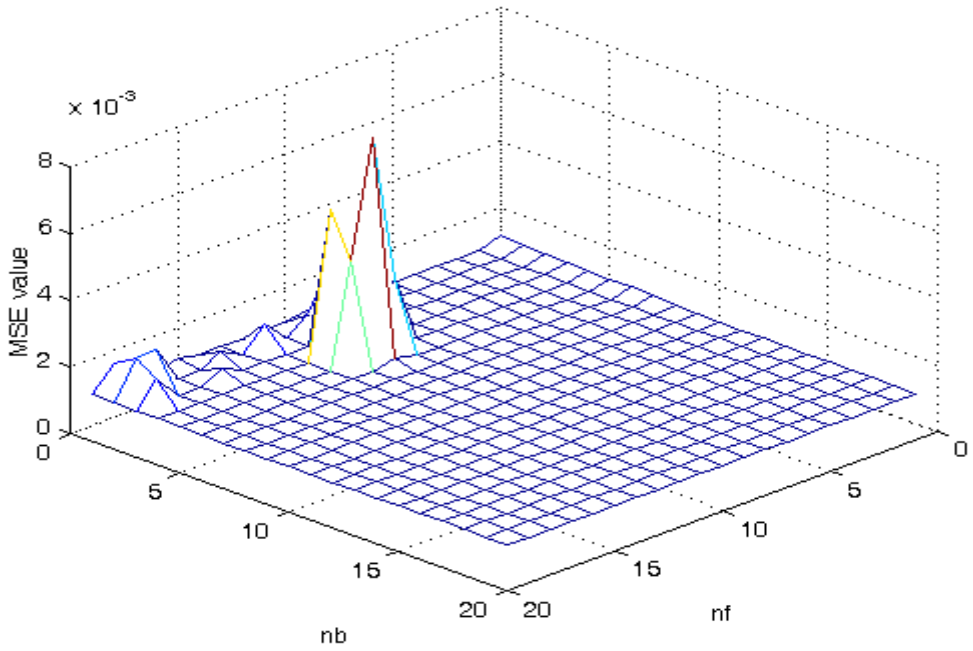

Figure 3.14 Plot of MSE values for OE model of Mn for 15 min of control data

3.2.1.1 Plots of estimated output and estimated frequency response of the ARX and OE models of Mn,Mp,Mt and Mh using M-1 and M-2 modeling schemes applied to 15 min of control data

In this section the plots for all models with order selected through M-1 and M-2 schemes for ARX and OE method are given. The output and the frequency response plots of Mn, Mp, Mt and Mh models are shown for orders estimated on the basis of lowest MSE values from M-1 and M-2 modeling schemes taking causality into consideration. The ARX, OE and NP models are estimated for same input-output data and their frequency response and estimated output is compared for all three estimation techniques. The above procedure is followed for Mn, Mp, Mt and Mh models. Figure 3.15 through Figure 3.7 show the plots for input-output, estimated output and frequency response for Mn. Similarly, Figure 3.18 through Figure3.20 gives plots for Mp, Figure

3.1 through Figure 3.23 give plots for Mt, and Figure 3.26 through Figure 3.6 gives plots for Mh. The frequency response for all the models is plotted in the range of 0.1 to 1Hz, which is the desired frequency range.

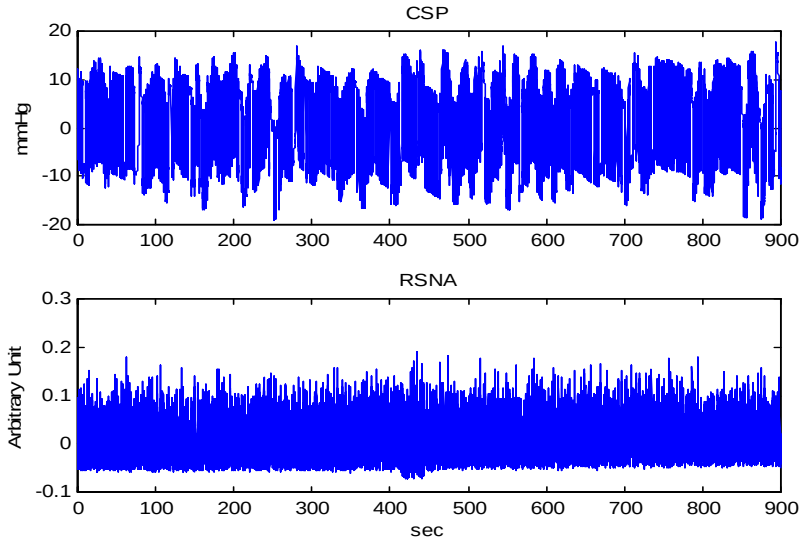

Figure 3.15 Plot for input (CSP) and output (RSNA) for 15 min for model Mn

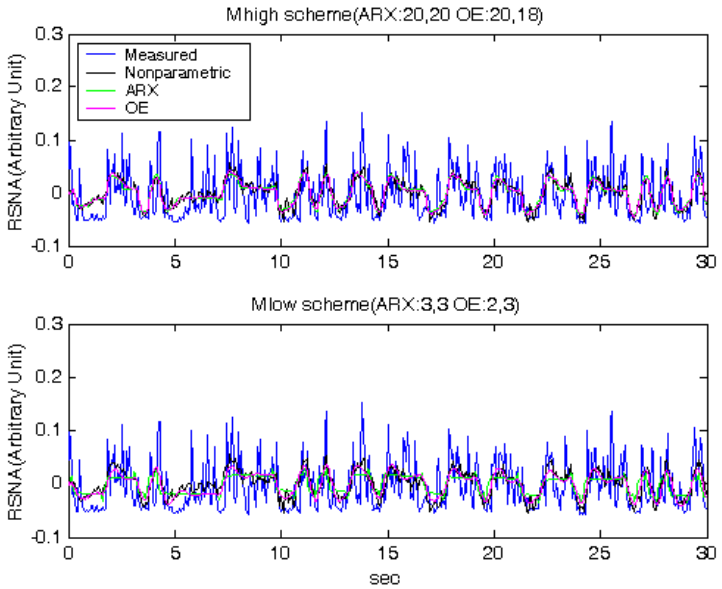

Figure 3.16 Plot for estimated output (RSNA) for 30 s of model Mn for NP and M-1(upper) and M-2 (lower) schemes of ARX and OE

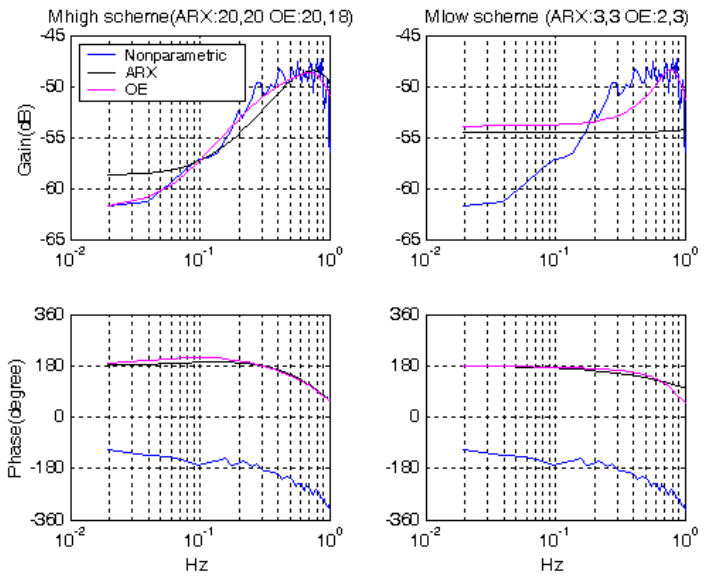

(i) (ii)

Figure 3.17 Plot estimated frequency response of ARX, OE and NP methods of Mn model for 15 min of control data (i) magnitude and phase plot for M-1 scheme (ii) magnitude and phase plot for M-2 scheme

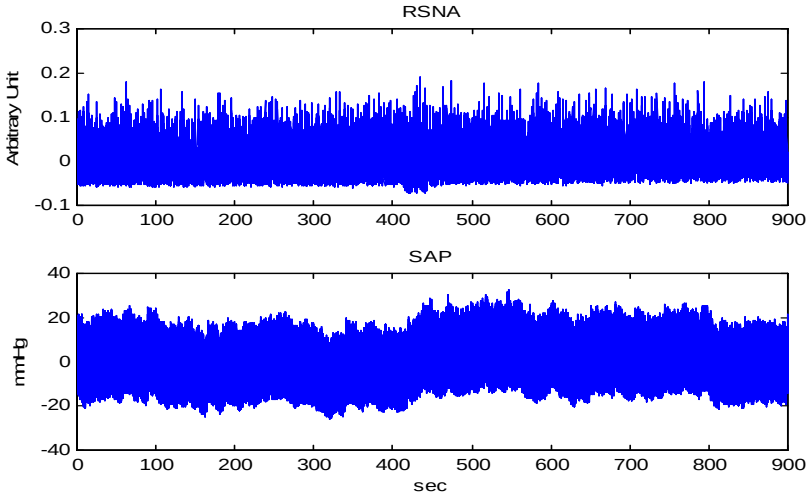

Figure 3.18 Plot for input (RSNA) and output (SAP) for 15 min for model Mp

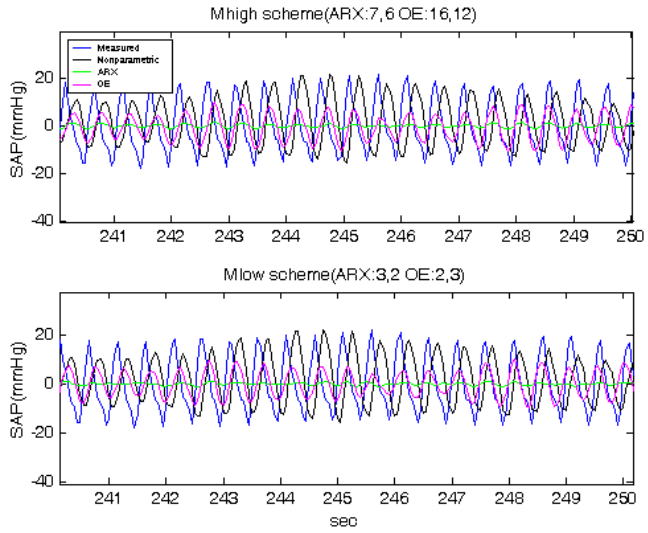

Figure 3.19 Plot for estimated output (SAP) for 5 s of control data of model Mp for M-1 (upper) and M-2 (lower) schemes of ARX and OE

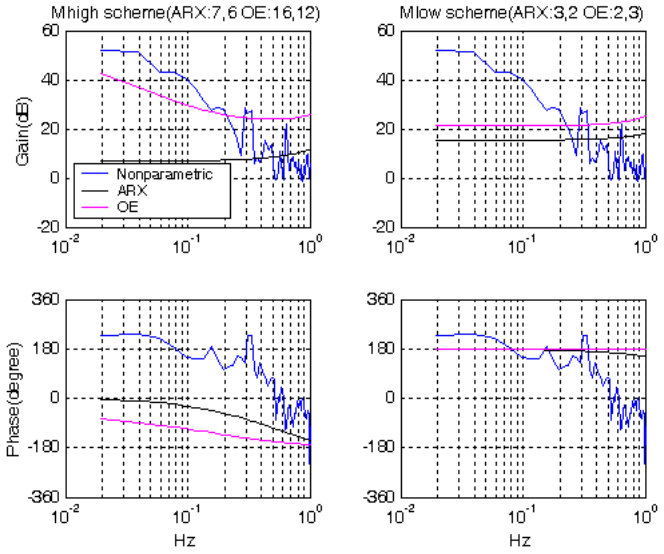

(i) (ii)

Figure 3.20 Plot estimated frequency response of ARX, OE and NP methods of Mp model for 15 min of control (i) magnitude and phase plot for M-1 scheme (ii) magnitude and phase plot for M-1 scheme

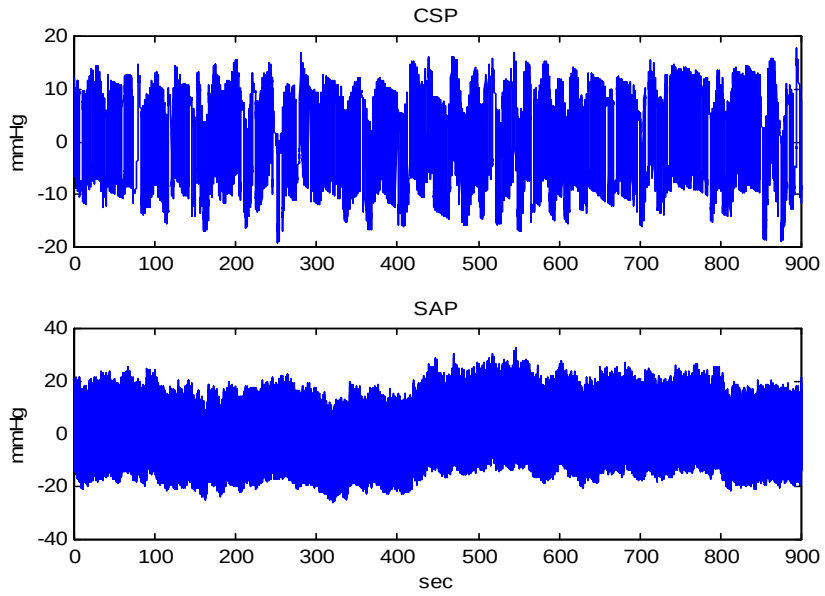

Figure 3.21 Plot for input (CSP) and output (SAP) for 15 min for model Mt

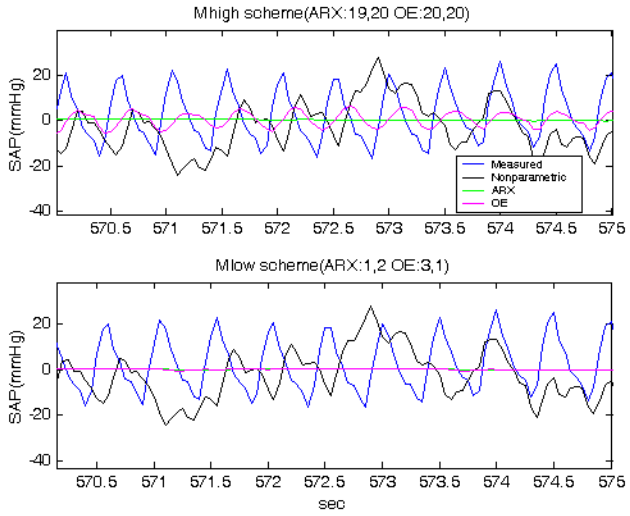

Figure 3.22 Plot for estimated output (SAP) for 5 s of control data of model Mt for M-1 and M-2 schemes of ARX and OE

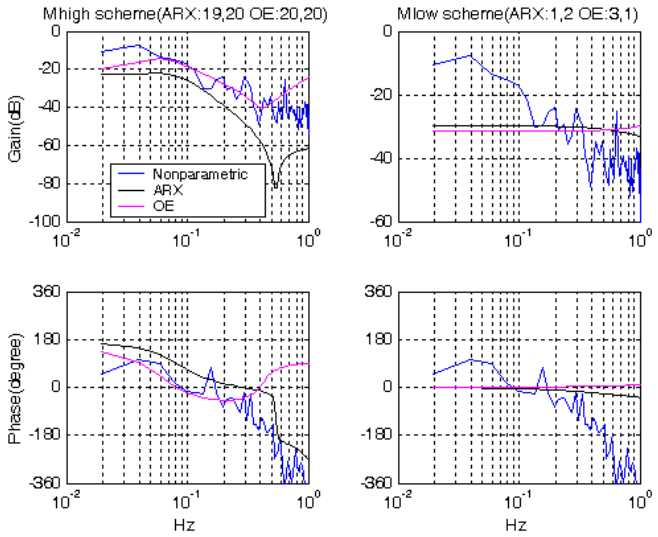

(i) (ii)

Figure 3.23 Plot estimated frequency response of ARX, OE and NP model of Mt for 15 min of control (i) magnitude and phase plot for M-1 (upper) scheme (ii) magnitude and phase plot for M-2 (lower) scheme

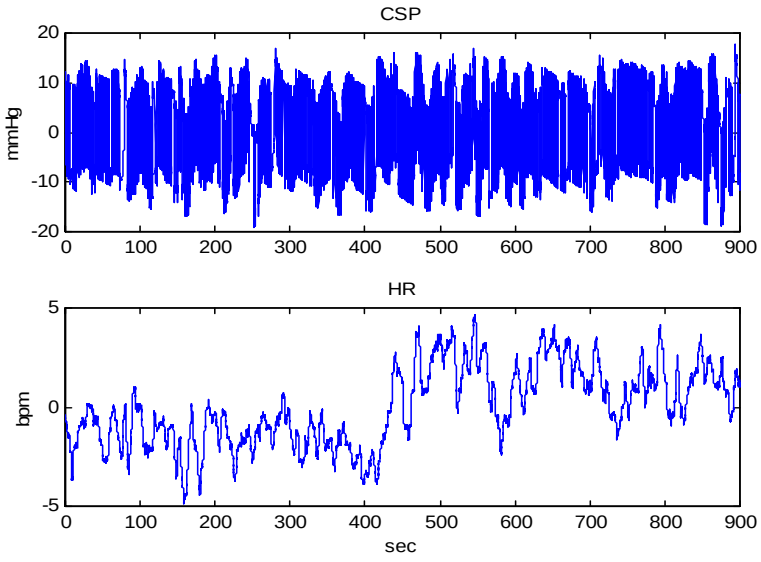

Figure 3.24 Plot for input (CSP) and output (HR) for 15 min for model Mh

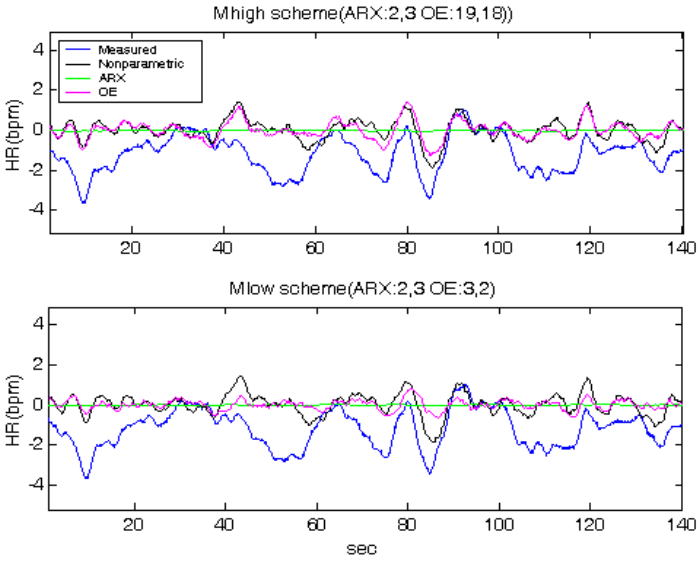

Figure 3.25 Plot for estimated output (HR) for 60 s of control data of model Mh for M-1 (upper) and M-2 (lower) schemes of ARX and OE

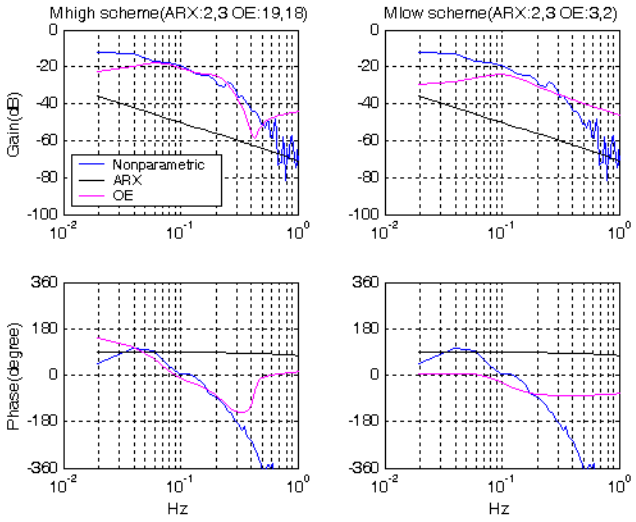

(i) (ii)

Figure 3.26 Plot estimated frequency response of ARX, OE and NP model of Mh for 15 min of control data (i) magnitude and phase plot for M-1 scheme (ii) magnitude and phase plot for M-2 scheme

3.2.2 M-1 and M-2 modeling schemes applied to short ensemble of control data from entire 15 min of data

The short ensembles of CSP, SAP, RSNA and HR data were selected from the 15 min of entire data length by visual inspection and run test was performed on them. The run test shows that the short ensembles are stationary compared to the non-stationary 15 min data, the result for which is given in appendix B. M-1 and M-2 modeling schemes were applied to the short ensembles. Figure 3.27 through Figure 3.30 give the plots for the selected ensembles which were used as input-output data for the Mn, Mp, Mt and the Mh.

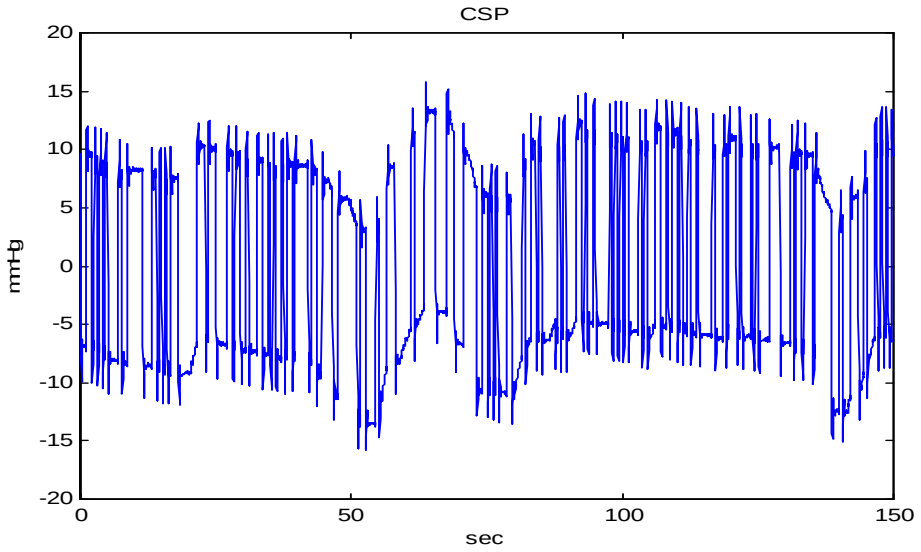

Figure 3.27 Plot of 150 s of measured CSP from Dog 5(control)

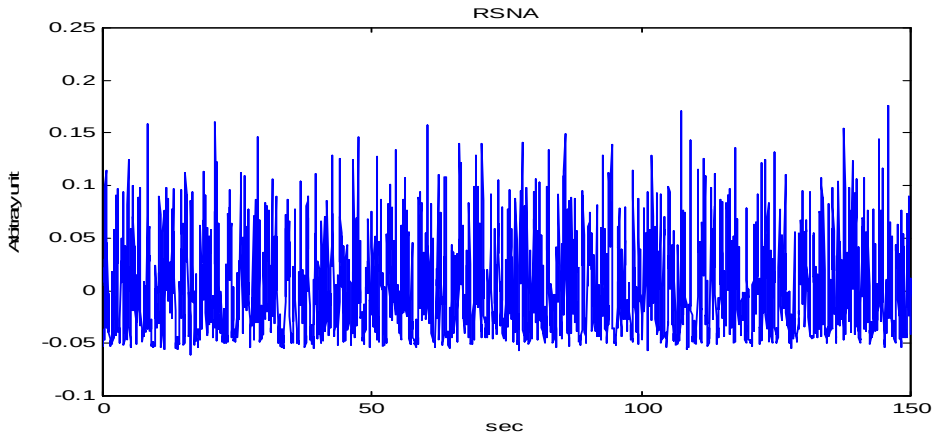

Figure 3.28 Plot of 150 s of measured RSNA from Dog 5(control)

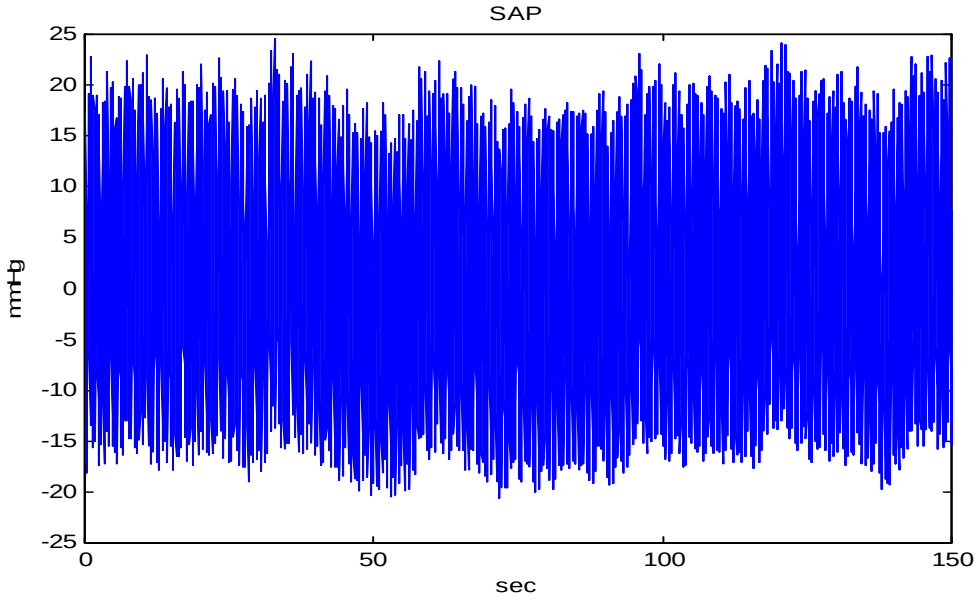

Figure 3.29 Plot of entire 150 s of measured SAP from Dog 5(control)

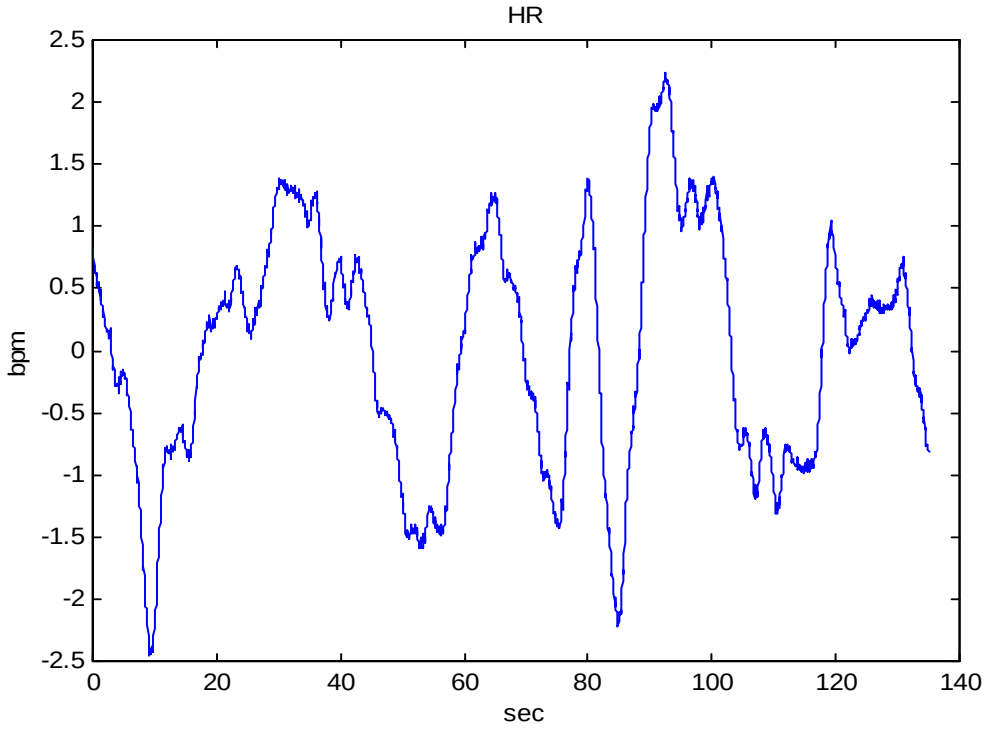

Figure 3.30 Plot of 140s of measured HR from Dog 5(control)

3.2.2.1 Plots of estimated output and estimated frequency response of the ARX and OE models of Mn, Mp, Mt and Mh using M-1 and M-2 modeling schemes applied to short ensembles of control data

In this section the plots for estimated output and the frequency response of the ARX, OE and NP models is illustrated. The order of ARX and OE models is selected by finding the lowest MSE values for M-1 and M-2 modeling schemes. The results for Mn,Mp,Mt and Mh models is shown along with the comparison between the ARX, OE and NP estimation techniques. Figure 3.31 through Figure 3.33 show the plots for input-output, estimated output and frequency response for Mn. Similarly, Figure 3.34 through Figure 3.36 give plots for Mp, Figure 3.37 through Figure 3.39 give plots for Mt, and

Figure 3.40 through Figure 3.42 give plots for Mh. The frequency response for all the models is plotted in the range of 0.1 to 1Hz, which is the desired frequency range

.

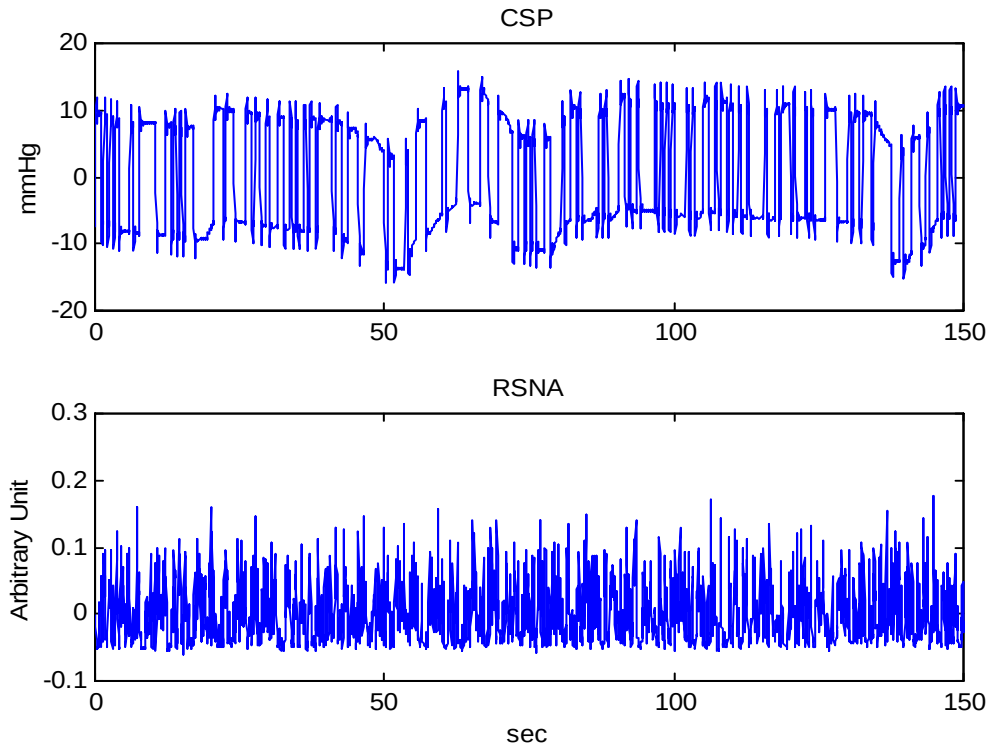

Figure 3.31 Plot for input (CSP) and output (RSNA) for 150 for model Mn

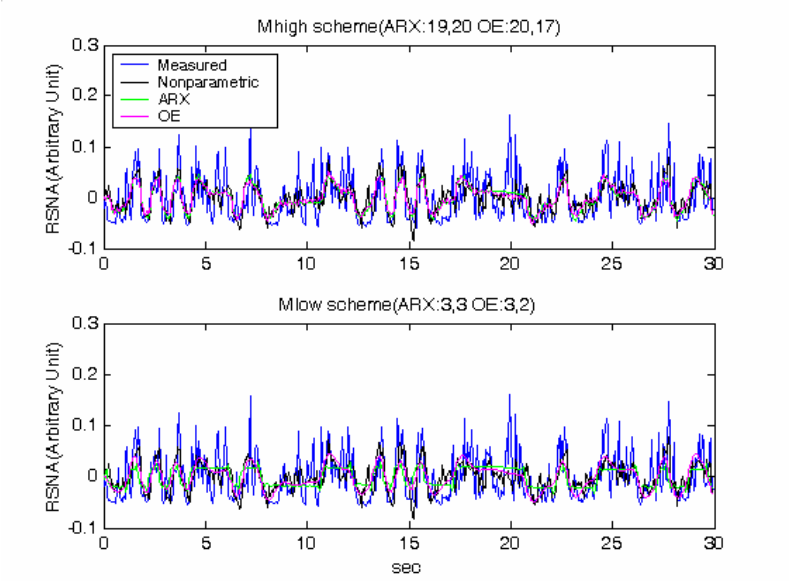

Figure 3.32 Plot for estimated output (RSNA) for 30 s of control data of model Mn for M-1 (upper) and M-2 (lower) schemes of ARX and OE

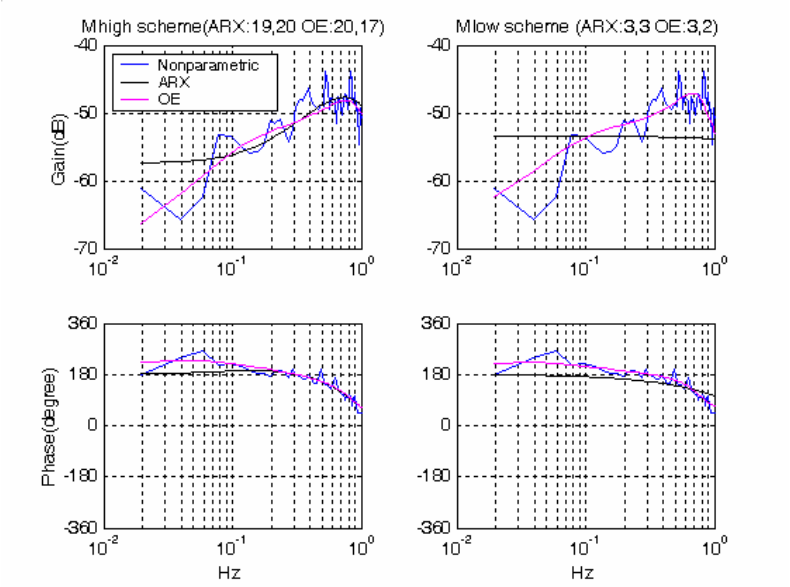

(i) (ii)

Figure 3.33 Plot estimated frequency response of ARX, OE and NP model of Mn for short ensemble (i) magnitude and phase plot for M-1 scheme (ii) magnitude and phase plot for M-2 scheme

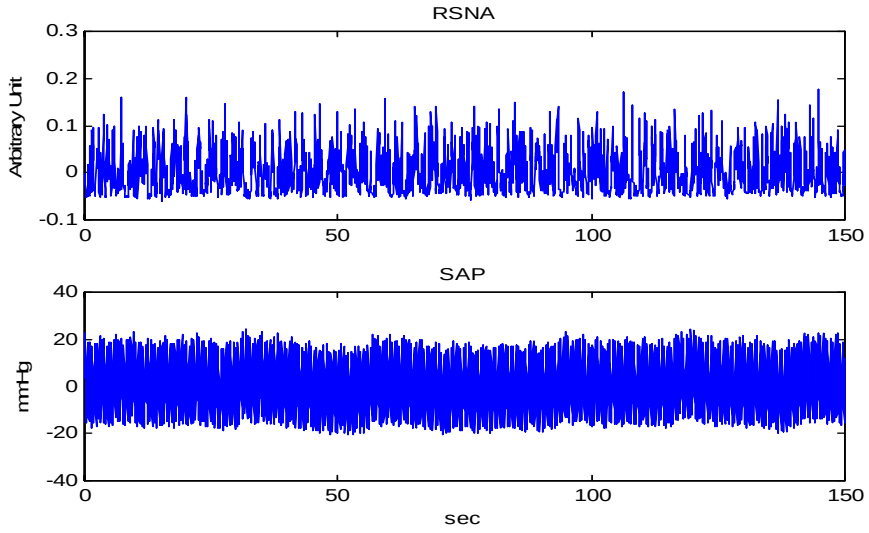

Figure 3.34 Plot for input (RSNA) and output (SAP) for 150 s for model Mp

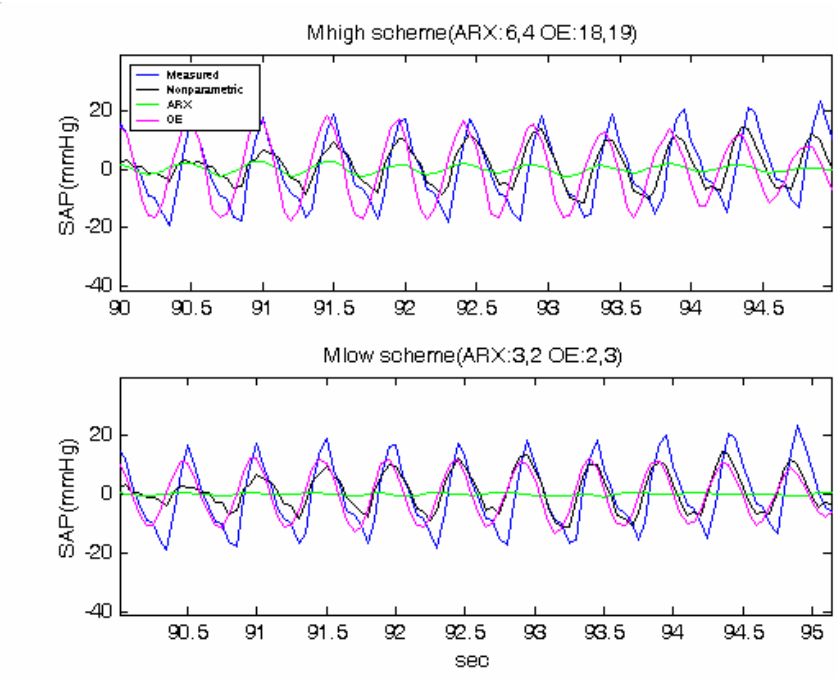

Figure 3.35 Plot for estimated output (SAP) for 10 s of control data of model Mp for M-1 (upper) and M-2 (lower) schemes of ARX and OE

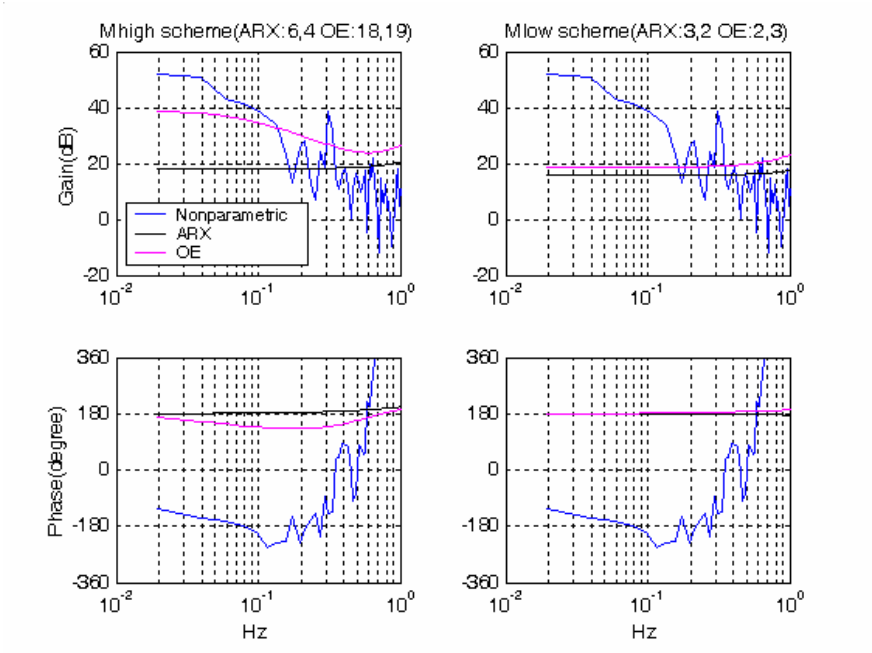

(i) (ii)

Figure 3.36 Plot estimated frequency response of ARX, OE and NP model of Mp for short ensemble (i) magnitude and phase plot for M-1 scheme (ii) magnitude and phase plot for M-1 scheme

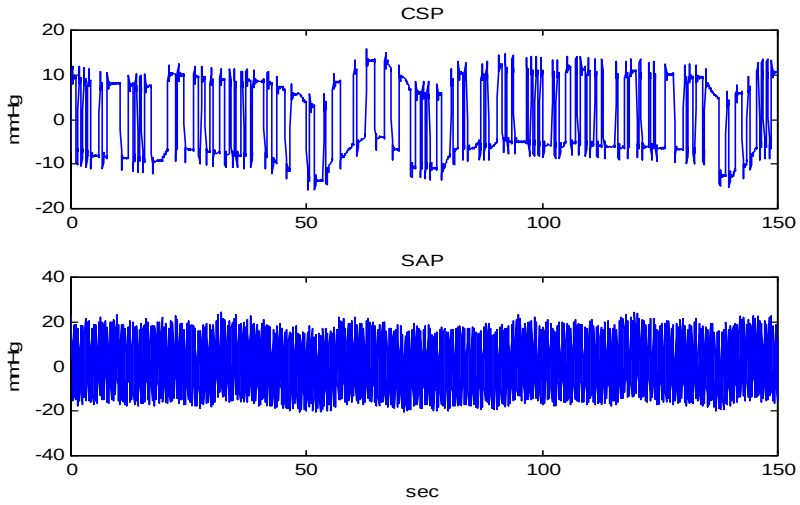

Figure 3.37 Plot for input (CSP) and output (SAP) for 150 s for model Mt

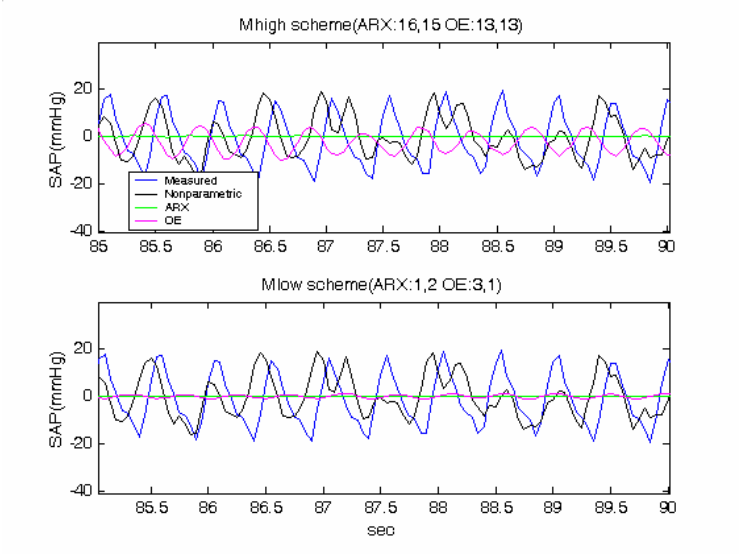

Figure 3.38 Plot for estimated output (SAP) for 10 s of control data of model Mt for M-1 (upper) and M-2 (lower) schemes of ARX and OE

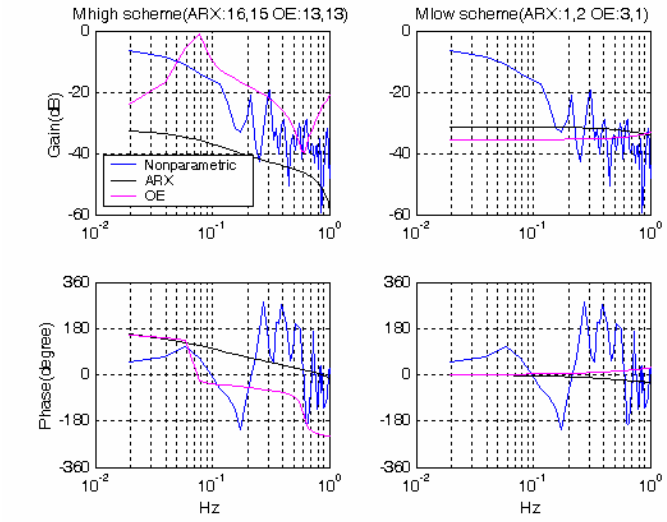

(i) (ii)

Figure 3.39 Plot estimated frequency response of ARX, OE and NP model of Mt for short ensemble of data (i) magnitude and phase plot for M-1 scheme (ii) magnitude and phase plot for M-2 scheme

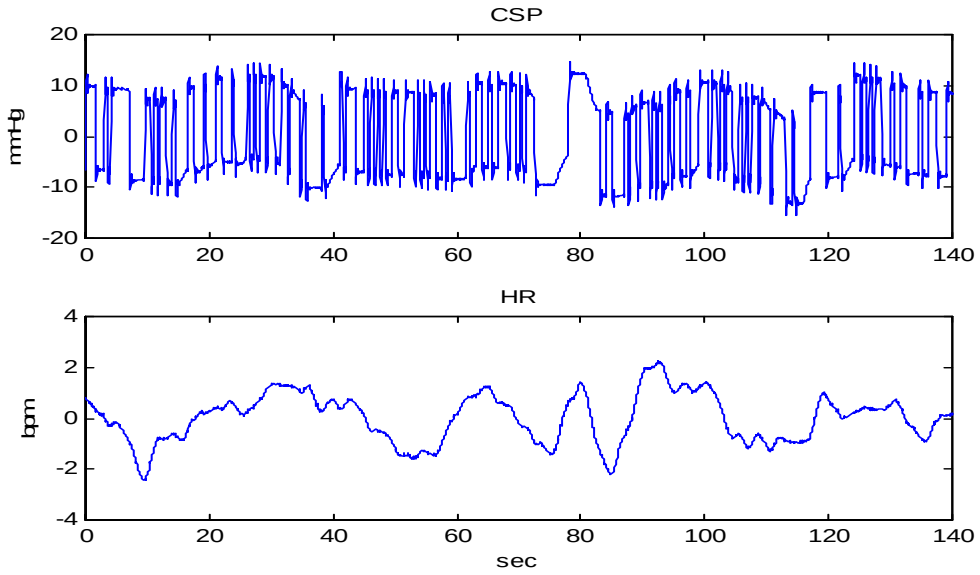

Figure 3.40 Plot for input (CSP) and output (HR) for 140 s for model Mh

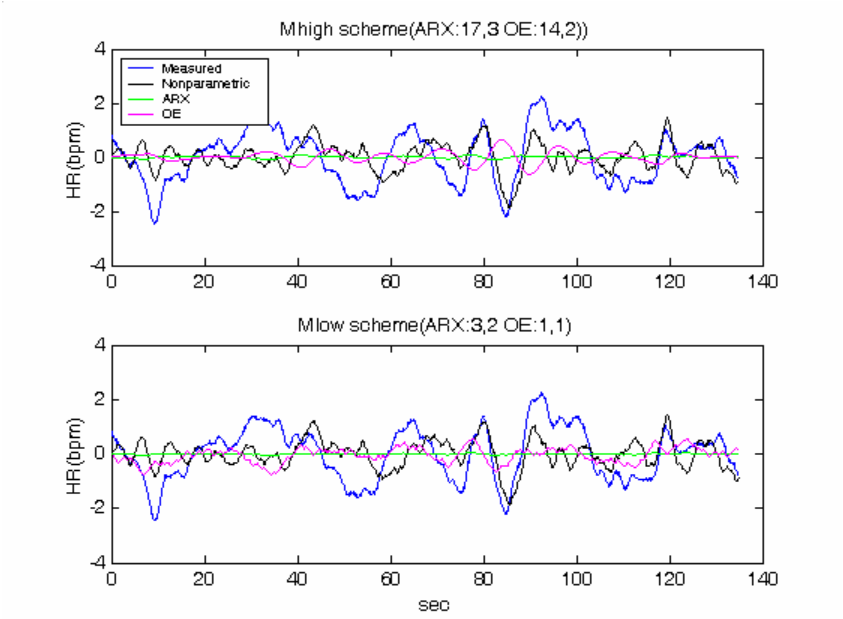

Figure 3.41 Plot for estimated output (HR) for 140 s of control data of model Mh for M-1 (upper) and M-2 (lower) schemes of ARX and OE

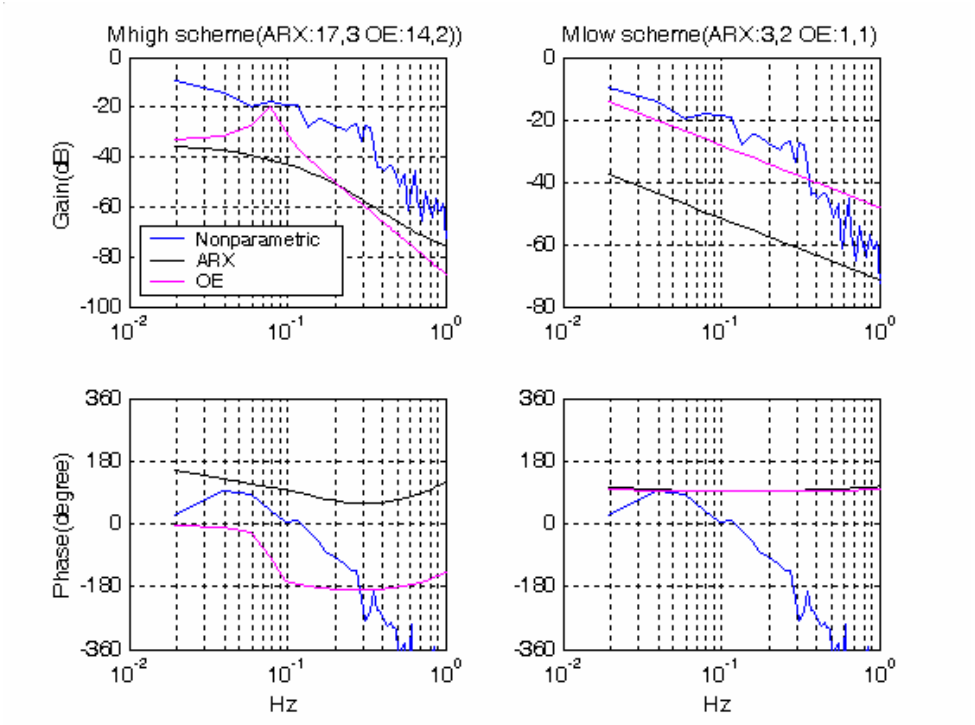

(i) (ii)

Figure 3.42 Plot estimated frequency response of ARX, OE and NP model of Mh for short ensemble of data (i) magnitude and phase plot for M-1 scheme (ii) magnitude and phase plot for M-2 scheme

3.2.3 Comparison between ARX and OE models using their MSE values for 15 min and short ensemble models from control data.

Table 3.3.6 tabulates the p-values for comparison of the M-1 and M-2 modeling schemes for ARX and OE models of Mn,Mp,Mt and Mh and the data length used for these models was 15 min. This test was conducted to see if there was any difference in the higher order and lower order models. Similarly, Table 3.3.7 gives the p-values for M-1 and M-2 model comparison using short ensembles of control data. Table 3.8 gives the p-values obtained from t-test for comparison of the 15 min models and the short ensemble models for all the transfer functions using MSE values obtained from M-1

modeling scheme by ARX and OE method. Similarly, Table 3.9 gives the p-values from t-test for 15 min and short ensemble model comparison using the M2 modeling scheme for ARX and OE models.

Table 3.6 T-test for comparison between the MSE values from ARX and OE method obtained from M-1 scheme and the MSE values obtained from M-2 scheme applied to 15 min of control data from all 6 dogs

	P-value	
	ARX	OE
Mn	0.31	0.10
Mp	0.01	0.15
Mt	0.03	0.004
Mh	0.23	0.27

Table 3.7 T-test for comparison between the MSE values from ARX and OE method obtained from M-1 scheme and the MSE values obtained from M-2 scheme applied to ensembles of control data from all 6 dogs

	P-value	
	ARX	OE
Mn	0.54	0.27
Mp	0.05	0.04
Mt	0.02	0.78
Mh	0.65	0.14

Table 3.8 T-test for comparison between the MSE values from ARX and OE method applied to 15 min of control data using M-1 scheme and the MSE values obtained from similar method for short ensemble of control data from all 6 dogs

	P-value	
	ARX	OE
Mn	0.17	0.19
Mp	0.00	0.02
Mt	0.01	0.11
Mh	0.06	0.03

Table 3.9 T-test for comparison between the MSE values from ARX and OE method applied to 15 min of control data using M-2 scheme and the MSE values obtained from similar method for short ensemble of control data from all 6 dogs

	P-value	
	ARX	OE
Mn	0.23	0.28
Mp	0.05	0.04
Mt	0.02	0.78
Mh	0.65	0.14

3.2.4 Comparison between the non-parametric models and the parametric models (ARX and OE models) for the control data condition

In this section the parametric models are statistically compared with the non-parametric models with the help of t-test for all the transfer functions, H_{RSNA}, $H_{RSNA-SAP}$, H_{SAP} and H_{HR}. The MSE values obtained from the estimated output and the measured output is used for comparison between ARX and NP, OE and NP and ARX and OE models for Mn, Mp, Mt and Mh models.

Table 3.10 gives the comparison between the ARX and OE, ARX and NP and OE and NP models for 15 min of control data for all 6 dogs and the ARX and OE models are estimated using M-1 modeling scheme in this case. Similarly, Table 3.11 has the p-values from t-test performed on the 15 min control data models for M-2 modeling scheme. Table 3.12 tabulates the t-test result for comparison of the ARX and OE, ARX and NP and OE and NP models using short ensemble of data models for higher orders and Table 13 give the result for lower order of short ensemble models.

Table 3.10 P-values from t-test comparison between the ARX and OE, ARX and NP and OE and NP models for 15 min higher order models using MSE values for control data from all 6 dogs

	P-value		
	ARX-OE	ARX-NP	OE-NP
Mn	0.246	0.112	0.108
Mp	0.034	0.884	0.749
Mt	0.001	0.281	0.020
Mh	0.193	0.114	0.215

Table 3.11 P-values from t-test comparison between the ARX and OE, ARX and NP and OE and NP models for 15 min lower higher order models using MSE values for control data from all 6 dogs

	P-value		
	ARX-OE	ARX-NP	OE-NP
Mn	0.307	0.419	0.112
Mp	0.039	0.081	0.053
Mt	0.017	0.289	0.273
Mh	0.102	0.077	0.207

Table 3.12 P-values from t-test comparison between the MSE values from ARX and OE, ARX and NP and OE and NP for short stationary ensemble higher order models for control data from all 6 dogs

	P-value		
	ARX-OE	ARX-NP	OE-NP
Mn	0.156	0.087	0.20
Mp	0.002	0.075	0.004
Mt	0.074	0.074	0.027
Mh	0.069	0.394	0.388

Table 3.13 P-values from t-test comparison between the MSE values from ARX and OE, ARX and NP and OE and NP for short stationary ensemble lower order models for control data from all 6 dogs

	P-value		
	ARX-OE	ARX-NP	OE-NP
Mn	0.591	0.332	0.091
Mp	0.009	0.185	0.016
Mt	0.058	0.058	0.024
Mh	0.129	0.174	0.417

3.3 Parametric estimation of baroreflex transfer functions applied to the electrical stimulation data

This section deals with the results obtained from parametric estimation of the carotid sinus baroreflex transfer functions, H_{RSNA}, $H_{RSNA-SAP}$, H_{SAP} and H_{HR} for the electrical stimulation measurement condition (exercise). ARX and OE methods were applied to the data using M-1 and M-2 modeling schemes as discussed in section 2.3.2 and section 2.3.3. Section 3.3.1 gives the ARX and OE method for estimation of Mn, Mp, Mt and Mh applied to the 15 min of measured data while section 3.3.2 gives the ARX and OE method for estimation of Mn, Mp, Mt and Mh applied to the short ensembles of data which are selected by visual inspection. The short ensembles were selected on the basis of stationarity from the 15 min data. Run test was performed on the selected ensembles to check if they were stationary. The input-output data to the non-parametric and parametric models, i.e. CSP, SAP, RSNA and HR is filtered, zero mean detrended and down-sampled which is explained in section 2.5. Total of 6 dogs were analyzed in this study but due to constraint of space, results of only dog 5 are shown in this section. The results obtained from dog 5 is similar to that obtained for all the remaining dogs Appendix B also gives results of run test performed on entire 15 min of CSP, SAP, RSNA and HR data for control to check whether the input and output time series is stationary .The run test results for the short data ensembles are also given here.

3.3.1 M-1 and M-2 modeling schemes applied to entire 15 min of control data

Figure 3.43 through Figure 3.46 gives the plots for CSP, RSNA, SAP and HR for entire 15 min data and the run test to check the stationarity of this plotted data is given in appendix B.

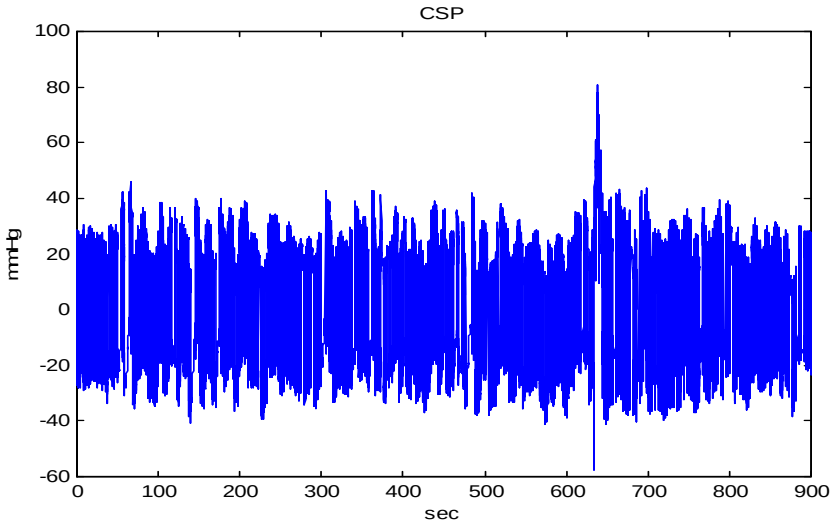

Figure 3.43 Plot of entire 15 minute of measured CSP from Dog 5 (electrical stimulation)

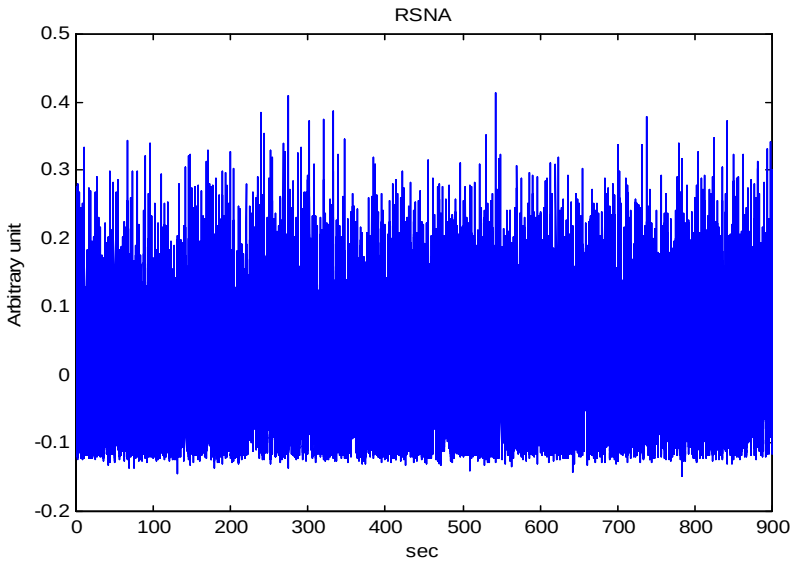

Figure3.44 Plot of entire 15 minute of measured RSNA from Dog 5 (electrical stimulation)

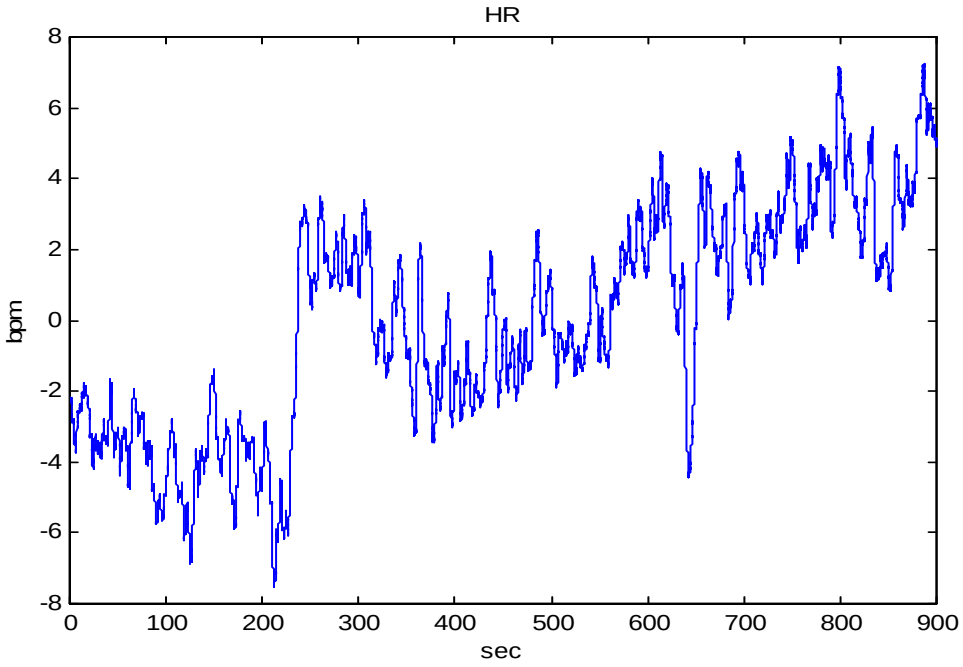

Figure 3.45 Plot of entire 15 minute of measured HR from Dog 5(electrical stimulation)

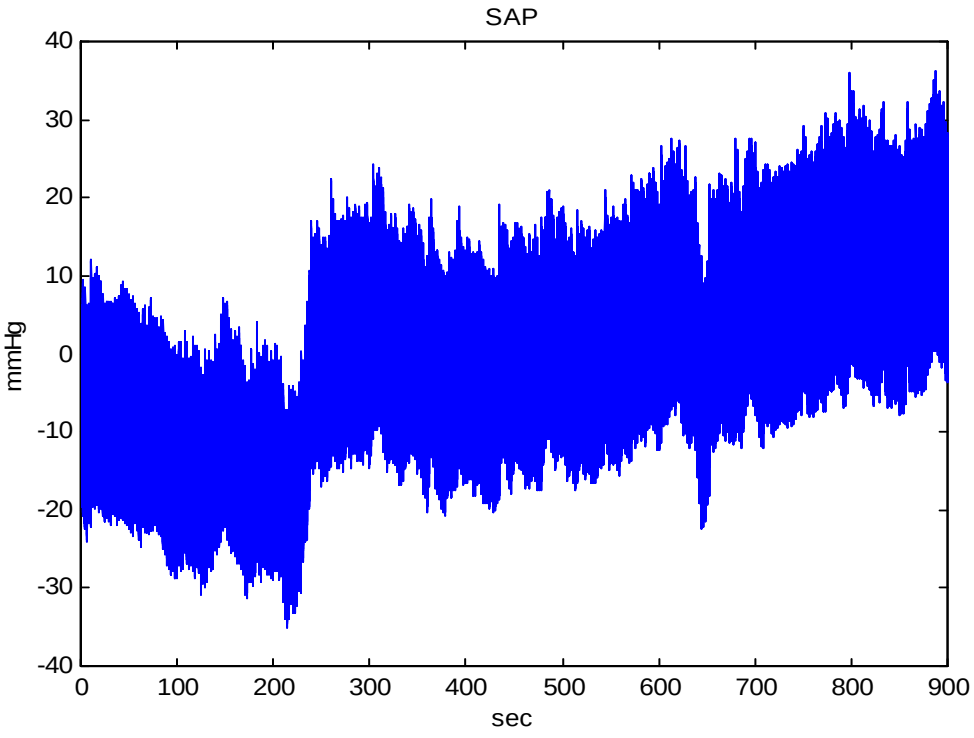

Figure3.46 Plot of entire 15 minute of measured SAP from Dog 5 (electrical stimulation)

MSE is used as criterion in selection of the model order in case of both the ARX and OE models. In this section 3-D plots of MSE value are shown, obtained by applying the 15 min measured data to M-1 modeling scheme for ARX and OE method. The MSE value is seen to decrease with increase in the model order for ARX as well as OE models. Figure 3.47 and Figure 3.48 give the sample MSE plots for ARX and OE Mn models

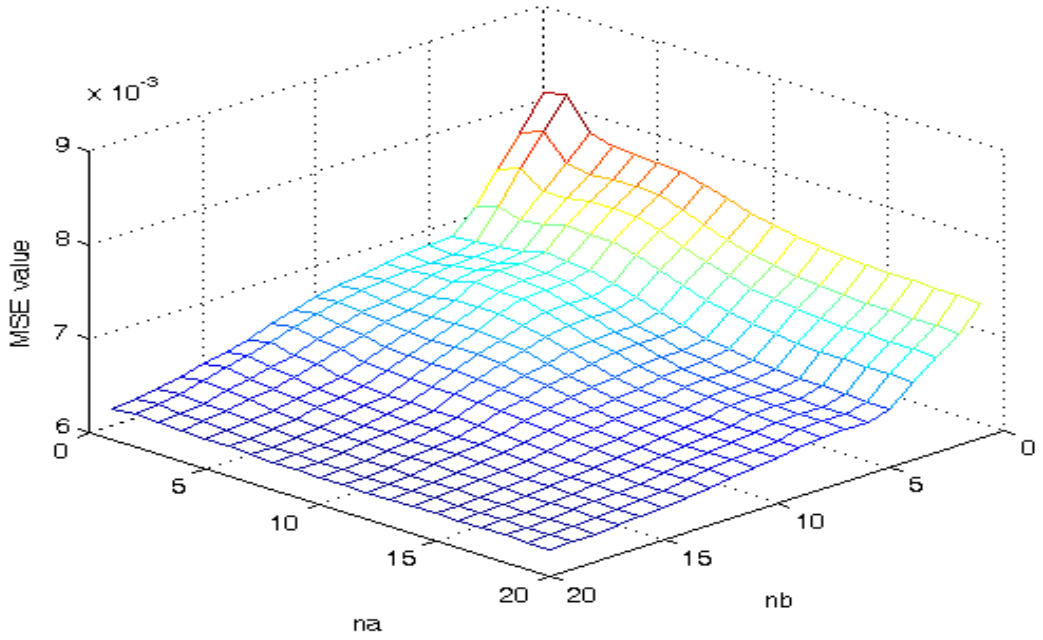

Figure3.47 Plot of MSE values for ARX model of Mn for 15 min of electrical stimulation data

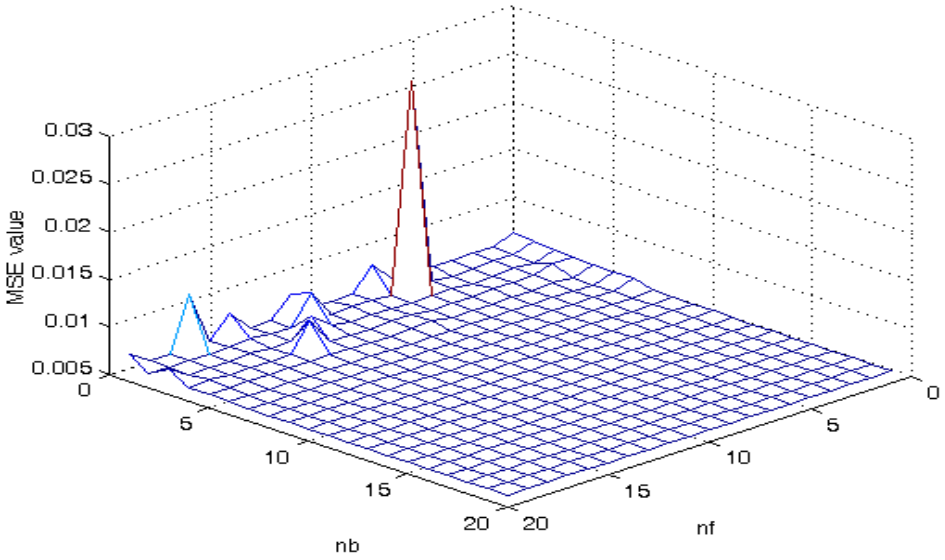

Figure 3.48 Plot of MSE values for OE model of Mn for 15 min of electrical stimulation data

3.3.1.1 Plots of estimated output and estimated frequency response of the ARX and OE models of Mn, Mp, Mt and Mh using M-1 and M-2 modeling schemes applied to 15 min of electrical stimulation data

In this section the plots for all models with order selected through M-1 and M-2 schemes for ARX and OE method are given. The output and the frequency response plots of Mn, Mp, Mt and Mh models are shown for orders estimated on the basis of lowest MSE values from M-1 and M-2 modeling schemes taking causality into consideration. The ARX, OE and NP models are estimated for same input-output data and their frequency response and estimated output is compared for all three estimation techniques. The above procedure is followed for Mn, Mp, Mt and Mh models. Figure 3.49 through Figure 3.51 show the plots for input-output, estimated output and frequency response for Mn. Similarly, Figure 3.52 through Figure 3.54 gives plots for Mp, Figure 3.55 through Figure 3.58 give plots for Mt, and Figure 3.59 through Figure

3.61 give plots for Mh. The frequency response for all the models is plotted in the range of 0.1 to 1Hz, which is the desired frequency range.

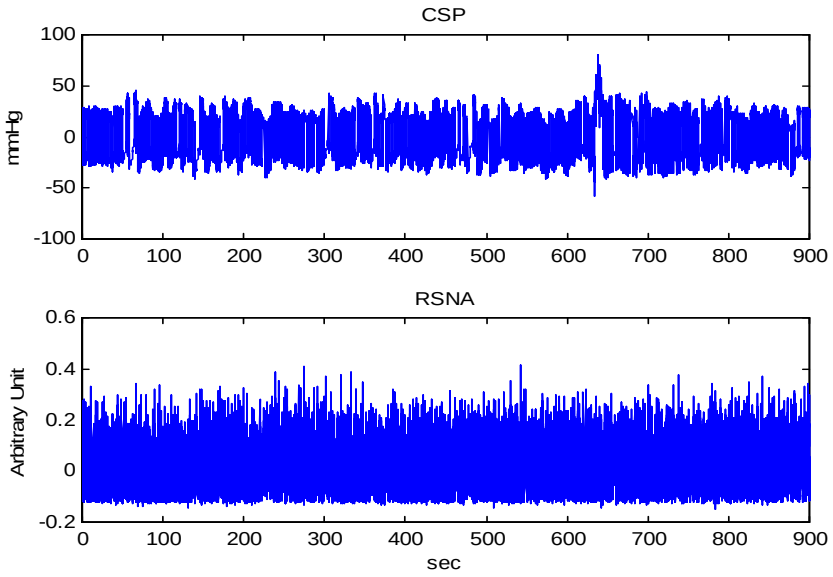

Figure 3.49 Plot for input (CSP) and output (RSNA) for 15 min for model Mn

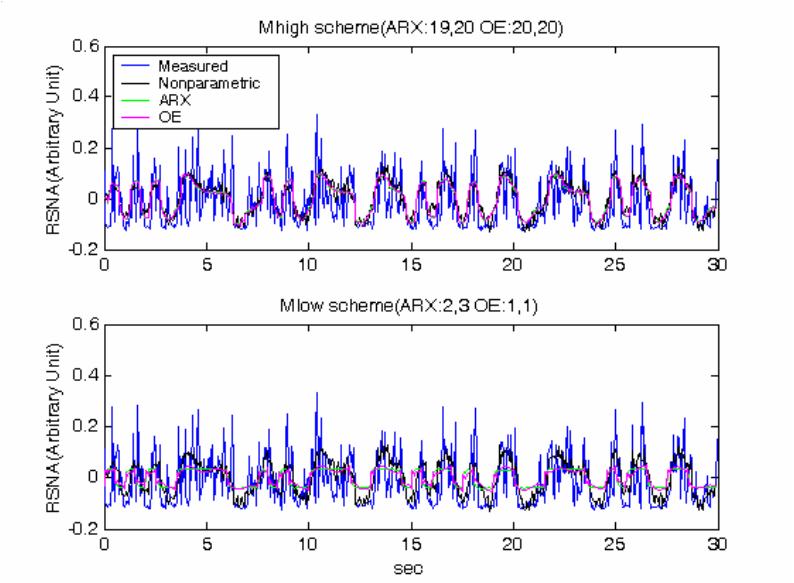

Figure 3.50 Plot for estimated output (RSNA) for 30 s of electrical stimulation data of model Mn for M-1 (upper) and M-2 (lower) schemes of ARX and OE

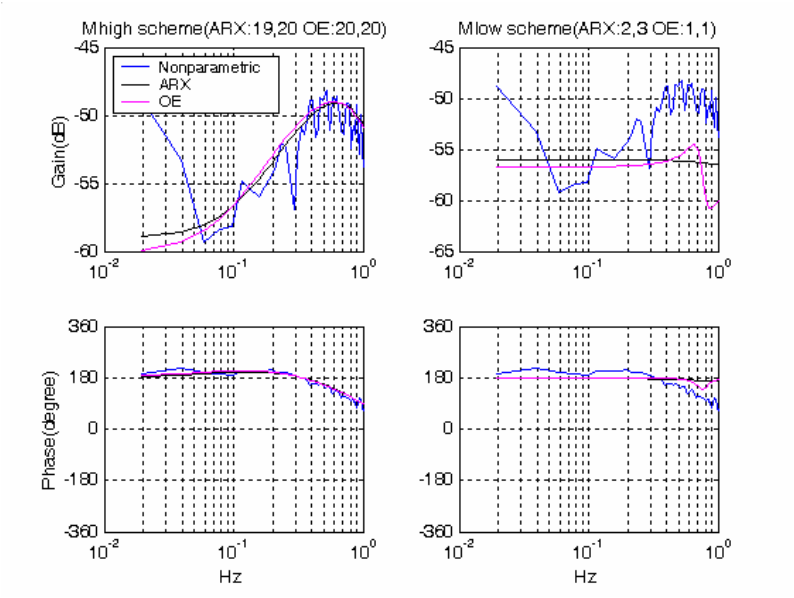

(i) (ii)

Figure 3.51 Plot estimated frequency response of ARX, OE and NP model of Mn (i) magnitude and phase plot for M-1 scheme (ii) magnitude and phase plot for M-2 scheme

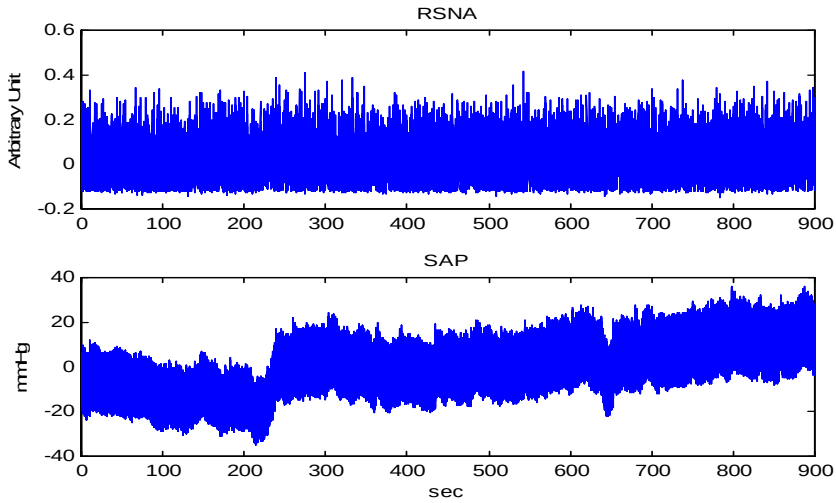

Figure 3.52 Plot for input (RSNA) and output (SAP) for 15 min of electrical stimulation for model Mp

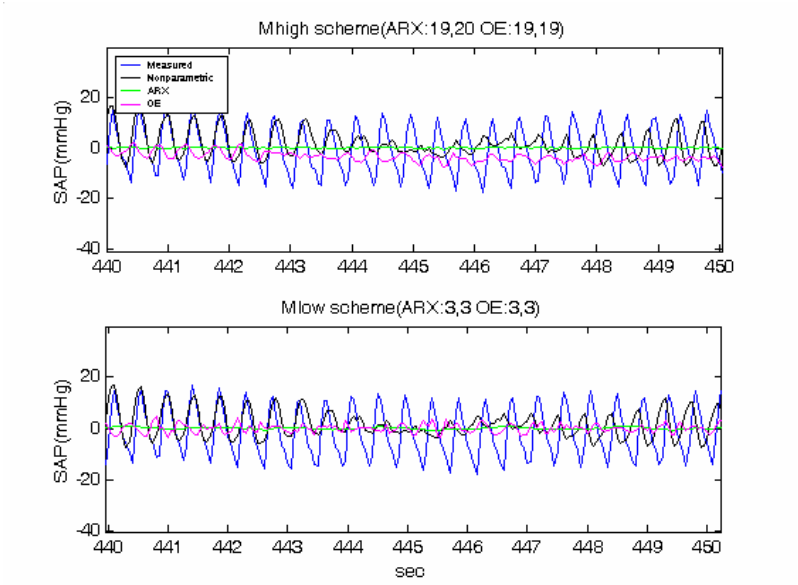

Figure 3.53 Plot for estimated output (SAP) for 10 s of electrical stimulation data of model Mp for M-1 (upper) and M-2 (lower) schemes of ARX and OE

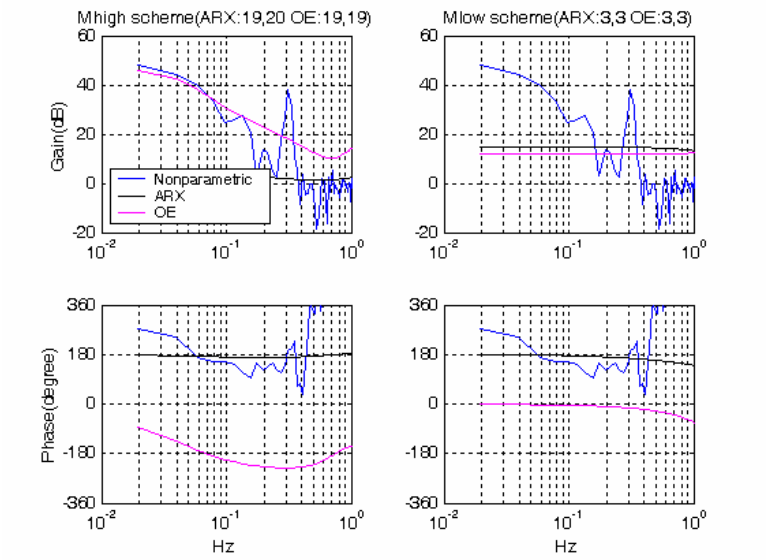

(i) (ii)

Figure 3.54 Plot estimated frequency response of ARX, OE and NP model of Mp for electrical stimulation (i) magnitude and phase plot for M-1 scheme (ii) magnitude and phase plot for M-2 scheme

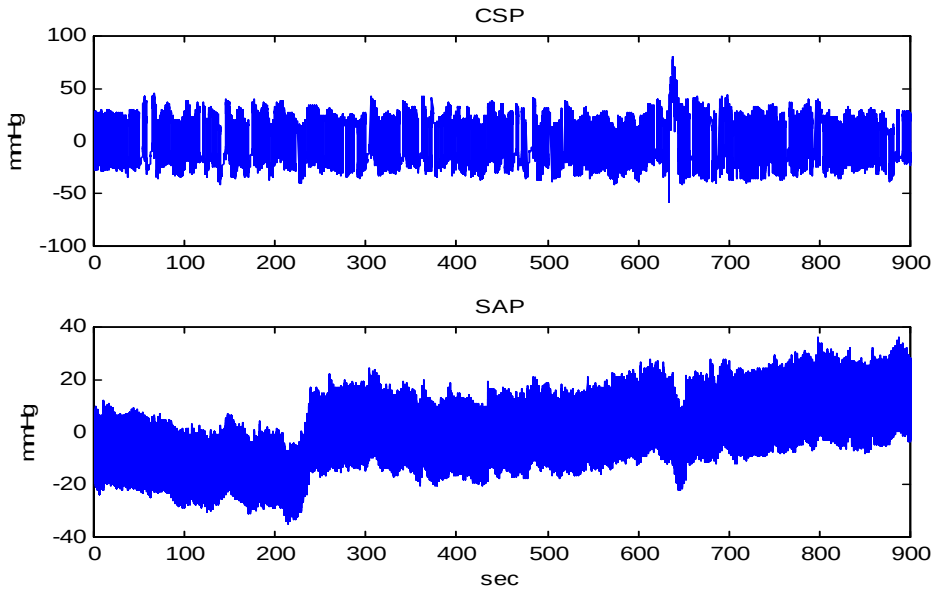

Figure 3.55 Plot for input (CSP) and output (SAP) for 15 min for model Mt

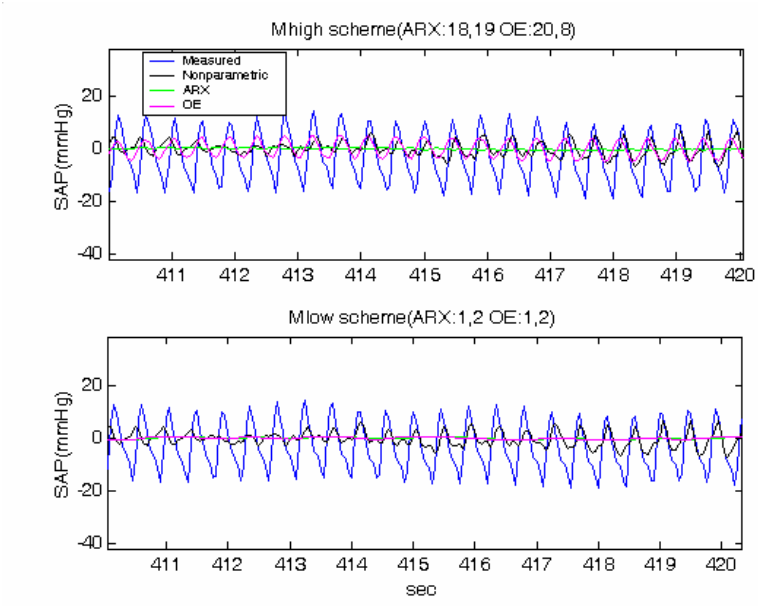

Figure 3.56 Plot for estimated output (SAP) for 10 s of electrical stimulation data of model Mt for M-1 (upper) and M-2 (lower) schemes of ARX and OE

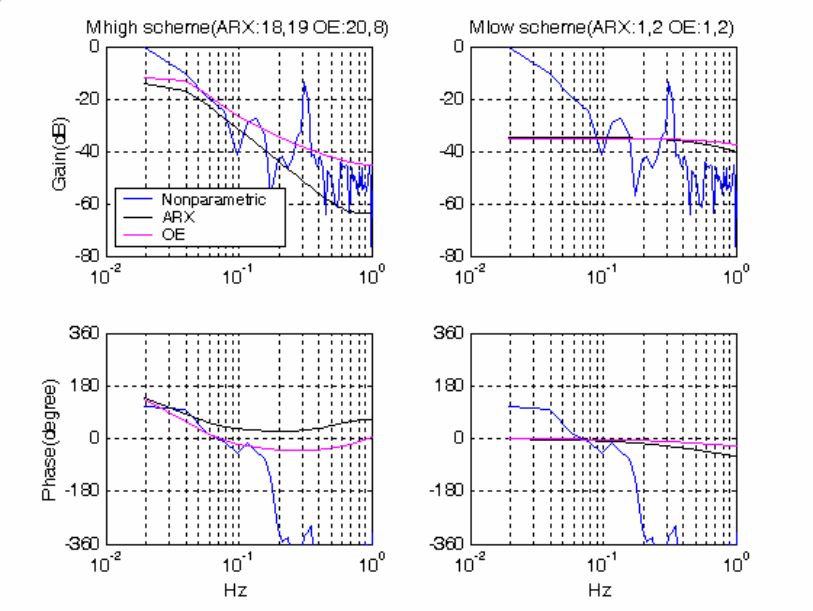

(i) (ii)

Figure 3.57 Plot estimated frequency response of ARX, OE and NP model of Mt from 15 min of electrical stimulation data (i) magnitude and phase plot for M-1 scheme (ii) magnitude and phase plot for M-2 scheme

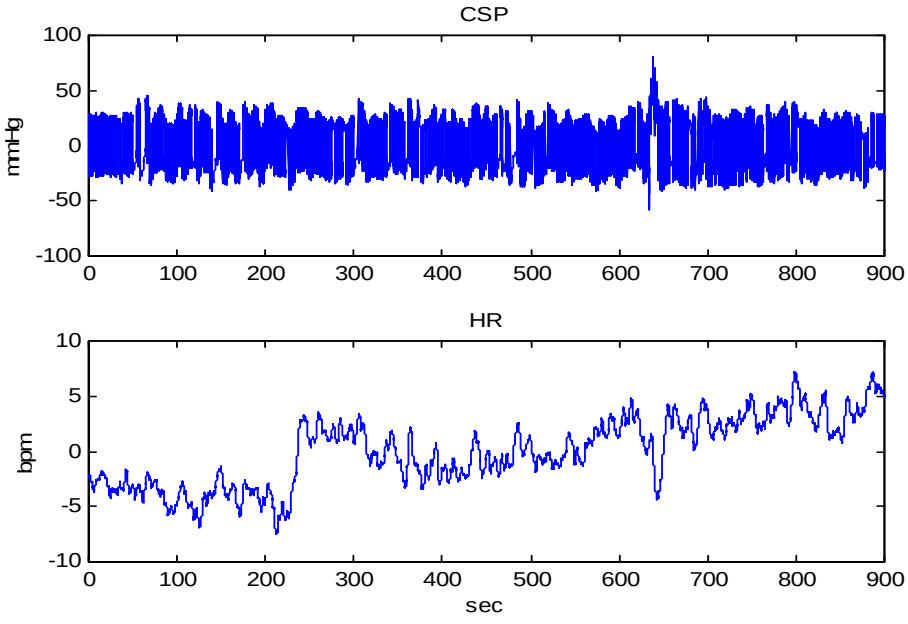

Figure 3.58 Plot for input (CSP) and output (HR) for 15 min for model Mh

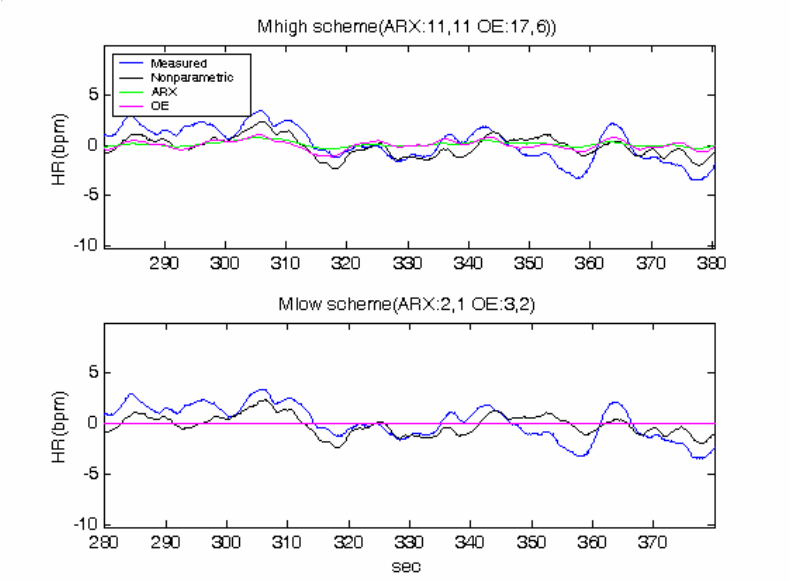

Figure 3.59 Plot for estimated output (HR) for 200 s of electrical stimulation data of model Mh for M-1 (upper) and M-2 (lower) schemes of ARX and OE

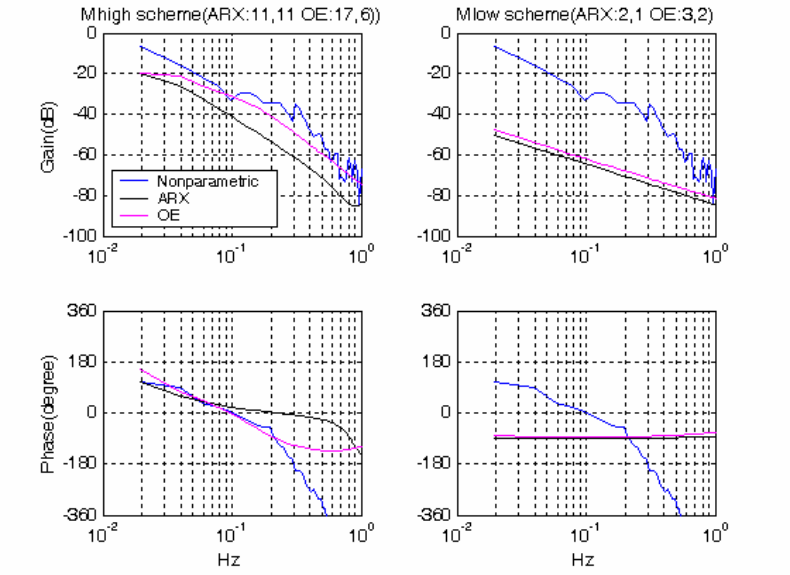

(i) (ii)

Figure 3.60 Plot estimated frequency response of ARX, OE and NP model of Mh for electrical stimulation (i) magnitude and phase plot for M-1 scheme (ii) magnitude and phase plot for M-1 scheme

3.3.2 M-1 and M-2 modeling schemes applied to short ensemble of electrical stimulation data from entire 15 min of data

The short ensembles of CSP, SAP, RSNA and HR data were selected from the 15 min of entire data length by visual inspection and run test was performed on them. The run test shows that the short ensembles are stationary compared to the non-stationary 15 min data, the result for which is given in appendix B. M-1 and M-2 modeling schemes were applied to the short ensembles. Figure 3.61 through Figure 3.65 give the plots for the selected ensembles which were used as input-output data for the Mn, Mp, Mt and the Mh.

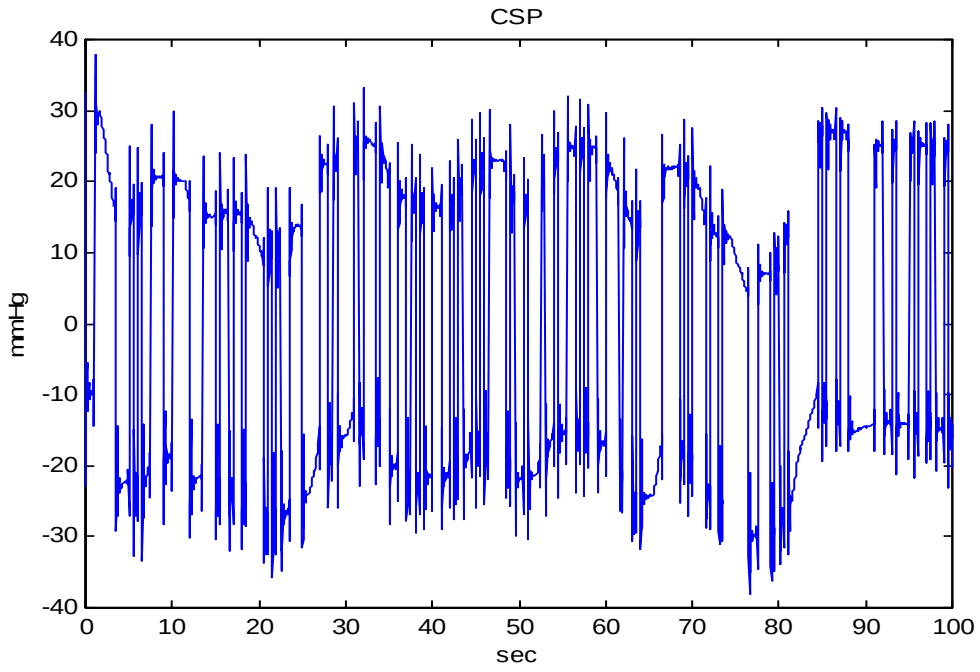

Figure 3.61 Plot of 100 s of measured CSP from Dog 5(electrical stimulation)

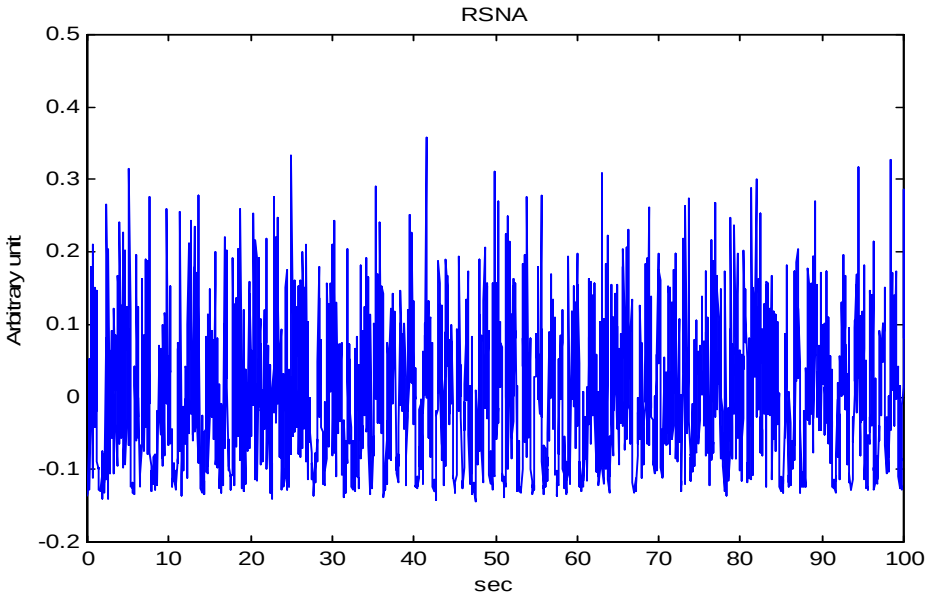

Figure 3.62 Plot of 100 s of measured RSNA from Dog 5(electrical stimulation)

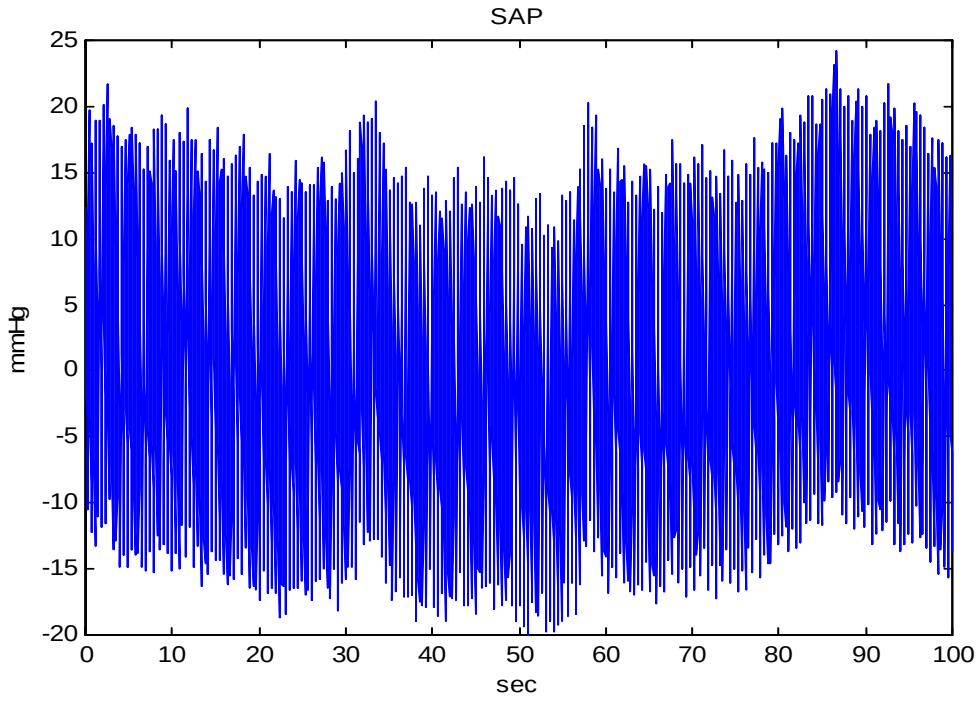

Figure 3.63 Plot of 100 s of measured SAP from Dog 5(electrical stimulation)

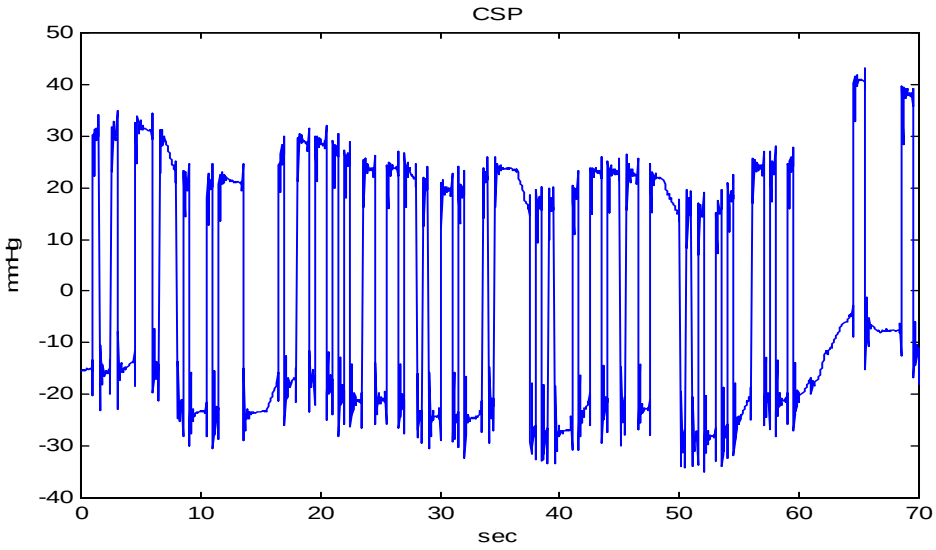

Figure 3.64 Plot of 70 s of measured CSP from Dog 5(electrical stimulation)

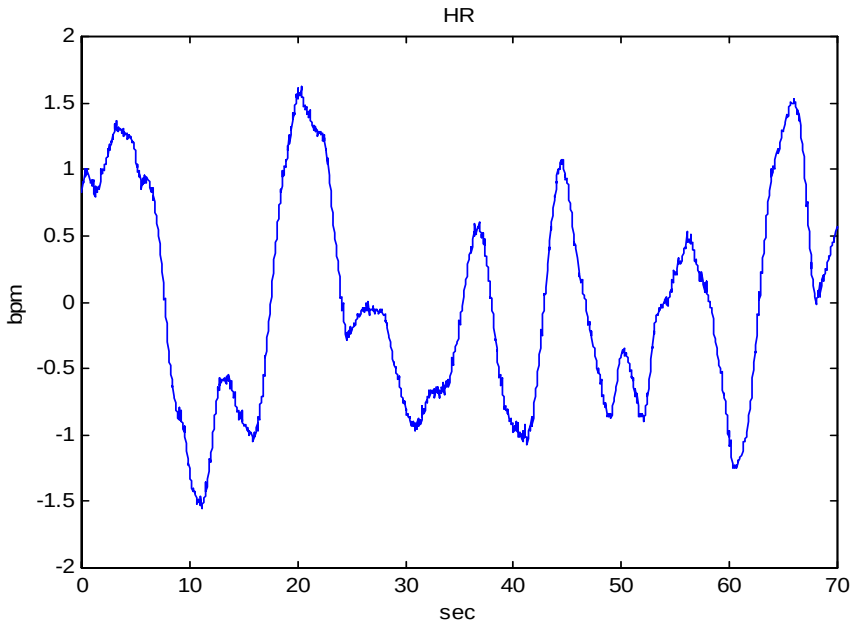

Figure 3.65 Plot of 70 s of measured HR from Dog 5(electrical stimulation)

3.3.2.1 Plots of estimated output and estimated frequency response of the ARX and OE models using short ensembles of data for all transfer functions for electrical stimulation

In this section the plots for estimated output and the frequency response of the ARX, OE and NP short ensemble models is illustrated. The order of ARX and OE models is selected by finding the lowest MSE values for M-1 and M-2 modeling schemes. The results for Mn,Mp,Mt and Mh models is shown along with the comparison between the ARX, OE and NP estimation techniques. Figure 3.66 through Figure 3.68 show the plots for input-output, estimated output and frequency response for Mn. Similarly, Figure 3.69 through Figure 3.71 give plots for Mp, Figure 3.72 through Figure 3.74 give plots for Mt, and Figure 3.75 through Figure 3.77 give plots for Mh. The frequency response for all the models is plotted in the range of 0.1 to 1Hz, which is the desired frequency range.

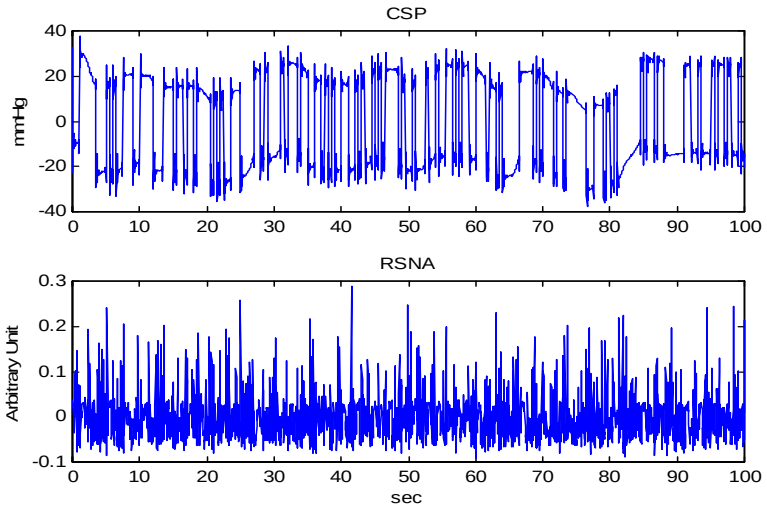

Figure 3.66 Plot for input (CSP) and output (RSNA) for 100 s for model Mn

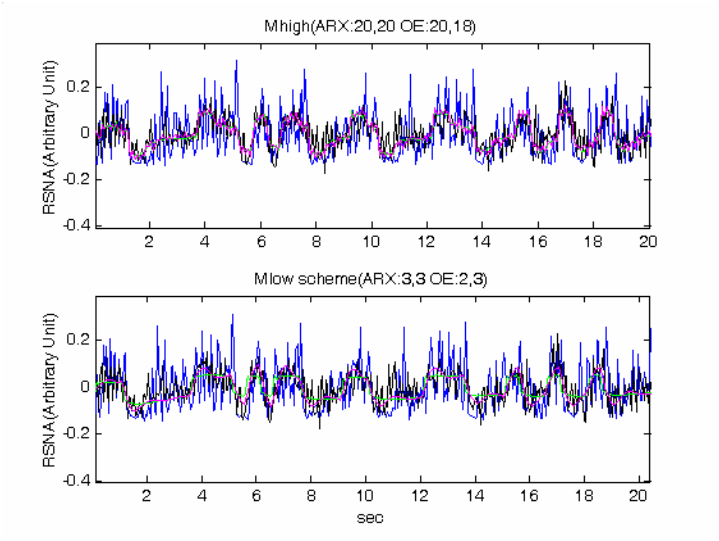

Figure 3.67 Plot for estimated output (RSNA) for 30 s of electrical stimulation data of model Mn for M-1 (upper) and M-2 (lower) schemes of ARX and OE

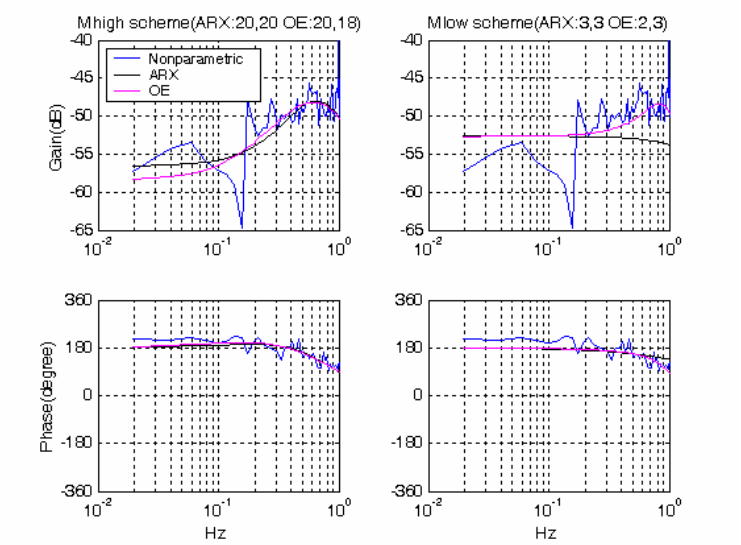

(i) (ii)

Figure 3.68 Plot estimated frequency response of ARX, OE and NP model of Mn for electrical stimulation (i) magnitude and phase plot for M-1 scheme (ii) magnitude and phase plot for M-2 scheme

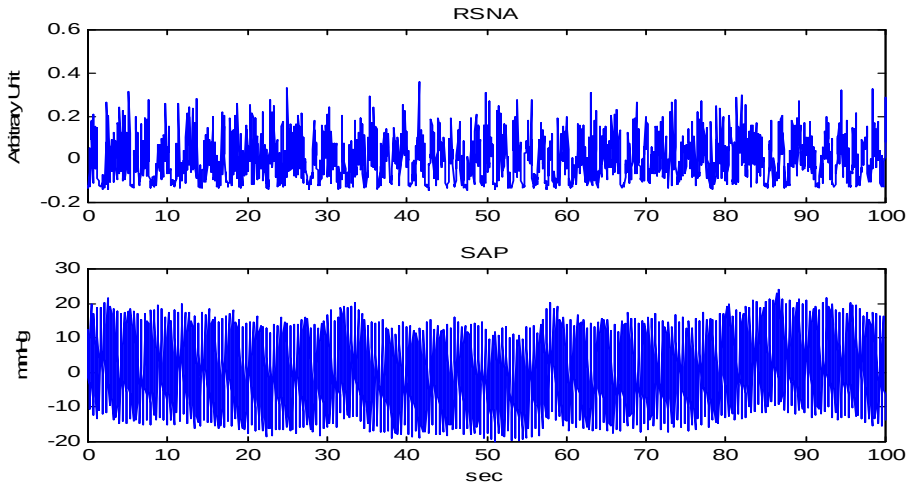

Figure 3.69 Plot for input (RSNA) and output (SAP) for 100 s for model Mp for electrical stimulation

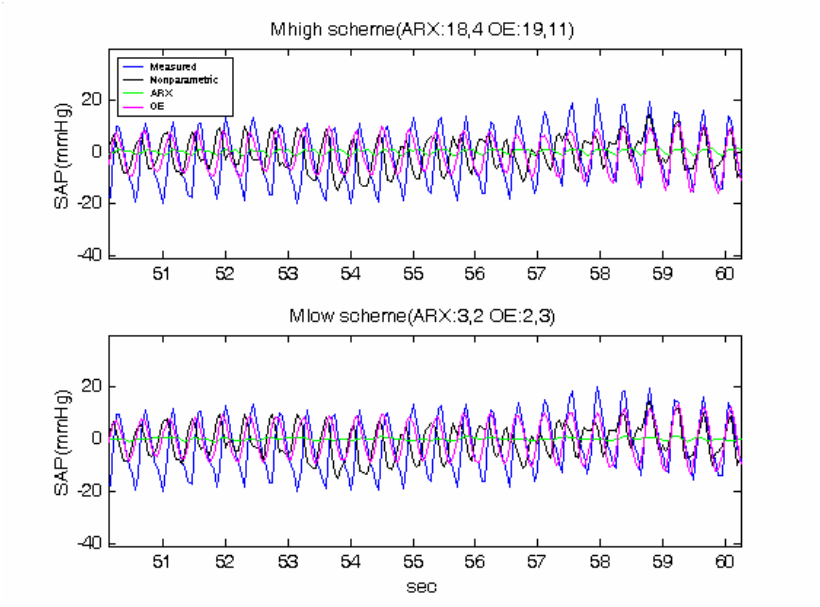

Figure 3.70 Plot for estimated output (SAP) for 10 s of electrical stimulation data of model Mp for M-1 (upper) and M-2 (lower) schemes of ARX and OE

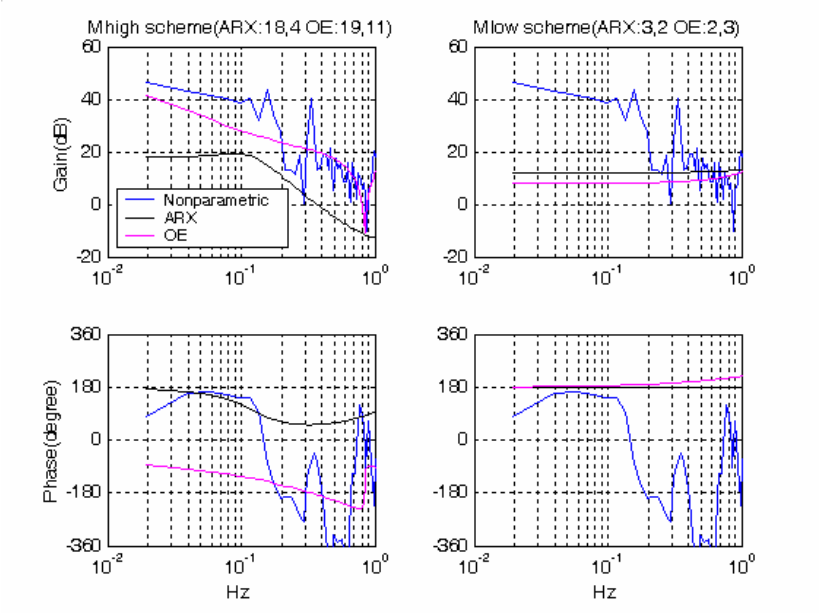

(i) (ii)

Figure 3.71 Plot estimated frequency response of ARX, OE and NP model of Mp electrical stimulation (i) magnitude and phase plot for M-1 scheme (ii) magnitude and phase plot for M-2 scheme

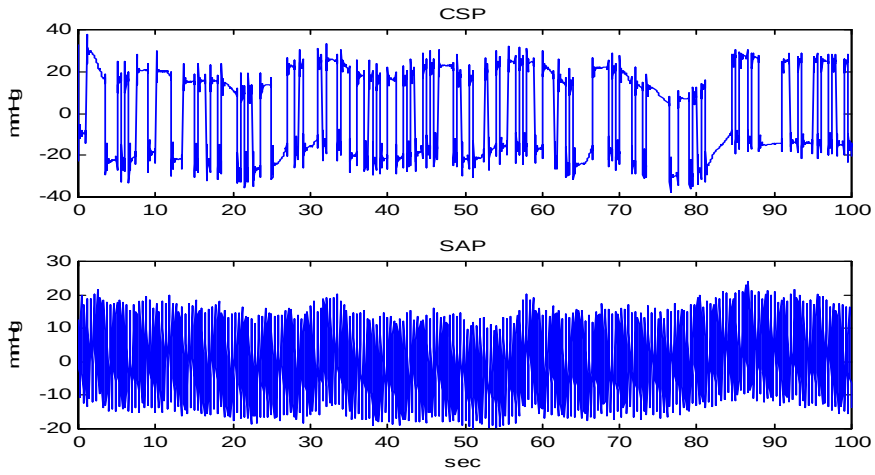

Figure 3.72 Plot for input (CSP) and output (SAP) for 100 s for model Mt

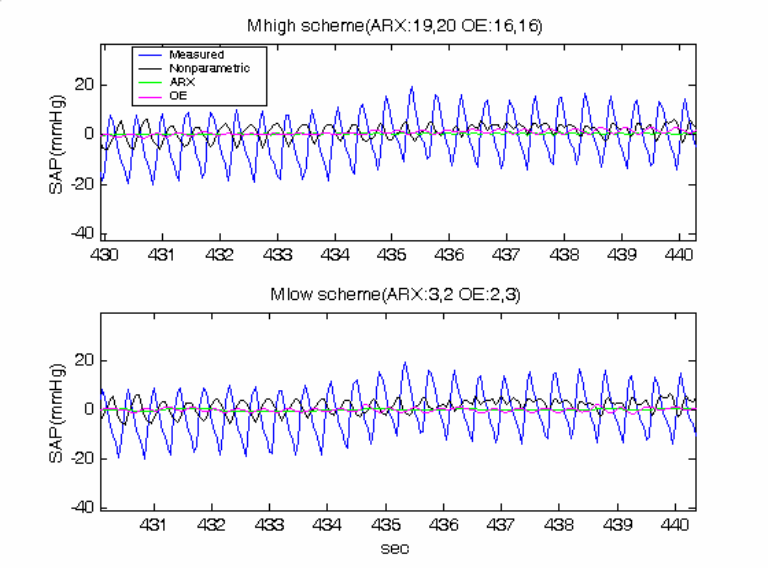

Figure 3.73 Plot for estimated output (SAP) for 10 s of electrical stimulation data of model Mt for M-1 (upper) and M-2 (lower) schemes of ARX and OE

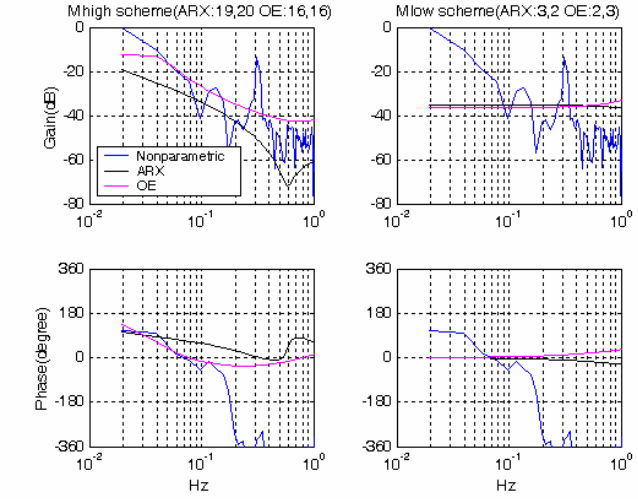

(i) (ii)

Figure 3.74 Plot estimated frequency response of ARX, OE and NP model of Mp electrical stimulation (i) magnitude and phase plot for M-1 scheme (ii) magnitude and phase plot for M-2 scheme

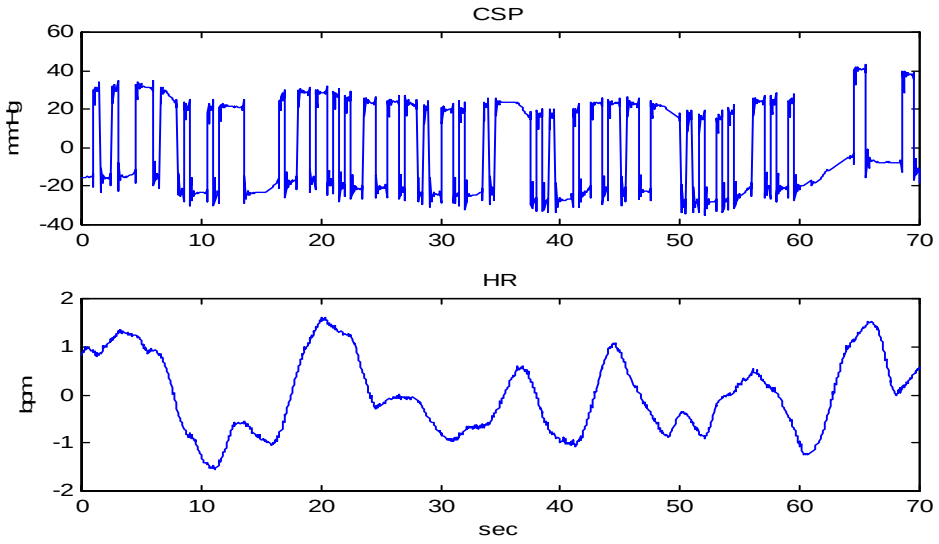

Figure 3.75 Plot for input (CSP) and output (HR) for 70 s electrical stimulation data for model Mh

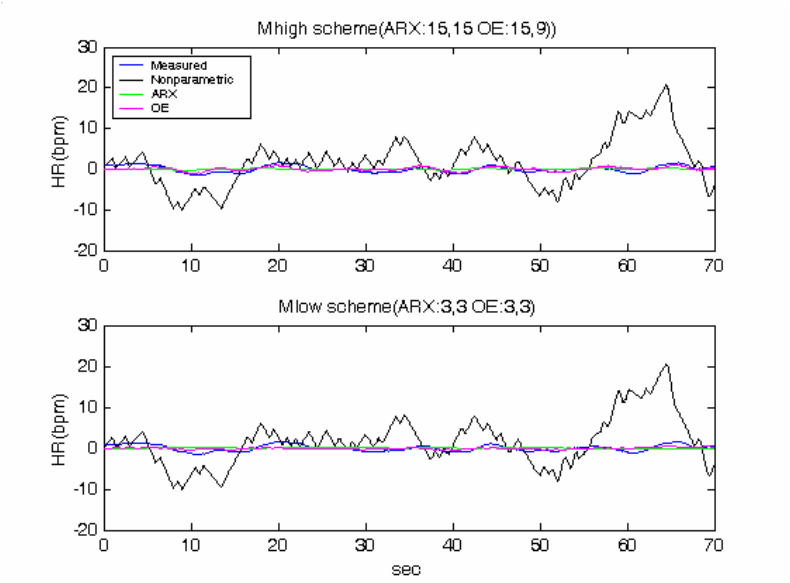

Figure 3.76 Plot for estimated output (HR) for 70 s of electrical stimulation data of model Mh for M-1 (upper) and M-2 (lower) schemes of ARX and OE

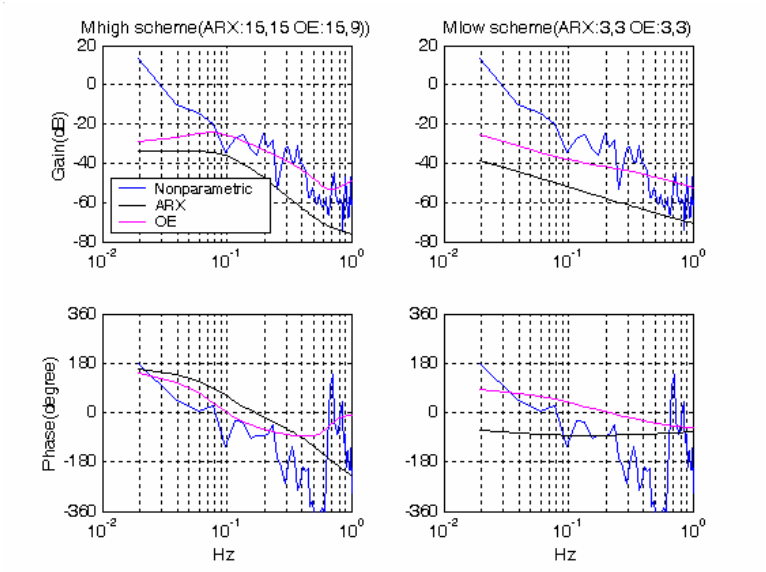

(i) (ii)

Figure 3.77 Plot estimated frequency response of ARX, OE and NP model of Mh electrical stimulation (i) magnitude and phase plot for M-1 scheme (ii) magnitude and phase plot for M-2 scheme

3.3.3 Comparison between ARX and OE models using their MSE values for 15 min and short ensemble models from electrical stimulation data.

Table 3.14 tabulates the p-values for comparison of the M-1 and M-2 modeling schemes for ARX and OE models of Mn,Mp,Mt and Mh and the data length used for these models was 15 min. This test was conducted to see if there was any difference in the higher order and lower order models. Similarly, Table 3.3.15 gives the p-values for M-1 and M-2 model comparison using short ensembles of control data. Table 3.16 gives the p-values obtained from t-test for comparison of the 15 min models and the short ensemble models for all the transfer functions using MSE values obtained from M-1 modeling scheme by ARX and OE method. Similarly, Table 3.17 gives the p-values

from t-test for 15 min and short ensemble model comparison using the M2 modeling scheme for ARX and OE models.

Table 3.14 P-values from t-test for comparison between the MSE values from ARX and OE method obtained from M-1 scheme and the MSE values obtained from M-2 scheme applied to 15 min of electrical stimulation data from all 6 dogs

Pval	ARX	OE
Mn	0.39	0.56
Mp	0.23	0.59
Mt	0.01	0.71
Mh	0.12	0.32

Table 3.15 P-values from t-test for comparison between the MSE values from ARX and OE method obtained from M-1 scheme and the MSE values obtained from M-2 scheme applied to ensembles of electrical stimulation data from all 6 dogs

Pval	ARX	OE
Mn	0.20	0.34
Mp	0.36	0.07
Mt	0.36	0.52
Mh	0.03	0.05

Table 3.16 P-values from t-test for comparison between the MSE values from ARX and OE method applied to 15 min of electrical stimulation data using M-1 scheme and the MSE values obtained from similar method for short ensemble of electrical stimulation data from all 6 dogs

Pval	ARX	OE
Mn	0.17	0.19
Mp	0.00	0.02
Mt	0.01	0.11
Mh	0.06	0.03

Table 3.17 P-values from t-test for comparison between the MSE values from ARX and OE method applied to 15 min of electrical stimulation data using M-2 scheme and the MSE values obtained from similar method for short ensemble of electrical stimulation data from all 6 dogs

Pval	ARX	OE
Mn	0.23	0.28
Mp	0.05	0.04
Mt	0.02	0.78
Mh	0.65	0.14

3.3.4 Comparison between the non-parametric models and the parametric models (ARX and OE) for the electrical stimulation

In this section the parametric models are statistically compared with the non-parametric models with the help of t-test for all the transfer functions, H_{RSNA}, $H_{RSNA-SAP}$, H_{SAP} and H_{HR}. The MSE values obtained from the estimated output and the measured output is used for comparison between ARX and NP, OE and NP and ARX and OE models for Mn, Mp, Mt and Mh models.

Table 3.18 gives the comparison between the ARX and OE, ARX and NP and OE and NP models for 15 min of electrical stimulation data for all 6 dogs and the ARX and OE models are estimated using M-1 modeling scheme in this case. Similarly, Table 3.19 has the p-values from t-test performed on the 15 min electrical stimulation data models for M-2 modeling scheme. Table 3.20 tabulates the t-test result for comparison of the ARX and OE, ARX and NP and OE and NP models using short ensemble of data models for higher orders and Table 21 give the result for lower order of short ensemble models.

Table 3.18 P-values from t-test comparison between the MSE values from ARX and OE, ARX and NP and OE and NP for 15 min higher order models for electrical stimulation data from all 6 dogs

	P-value		
	ARX-OE	ARX-NP	OE-NP
$H_{CSP-RSNA}$	0.306	0.092	0.098
$H_{RSNA-SAP}$	0.027	0.027	0.054
$H_{CSP-SAP}$	0.019	0.001	0.003
H_{CSP-HR}	0.135	0.933	0.139

Table 3.19 P-values from t-test comparison between the MSE values from ARX and OE, ARX and NP and OE and NP for 15 min lower order models for electrical stimulation data from all 6 dogs

	P-value		
	ARX-OE	ARX-NP	OE-NP
$H_{CSP-RSNA}$	0.193	0.412	0.047
$H_{RSNA-SAP}$	0.027	0.200	0.057
$H_{CSP-SAP}$	0.136	0.771	0.004
H_{CSP-HR}	0.192	0.404	0.279

Table 3.20 P-values from t-test comparison between the MSE values from ARX and OE, ARX and NP and OE and NP for short stationary ensemble higher order models for electrical stimulation data from all 6 dogs

	P-value		
	ARX-OE	ARX-NP	OE-NP
$H_{CSP-RSNA}$	0.070	0.327	0.080
$H_{RSNA-SAP}$	0.363	0.363	0.051
$H_{CSP-SAP}$	0.018	0.141	0.007
H_{CSP-HR}	0.007	0.350	0.111

Table 3.21 P-values from t-test comparison between the MSE values from ARX and OE, ARX and NP and OE and NP for short stationary ensemble higher order models for electrical stimulation data from all 6 dogs

	P-value		
	ARX-OE	ARX-NP	OE-NP
$H_{CSP-RSNA}$	0.060	0.640	0.123
$H_{RSNA-SAP}$	0.131	0.885	0.071
$H_{CSP-SAP}$	0.363	0.363	0.041
H_{CSP-HR}	0.008	0.430	0.135

CHAPTER 4

DISCUSSION AND LIMITATIONS

Chapter 4 presents the discussion of the results given in the chapter 3 and important inferences obtained from the results.

4.1 Discussion for the non-parametric analysis for comparison between control and electrical stimulation transfer functions

This section details on the dynamic transfer function characteristics of H_{RSNA}, $H_{SAP,}$ $H_{RSNA\text{-}SAP}$ and H_{HR} and their comparison between the control and the electrical stimulation measurement conditions using their slope (dB/octave),coherence, phase, DC gain and ratio and difference of their respective gains. Section 3.1.1 gives the illustrations for the averaged frequency response of the all four transfer functions from all 6 dogs for both control and the electrical stimulation and section 3.1.2 gives the t-tests for the slope, coherence and DC gain comparison between the control and electrical stimulation.

Neural arc has CSP as input and RSNA as the output. The plot for the frequency response of the neural arc is given in Figure 3.1 and Figure 3.5. From the magnitude plot for the H_{RSNA} it can be observed that the neural arc has a high pass filter

characteristic. Both the transfer functions, H_{NC} and H_{NS} show similar nature of the magnitude response that of a high pass filter. The phase of H_{RSNA} is out of phase for control as well as electrical stimulation for a frequency range of 0.002Hz to 0.4 Hz and further lags for the control condition and leads in case of electrical stimulation. Coherence plot shows linearity between the CSP and RSNA as coherence is >0.5 in range of 0.1 to 1 Hz. Hence the neural arc shows linear system characteristics showing low pass filter nature. From Figure 3.1 it is observed that the DC gain of the electrical stimulation is greater than the control w

hich shows the anticipated change in the baroreflex set-point due to the reason explained in section 1.2.

Comparison t-test was performed between the slopes of average H_{NC} and H_{NS} from all 6 dogs and the p-value obtained is 0.212 > 0.05, where 0.05 is the assumed level of statistical significance. Hence the slopes of the magnitude response for the H_{RSNA}, from both control (rest) and electrical stimulation (exercise) are not significantly different showing that the sensitivity of the neural arc is not affected due to the exercise. Also the linearity of the H_{RSNA} is not affected by stimulation as the p-value from the t-test of coherence function from all 6 dogs is 0.068>0.05 .The DC gain is obtained by calculating the average gain in dB below 0.1 Hz frequency. P-value obtained by performing t-test between the DC gain for averaged H_{NC} and H_{NS} from all 6 dogs is 0.6053>0.05. Hence there is no significant difference observed in the DC gain before and after electrical stimulation indicating no shift in the set-point. The baroreflex

sensitivity also does not change as the slope of the magnitude plots remained unchanged.

The peripheral arc is the path from the medulla oblongata to the effector organs and has RSNA as input and SAP as the output. The $H_{RSNA-SAP}$ shows a low-pass filter characteristic for both the control as well as the electrical stimulation condition. Comparison t-test between the slopes of average H_{PC} and H_{PS} from all 6 dogs gives the p-value as 0.573>0.05, this shows that the sensitivity of the peripheral arc is unaltered even after the electrical stimulation of the L1 and S7 ventral roots indicating no change in the baroreflex sensitivity. The phase for both the H_{PC} and H_{PS} is out of phase and it leads for the control and lags for the electrical stimulation after approximately 0.1Hz. T-test performed on average coherence from 6 dogs obtained in the range of 0.2 Hz to 0.4 Hz has the p-value 0.0184<0.05.This shows the non-linear nature of the peripheral arc and a significant difference between the coherence function between the control and the electrical stimulation. T-test was also conducted to check for change in the DC gain between the H_{PC} and H_{PS}. The p-value obtained was 0.059>0.05, hence there is no significant change in the DC gain for the control and the electrical stimulation.

The baroreflex arc comprises of the neural arc and the peripheral arc. $H_{CSP-SAP}$ has low-pass filter characteristics for both the control as well as the electrical stimulation. P-value obtained from the t-test between the slopes of the control and stimulation is 0.158>0.05, hence there is no significant difference seen in the slopes. This shows that the sensitivity of the baroreflex loop does not change after electrical stimulation (during exercise). Also from the t-test between the coherence function of

H_{TC} and H_{TS}, the p-value obtained is 0.661 >0.05 which shows that there is also no significant difference in the coherence function after electrical stimulation. Hence the linearity of the H_{SAP} is not affected after stimulation. Also the p-value obtained from the t-test between the average DC gains of H_{TC} and H_{TS} from 6 dogs is 0.112>0.05. Thus, there is no significant difference in the DC gain after and before the electrical stimulation indicating that the operating point for baroreflex activity does not shift for the population of dogs analyzed in this study.

The CSP-HR transfer function is also evaluated in this study. This transfer function has characteristics of a low-pas filter. The p-value obtained from the t-test between the slopes of the average H_{HC} and H_{HS} from 6 dogs is 0.727>0.05, hence there is no significant difference in the slope before and after electrical stimulation keeping the sensitivity of the baroreflex arc unchanged. T-test was also performed on the coherence function between from the averaged H_{HC} and H_{HS} from 6 dogs to give a p-value of 0.003<0.05. This shows that there is a significant difference in the coherence function before and after electrical stimulation. The linearity of the CSP-HR transfer function is significantly affected due to electrically induced muscle contraction. The t-test for comparison of the DC gains for control and electrical stimulation done for all the 4 averaged transfer functions show that there is no significant difference in the DC gains before and after electrical stimulation. This has also been graphically validated in section 3.1.1 for each transfer function with the help of the difference and the ratio plots of the control and the electrical stimulation gains.

In the previous study done in this area, researchers have analyzed the baroreflex transfer functions to obtain the nature of the neural arc, peripheral arc and the total baroreflex loop. In this thesis the transfer functions were estimated for the control (rest) and electrical stimulation (exercise) condition and comparison was done in terms of the sensitivity and functioning of the baroreflex loop.

4.2 Discussion for the parametric analysis of the baroreflex transfer functions

The results of ARX and OE models for comparison of M-1 and M-2 modeling schemes is discussed in this section. ARX and OE method was applied to the CSP, SAP, RSNA and HR of 15 min of data and short ensembles of data for both control as well as the electrical stimulation data set. The results for dog 5 are discussed which is similar to all the remaining dogs.

Section 3.2.1.1 gives the illustrations for all four models Mn, Mp, Mt and Mh, showing comparison between the ARX, OE and NP models for each. The input-output data used in estimating these models was the 15 min CSP, SAP, RSNA and HR control data from dog 5. In this section the ARX and OE models of all four transfer functions are estimated by M-1 (order restricted from 1 to 20) and M-2 (order restricted from 1 to 3) modeling schemes. The Mn model estimated by ARX and OE method has CSP as input and RSNA as output, these input-output signals are weakly stationary as discussed earlier. Illustrations for the time domain as well as frequency domain response for Mn are given. The time domain response shows the estimated RSNA from the NP, ARX and the OE models for the same CSP as input. It can be observed that for

higher order estimated ARX and OE models follow the NP output and the measured output very well, while in case of the lower order models, the OE model does a better job compared to the ARX model. The estimated frequency response obtained from ARX and OE Mn models it can be observed that the magnitude response obtained from the higher order estimated models is agreeable to the magnitude plot from the NP method. The Mp model has RSNA as input and SAP as the output, where RSNA is weakly stationary and SAP is non-stationary. From the illustration of the time domain response of the estimated SAP from Mp model show that the ARX, OE as well Np model fail to estimate SAP due to the non-stationary input to the model. Similarly, Mt and Mh have the same problem in estimating the measured output due to non-stationary SAP and HR given as input to the models. Also from the visual inspection of the time domain and frequency domain responses, it can be observed that the higher order Mp, Mt and Mh models estimate better than the lower order models. The OE models are observed to perform a better good job compared to the ARX models in case of all 4 estimated models as the error in the OE structure is considered at the output rather the system. Hence the error is estimated with the output and hence better fit is obtained compared to the ARX models.

T-test was conducted to compare MSE values for the estimated output obtained from the M-1 modeling scheme and the M-2 modeling scheme for Mn, Mp, Mt and Mh models for the 15 min of control data, the p-values are tabulated in Table 3.6 . MSE values were obtained from the estimated and measured output from all 6 dogs and for all 4 models. The p-value for ARX Mn model is 0.31>0.05 and that for the OE model

is 0.10 >0.05, which shows that there is no significant difference in the estimated output for the higher order and lower order ARX and OE Mn models. For Mp the p-value for ARX model is 0.01<0.05 showing a significant difference in the ARX Mp model for higher and lower orders. The p-value for OE Mp model is 0.15 >0.05 which shows that there is not a significant change in the estimated time domain response for higher and lower order OE Mp models. In case of Mt the p-values for ARX and OE are 0.03<0.05 and 0.004<0.05 which shows that there exists a significant difference in the estimates output for the higher and lower order ARX Mt models and the higher and lower order OE Mt models. P-values for Mh model for ARX and OE respectively are 0.23>0.05 and 0.27>0.05 which tells that the model output does not change significantly when the order of the model is lowered for both ARX as well as the OE models.

The Mp, Mt and Mh models estimated from the 15 min length of data do not show good time domain response as apposed to good frequency domain response. This is due to the non-stationary nature of the data given as input and output for the estimated models as discussed earlier. Hence to solve this problem short ensemble of CSP, SAP, RSNA and HR data were selected from the 15 min data set by visual inspection. The ensembles selected were such that the mean values of the signal was approximately constant for that selected epoch. Run test was performed on these ensembles to validate that the selected ensembles are weakly stationary.

Section 3.2.2.1 gives the ARX and OE estimation for the Mn, Mp, Mt and Mh models using the selected ensembles as input and output to the model and also t-test comparison for the MSE values from models estimated for higher and lower orders. For

Mn model it is seen that there is no significant change in the estimated output for ARX and OE methods for the higher and lower order model as the p-values are 0.54>0.05 and 0.27>0.05 for ARX and OE models respectively. In case of Mp model the p-values for ARX and OE Mp models are 0.05 and 0.04 <0.05 which show that there exists a significant change in the estimated time domain response of the ARX and OE Mp models. The Mt model shows a significant difference for the ARX model for the higher and lower order models as the p-value is 0.02<0.05 and the p-value for the OE Mt model is 0.78>0.05 which shows that there is no significant change between the higher and lower order OE Mt models. The Mh model also shows no significant difference in the higher and lower order estimation of ARX and OE models as the p-values are 0.65>0.05 and 0.14>0.05 for ARX and OE respectively.

The 15 min models are also compared to the short ensemble models for both M-1 and M-2 modeling schemes. T-test was performed between the MSE values for the ARX 15 min models and ARX short ensemble models and similar test was carried for the OE models. This comparison t-test was conducted for Mn, Mp, Mt and Mh models. Table 3.8 gives the p-values for the lower order models i.e. for M-1 scheme. In case of Mn model CSP is the input and RSNA is the output, both of which are weakly stationary for 15 min of data. Hence it is seen that there exists no significant change in the 15 min higher order models (ARX and OE) and short ensemble higher order models (ARX and OE) of Mn as the p-values for ARX and OE are 0.17>0.05 and 0.19>0.05 respectively. In case of Mp the p-values are 0.003 <0.05 and 0.02<0.05 for t-test between the 15 min ARX and short ensemble ARX models and the 15min OE and

short ensemble OE models for M-1 scheme showing that there exists a significant difference in the estimated output after selection of stationary ensemble of input and output to the model. The ARX models show a difference in case of the Mt model as the p-value is 0.01<0.05 and for the OE model there is no difference as p-value is 0.11>0.05. The estimated output in case of the Mh model for 15 min and Mh model for short ensemble significant differ for OE models as the p-values is 0.03<0.05. Similar t-test was carried for the lower order models, between the MSE value from the 15 min model and the MSE value from the short ensemble model. In case of the ARX and OE models of Mn the p-values are 0.23>0.05 and 0.28>0.05 showing there is no difference in the output estimation, while in case of Mp model there is seen a significant difference in for both ARX and OE models as the p-values are 0.05 and 0.04<0.05. Mt model shows difference for the ARX model as p-value is 0.02<0.05 and there is no difference in case of the OE model as the p-value is 0.78.>0.05. The Mh models for ARX and OE methods do not show any difference for 15 min and short ensemble models as the p-values for both are >0.05, which are 0.65 and 0.14 respectively.

4.3 Discussion for the comparison of the non-parametric and parametric analysis

Section 3.2.1.1 gives the graphical comparison of the ARX and OE models with the NP models in time domain as well as frequency domain for 15 min of control data. The magnitude of Mn model estimated from the ARX and OE methods by M-1 modeling scheme show a high pass filter characteristics which is same as that of the magnitude plot obtained for the NP model. The parametric models estimated from M-2

modeling scheme does not show favorable results in the frequency domain and fail to estimate the magnitude and phase as that of the non-parametric model. Similarly for all the Mp, Mt and Mh models, their parametric ARX and OE models follow the magnitude and phase estimated from the respective NP models for higher order models, order restricted to 20.In case of the lower order models where the order is restricted to 3 the estimated frequency response from the parametric models fails to compare the frequency response from the non-parametric model.

Section 3.2.2.1 gives the time domain and frequency domain plots for parametric and the non-parametric models applied to the short ensemble of stationary data fro control. It is observed in case of all the models, Mn, Mp, Mt and Mh that the non-parametric estimation of the transfer function in frequency domain does not give good results as the data length is reduced compared to the 15 min models. The time domain response for both parametric and the nonparametric models improve for the short stationary ensemble models. Again better results are observed for higher order models.

The parametric and the non-parametric models are statistically compared in with the help of t-test. The MSE values obtained from Mn, Mp, Mt and Mh models for ARX, OE and Np models is compared with each other for control data from all the 6 dogs.

Table **3.**10 gives the p-values for the 15 min higher order models from control data. It can be observed that for Mn model the p-values from the t-test between ARX-OE, ARX-NP and OE-NP are 0.246, 0.112 and 0.108 respectively, which are >0.05. Hence

there is no significant difference in the parametric and the non-parametric Mn models. In case of the Mp model, p-value for ARX-OE comparison is 0.034<0.05 showing a significant difference between the two models, while the p-values for ARX-NP and OE-NP are 0.884 and 0.749 such that they are >0.05 which shows that there is no significant difference between the parametric and the NP Mp models. For the Mt models there is significant difference found between the ARX and OE models as the p-value is 0.001<0.05 and also there was difference in the OE and NP models estimated as the p-value for them was 0.020<0.05, the ARX and NP models did not show any significant difference.

Table 3.11 tabulates the p-values incase of the 15 min lower order models. The p-values given in this table show that there is no significant difference between the ARX - OE, ARX -NP and OE -NP models for the Mn model. In case of Mp only the ARX and OE models showed a significant difference as the p-value obtained was 0.039<0.05. Also for the Mt model the ARX and OE showed a difference in estimation. In case of the Mh model there is no significant difference found between any of 3 modeling techniques.

Table 3.12 gives the t-test comparison for the short stationary ensemble models of higher order. From the p-values tabulated it can be observed that the Mn and Mh models show no significant difference between the parametric and non-parametric models and also there is no difference between the ARX and OE models as the p-values obtained for them is >0.05 .In case of the Mp model there is difference found between

the ARX-OE and the OE-NP models while for Mt model the OE and NP models show a significant difference.

Table 13 gives the p-values for the t-test performed on the short stationary ensemble lower order models. From the p-values it is observed that in case of the Mn and Mh models there is no significant difference between the parametric and non-parametric models and also no difference found between the ARX and The OE models.For the Mp model significant difference is found between the ARX and OE models as well as the OE and NP models as the p-values are <0.05 and the ARX and the NP models do not differ. In case of the Mt model only the OE and the NP models differ as the p-value is $0.024<0.05$.

4.4 Limitations

This study is performed on the linear system assumption of the carotid sinus baroreflex system. The models of the $H_{RSNA,}$ $H_{RSNA-SAP,}$ H_{SAP} and H_{HR} transfer functions were estimated using the measured data which was recorded in the linear region of the baroreflex curve and hence linear relation between the input and output was assumed. The coherence function obtained was <0.5 in some cases showing nonlinearity in the system giving varied results in case of different subjects The DC gain which was used as an index for change in the set-point during exercise derived from the non-parametric models assumed the baroreceptor analyzed in an animal to be a linear system, and hence this may lead in discrepancy in determining the change in the DC gain for the two measurement conditions. The CSP-RSNA, RSNA-SAP, CSP-SAP

and CSP-HR parametric models were estimated on the assumption that the input-output data to the models was stationary. It was observed that there were variations in the mean of the data along its entire length of 15 min.

CHAPTER 5

CONCLUSION AND DIRECTIONS FOR FUTURE WORK

5.1 Conclusions

The present study is focused on the non-parametric and parametric estimation of the baroreflex transfer functions for two measurement conditions, control and the electrically induced muscle contraction. The models considering CSP as input and RSNA as output, RSNA as input and SAP as output, CSP as input SAP as output and CSP as input and HR as output were estimated by ARX and OE method for higher and lower order models. Non-parametric method was also employed to the above mentioned combination of input and output. The main objective of this study was to observe if there exists change in the DC gain of CSP-RSNA and CSP-HR transfer functions when the L7 and S1 ventral roots were stimulated by electrical pulses, which mimicked exercise. Another purpose of this study was to compare the transfer function models obtained by the parametric (ARX and OE) method to the non-parametric estimated models. Parametric models were also tested for the 15min long non-stationary data and the short stationary ensembles of data.

As discussed in chapter 4, there is seen to be a variation in the gain of the CSP-RSNA and the CSP-HR transfer function. The gain was observed to decreased when the electrical stimulation was applied which depict that there might be a change in the set point of the baroreflex activity. But the change was not significant as proved from the comparison t-test. The OE method for higher order models produced superior results compared to the ARX method for the same. Also CSP-RSNA model was best estimated using both the ARX and OE method. The CSP-SAP and the RSNA-SAP models were poorly estimated by the parametric method due to the nonlinear nature of the peripheral arc and also due to the non-stationary input-output data to the model. The CSP-HR data was well estimated for the short ensemble parametric models. It is also observed that the short ensemble parametric models show better fit in time domain compared to the 15 min models, but the estimated frequency response was better in case of the 15 min models. Again the higher order models are observed to estimate better than the lower order models.

5.2 Future Work

In this study the neural arc, peripheral arc and the baroreflex arc were modeled using the linear parametric modeling techniques and then compared with the standard non-parametric method. The peripheral arc of the baroreflex system is nonlinear in nature and hence estimation of non-linear ARX models of RSNA-SAP and CSP-SAP transfer functions can improve their time domain and the frequency-domain response of the models. Also cascade arrangement of the parametric models could be examined to

obtain the transfer function of the total baroreflex loop.

APPENDIX A

SLOPE, COHERENCE AND DC GAIN VALUES

Table A1 Slope and coherence values between 0.2Hz to 0.4Hz for each transfer function from 6 dogs for control and electrical stimulation

		Control		Electrical stimulation	
	Transfer Function	Slope (dB/octave)	Coherence	Slope (dB/octave)	Coherence
Dog 1	H_{RSNA}	7.84	0.51	7.78	0.28
	$H_{RSNA-CSP}$	-13.50	0.50	-4.26	0.20
	H_{SAP}	-6.38	0.82	-12.96	0.76
	H_{HR}	-0.96	0.68	-10.58	0.07
Dog 2	H_{RSNA}	5.06	0.62	4.52	0.07
	$H_{RSNA-CSP}$	-9.99	0.54	-13.75	0.11
	H_{SAP}	-11.10	0.70	-13.75	0.44
	H_{HR}	-5.05	0.86	-5.60	0.05
Dog 3	H_{RSNA}	0.56	0.34	0.52	0.09
	$H_{RSNA-CSP}$	-11.57	0.32	-4.04	0.08
	H_{SAP}	-13.66	0.63	-13.63	0.70
	H_{HR}	-6.83	0.53	-17.34	0.08
Dog 4	H_{RSNA}	0.22	0.11	4.58	0.10
	$H_{RSNA-SAP}$	-6.00	0.29	-9.91	0.11
	H_{SAP}	-8.88	0.14	-9.54	0.52
Dog5	H_{RSNA}	2.61	0.70	4.37	0.75
	$H_{RSNA-SAP}$	-6.75	0.64	-13.68	0.45
	H_{SAP}	-8.05	0.50	-9.42	0.30
	H_{HR}	-3.80	0.64	-2.04	0.06
Dog 6	H_{RSNA}	7.58	0.74	10.89	0.51
	$H_{RSNA-SAP}$	-20.13	0.53	-11.37	0.56
	H_{SAP}	-12.64	0.38	-12.03	0.18

Table A2 DC gain values for each transfer function from 6 dogs for control and electrical stimulation

		DC gain (dB)	
	Transfer Function	Control	Electrical stimulation
Dog 1	H_{RSNA}	-64.30	-69.50
	$H_{RSNA-SAP}$	43.77	40.65
	H_{SAP}	-15.96	-16.17
	H_{HR}	-24.35	-28.07

Table A2 continued

Dog 2	H_{RSNA}	-73.53	-76.72
	$H_{RSNA-SAP}$	52.28	48.29
	H_{SAP}	-10.06	-21.14
	H_{HR}	-16.51	-21.14
Dog 3	H_{RSNA}	-69.41	-71.59
	$H_{RSNA-SAP}$	54.25	43.15
	H_{SAP}	-3.78	-4.84
	H_{HR}	-17.09	-20.39
Dog 4	H_{RSNA}	-75.48	-80.48
	$H_{RSNA-SAP}$	36.35	32.38
	H_{SAP}	-22.62	-32.38
Dog5	H_{RSNA}	-73.91	-54.55
	$H_{RSNA-SAP}$	44.18	38.19
	H_{SAP}	-11.93	-17.59
	H_{HR}	-14.45	-33.10
Dog 6	H_{RSNA}	-81.88	-72.08
	$H_{RSNA-SAP}$	45.69	47.98
	H_{SAP}	-13.43	-11.23

APPENDIX B

RUN TEST RESULT AND MSE PLOTS

Table B1 Run test result for 15 minutes of CSP, SAP, RSNA and HR measured data from Dog5 (control)

	CSP		RSNA		SAP		HR	
No. of statistics	No. of runs	Pass=1 Fail=0	No. of runs	Pass=1 Fail=0	No. of runs	Pass=1 Fail=0	No. of runs	Pass=1 Fail=0
10	7	1	8	1	4	1	2	0
12	7	1	10	1	4	1	2	0
14	12	1	10	1	4	1	2	0
16	13	1	10	1	4	0	2	0
18	12	1	12	1	4	0	2	0
20	11	1	10	1	4	0	2	0
22	14	1	12	1	5	0	2	0
24	19	0	12	1	5	0	2	0
26	17	1	18	1	5	0	2	0
28	22	0	17	1	5	0	2	0
30	16	1	17	1	5	0	4	0
32	19	1	15	1	7	0	4	0
36	23	1	19	1	9	0	4	0
40	24	1	25	1	11	0	4	0
50	33	1	31	1	11	0	4	0
60	40	1	42	0	11	0	12	0
70	52	0	42	1	11	0	12	0
80	58	0	48	1	11	0	12	0
90	63	0	56	1	14	0	14	0
100	73	0	58	1	12	0	16	0
110	77	0	68	1	16	0	14	0
120	71	1	73	1	16	0	18	0
130	87	0	77	1	16	0	18	0
140	93	0	75	1	18	0	20	0
150	97	0	81	1	16	0	22	0
160	99	0	87	1	16	0	24	0
170	97	1	95	1	22	0	20	0
180	97	1	87	1	24	0	20	0
190	113	0	99	1	24	0	26	0
200	105	1	101	1	18	0	24	0

Table B2 Run test result for short ensemble of CSP, SAP, RSNA and HR measured data from Dog5 (control)

	CSP(650 to 800s)		RSNA(650 to 800s)		SAP(650 to 800s)		HR(0 to 140s)	
No. of statistics	No. of runs	Pass=1 Fail=0	No. of runs	Pass=1 Fail=0	No. of runs	Pass=1 Fail=0	No. of runs	Pass=1 Fail=0
10	7	1	6	1	5	1	6	1
12	11	1	10	1	5	1	8	1
14	10	1	9	1	7	1	8	1
16	11	1	11	1	11	1	8	1
18	11	1	12	1	11	1	10	1
20	13	1	12	1	7	1	10	1
22	15	1	11	1	9	1	8	1
24	15	1	15	1	13	1	9	1
26	16	1	17	1	13	1	12	1
28	15	1	17	1	15	1	12	1
30	17	1	23	0	13	1	11	1
32	19	1	22	1	15	1	12	1
36	19	1	21	1	15	1	12	1
40	21	1	33	0	17	1	12	0
50	29	1	39	0	15	0	14	0
60	34	1	38	1	15	0	16	0
70	41	1	41	1	27	1	14	0
80	45	1	52	0	23	0	14	0
90	46	1	53	1	39	1	14	0
100	46	1	62	1	26	0	14	0
110	52	1	62	1	33	0	14	0
120	54	1	69	1	59	1	14	0
130	62	1	86	0	67	1	14	0
140	66	1	82	1	44	0	16	0
150	66	1	86	1	44	0	16	0
160	70	1	101	0	35	0	16	0
170	80	1	97	1	51	0	16	1
180	80	1	101	1	78	1	0	0
190	92	1	113	0	114	0	16	0
200	88	1	117	1	134	0	16	0

Table B3 Run test result for 15 minutes of CSP, SAP, RSNA and HR measured data from Dog5 (electrical stimulation)

	CSP		RSNA		SAP		HR	
No. of statistics	No. of runs	Pass=1 Fail=0	No. of runs	Pass=1 Fail=0	No. of runs	Pass=1 Fail=0	No. of runs	Pass=1 Fail=0
10	5	1	4		4	1	4	1
12	7	1	4	1	4	1	4	1
14	11	1	4	1	4	1	4	1
16	10	1	6	1	6	1	4	0
18	14	1	4	1	4	0	4	0
20	16	1	4	0	6	1	4	0
22	15	1	4	0	4	0	4	0
24	16	1	6	0	4	0	4	0
26	18	1	4	0	6	0	6	0
28	17	1	8	0	6	0	6	0
30	21	1	4	0	6	0	8	0
32	23	1	8	0	6	0	6	0
36	25	1	6	0	6	0	8	0
40	27	1	6	0	8	0	8	0
50	32	1	10	0	6	0	8	0
60	38	1	16	0	8	0	10	0
70	40	1	12	0	10	0	12	0
80	53	0	20	0	10	0	14	0
90	67	0	18	0	10	0	14	0
100	58	1	22	0	10	0	14	0
110	74	0	30	0	10	0	16	0
120	90	0	46	0	12	0	16	0
130	94	0	56	0	10	0	16	0
140	102	0	50	1	10	0	18	0
150	104	0	46	0	10	0	16	0
160	110	0	60	0	10	0	16	0
170	106	0	60	0	14	0	16	0
180	116	0	76	0	14	0	18	0
190	124	0	76	1	22	0	18	0
200	130	0	78	0	14	0	18	0

Table B4 Run test result for ensemble (800 to 900 s) of CSP, RSNA and SAP measured data from Dog5 (electrical stimulation)

	CSP		RSNA		SAP	
No. of statistics	No. of runs	Pass=1 Fail=0	No. of runs	Pass=1 Fail=0	No. of runs	Pass=1 Fail=0
10	5	1	4	1	5	1
12	7	1	8	1	5	1
14	10	1	9	1	7	1
16	11	1	4	0	5	1
18	15	1	13	1	7	1
20	15	1	9	1	5	0
22	13	1	13	1	7	1
24	17	1	18	1	7	0
26	17	1	14	1	7	0
28	17	1	12	1	7	0
30	15	1	18	1	7	0
32	18	1	22	1	7	0
36	18	1	24	1	7	0
40	25	1	26	1	7	0
50	20	1	24	1	7	0
60	32	1	32	1	9	0
70	27	1	40	1	22	0
80	40	1	56	0	15	0
90	44	1	62	0	30	0
100	50	1	62	1	30	0
110	52	1	64	1	24	0
120	58	1	76	0	19	0
130	63	1	74	1	30	0
140	71	1	84	1	52	0
150	77	1	81	1	66	1
160	81	1	93	1	90	1
170	85	1	101	1	70	0
180	89	1	101	1	70	0
190	93	1	107	1	54	0
200	105	1	93	1	54	0

Table B5 Run test result for ensemble (240 to 310 s) of CSP and HR measured data from Dog5 (electrical stimulation)

	CSP(240 to 310s)		HR(240 to 310s)	
No. of statistics	No. of runs	Pass=1 Fail=0	No. of runs	Pass=1 Fail=0
10	7	1	7	1
12	7	1	9	1
14	10	1	9	1
16	10	1	9	1
18	10	1	11	1
20	14	1	11	1
22	12	1	11	1
24	16	1	11	1
26	14	1	11	1
28	16	1	11	1
30	18	1	11	1
32	14	1	13	1
36	18	1	11	0
40	18	1	13	0
50	24	1	13	0
60	26	1	13	0
70	30	1	13	0
80	34	1	13	0
90	46	1	13	0
100	46	1	13	0
110	50	1	13	0
120	59	1	13	0
130	65	1	13	0
140	75	1	13	0
150	69	1	13	0
160	71	1	13	0
170	73	1	13	0
180	73	0	13	0
190	73	0	13	0
200	73	0	15	0

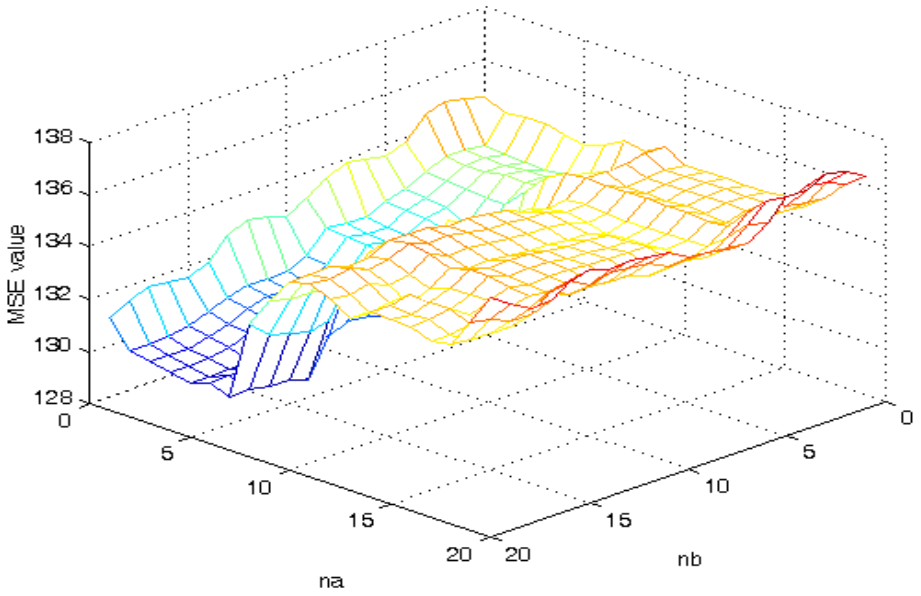

Figure B1 Plot of MSE values for ARX model of Mp for 15 min of control data

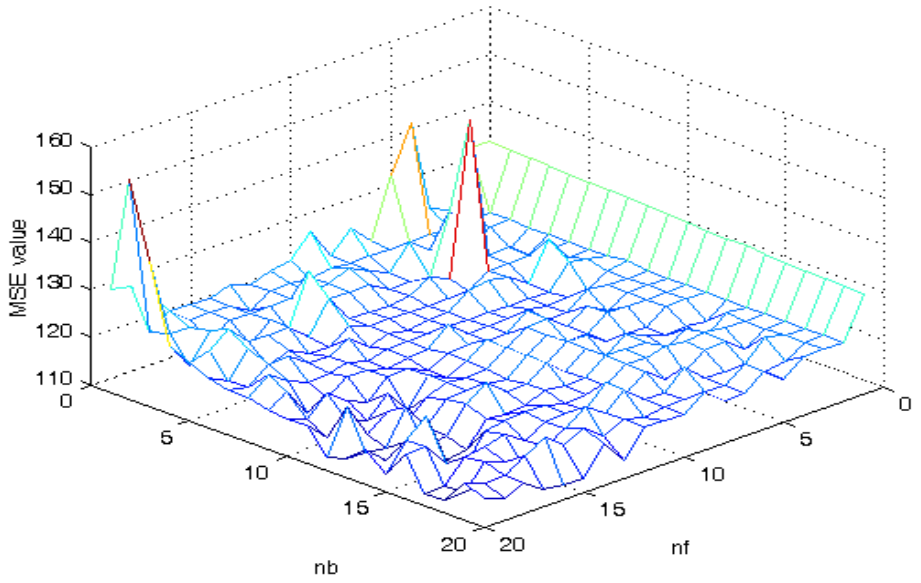

Figure B2 Plot of MSE values for OE model of Mp for 15 min of control data

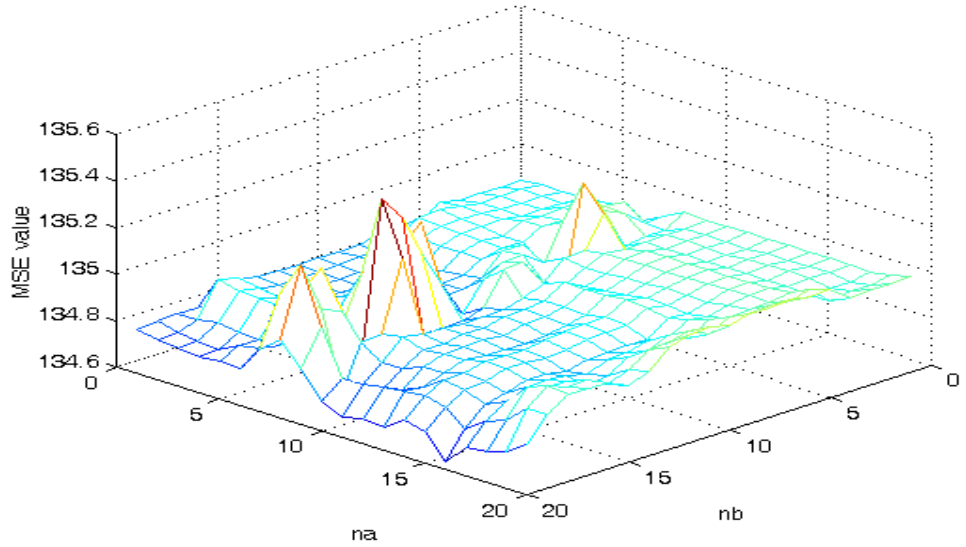

Figure B3 Plot of MSE values for ARX model of Mt for 15 min of control data

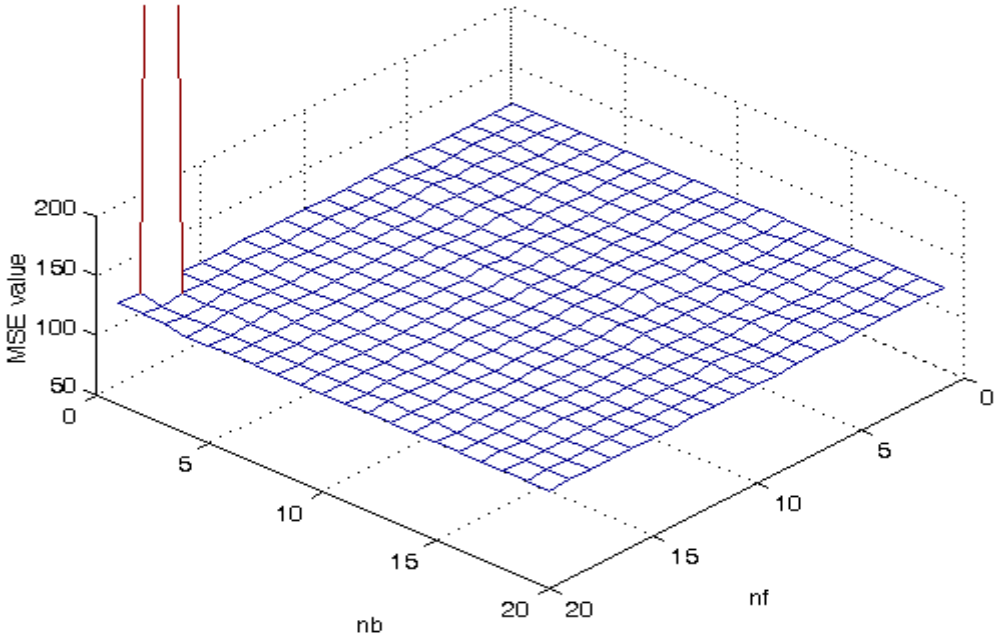

Figure B4 Plot of MSE values for OE model of Mt for 15 min of control data

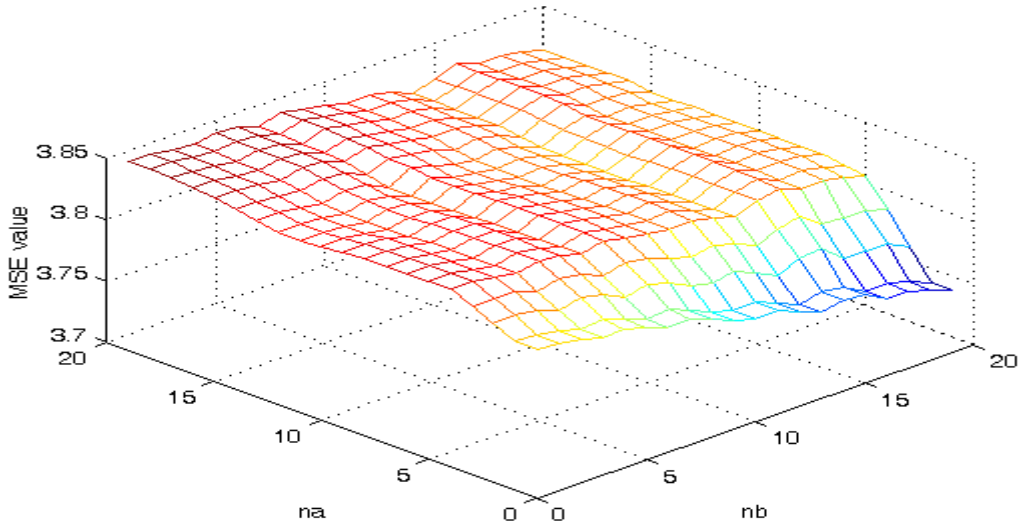

Figure B5 Plot of MSE values for ARX model of Mh for 15 min of control data

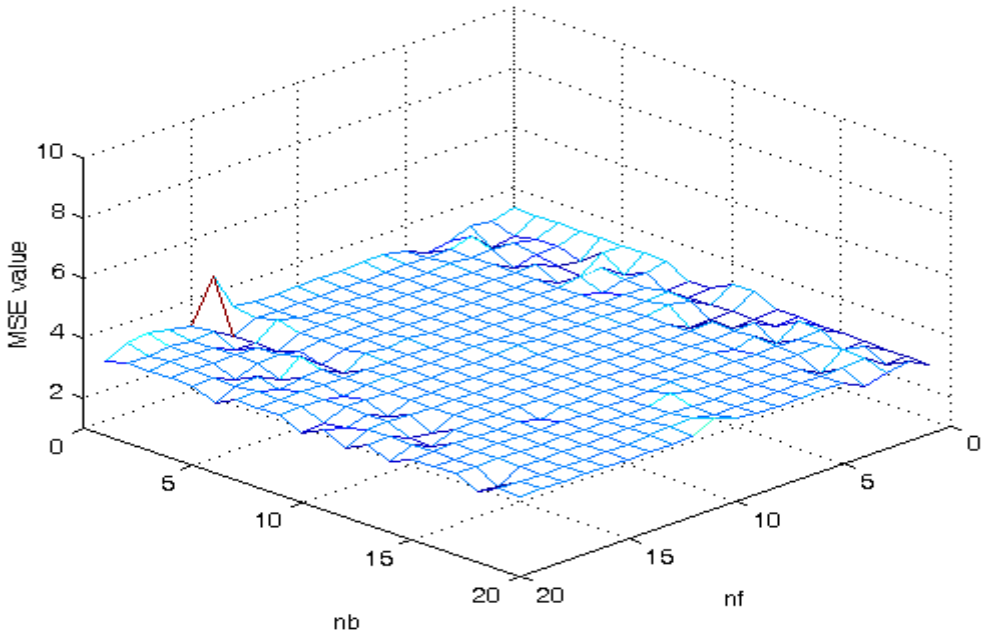

Figure B6 Plot of MSE values for OE model of Mh for 15 min of control data

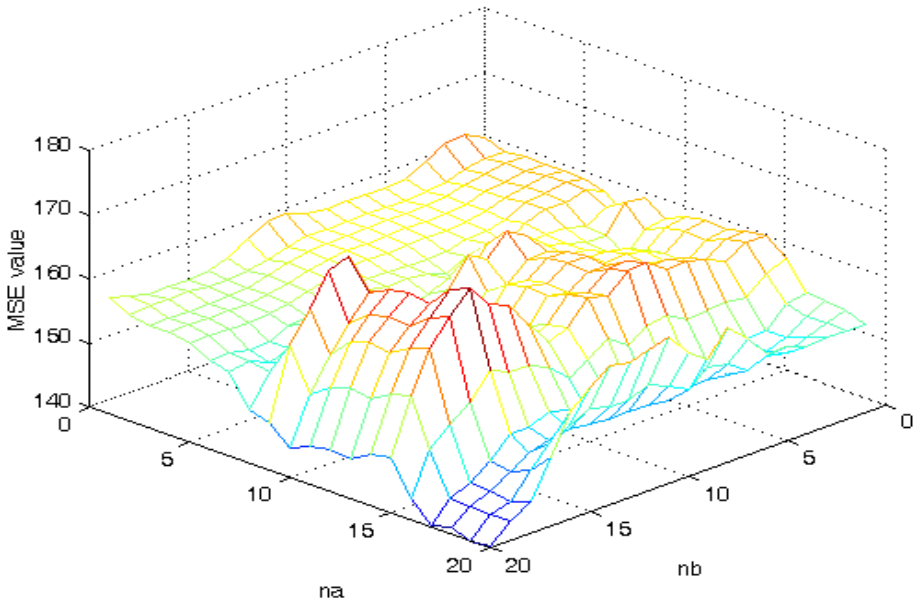

Figure B7 Plot of MSE values for ARX model of Mp for 15 min of electrical stimulation data

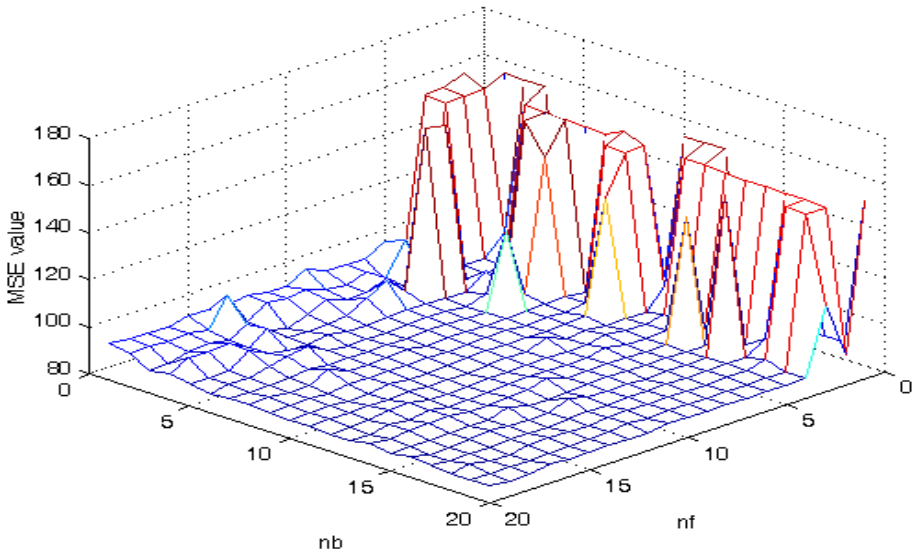

Figure B8 Plot of MSE values for OE model of Mp for 15 min of electrical stimulation data

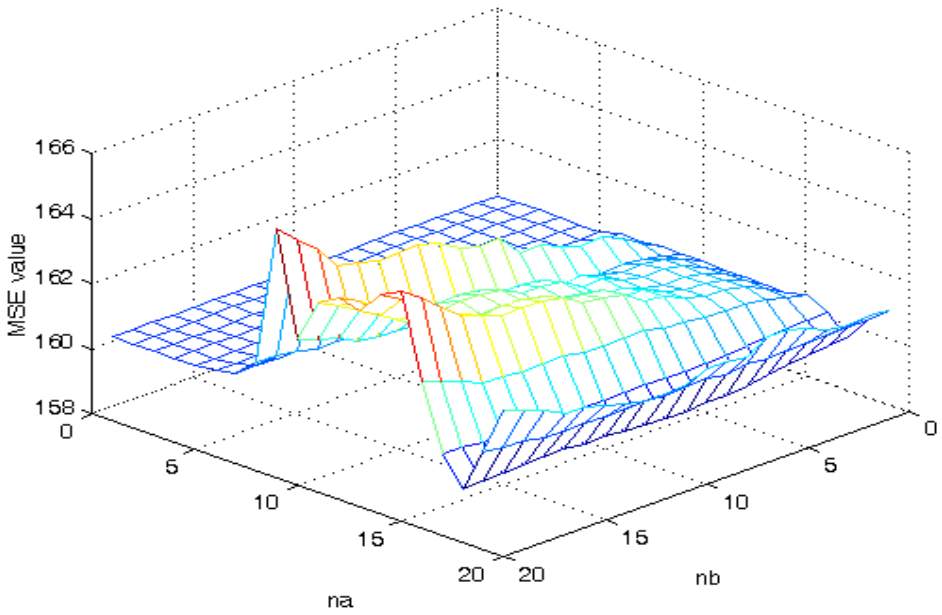

Figure B9 Plot of MSE values for ARX model of Mt for 15 min of electrical stimulation data

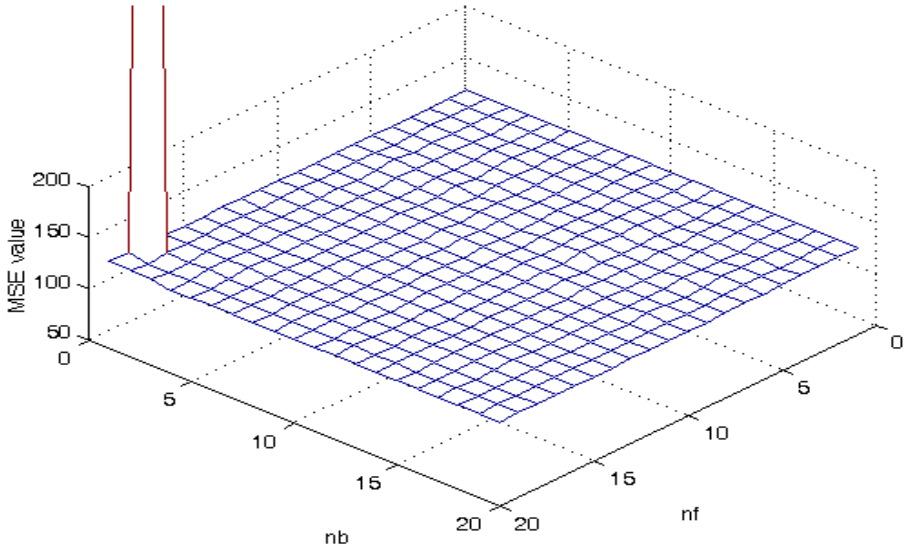

Figure B10 Plot of MSE values for OE model of Mt for 15 min of electrical stimulation data

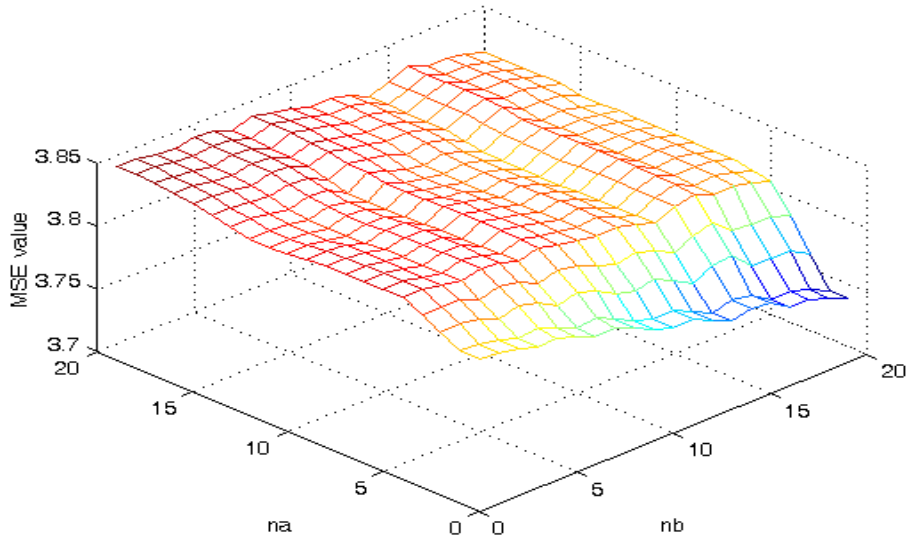

Figure B11 Plot of MSE values for ARX model of Mh for 15 min of electrical stimulation data

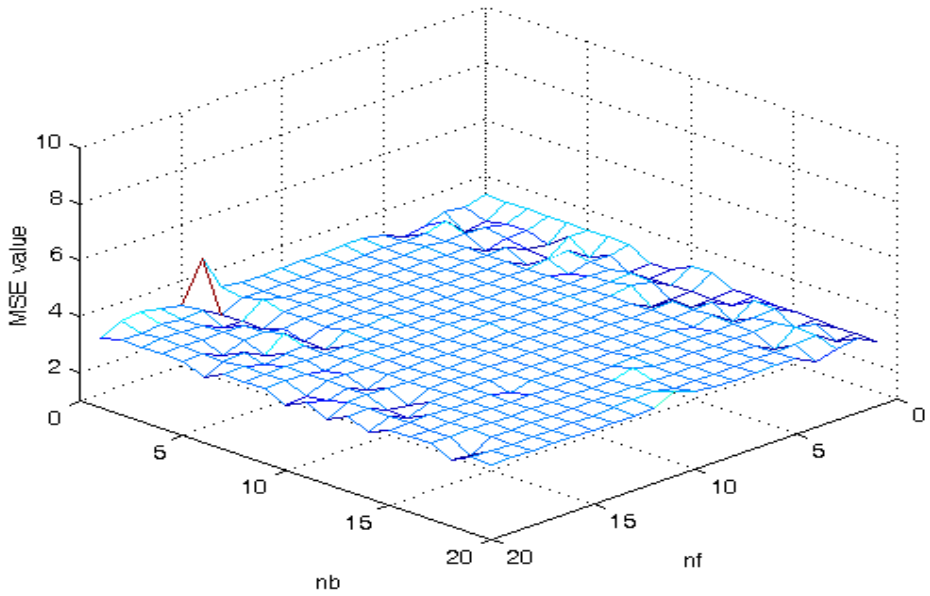

Figure B12 Plot of MSE values for OE model of Mh for 15 min of electrical stimulation data

REFERENCES

1. Kenji Sunagawa, Yasuhiro Ikeda, Toru Kawada, Masaru Sugimachi, Osamu Kawaguchi, Toshiaki Shishido, Takayuki Sato, Hiroshi Miyano, Wataru Matsuura, Joe Alexander Jr 1995. "Neural loop of baroreflex optimizes dynamic arterial pressure regulation." IEEE –EMBC and CMBEC Theme 6: Physiological systems/Modeling and Identification.

2.Yasuhiro Ikeda, Toru Kawada, Masaru Sugimachi , Osamu Kawaguchi, Toshiaki Shishido, Takayuki Sato, Hiroshi Miyano , Wataru matsuura, Joe Alexander, Jr., and Kenji Sunagawa 1996. American Journal of Physiology "Neural arc of baroreflex optimizes dynamic pressure regulation in achieving both stability and quickness." 271 (Heart Circ. Physiol. 40) H882-H890,

3. Toru Kawada, Masaru Sugimachi Takayuki Sato, Hiroshi Miyano, Toshiaki Shishido, Hiroshi Miyashita, Ryoichi Yoshimura, Hiroshi Takaki, Joe Alexander, Jr., and Kenji Sunagawa 1997. "Closed-loop identification of carotid sinus baroreflex open-loop transfer characteristics in rabbits." American Journal of Physiology." 273 (Heart Circ. Physiol.42):H1024-H1031.

4. Toru Kawada, Toshiaki Shishido, Masashi Inagaki, Teiji Tatewaki, Can Zheng , Yusuke Yanagiya, Masaru Sugimachi, and Kenji Sunagawa 2001. " Differential dynamic baroreflex regulation of cardiac and renal sympathetic nerve activities." American Journal Physiology Heart Circ Physiol 280: H1581- H1590.

5.Toshihiko Kubo, Tsutomu Imaizumi , Yasuhiko Harasawa, Shin-Ichi Ando, Tatsuya Tagawa, Toyonari Endo , Masanari Shiramoto, and Akira Takeshita 1996. ."Transfer function analysis of central arc of aortic baroreceptor reflex in rabbits." American Journal of Physiology.270 (Heart Circ. Physiology. 39): H1054-H1062.

6. Toru Kawada, Takayuki Sato , Toshiaki Shishido, Masashi Inagaki, Teiji Tatewaki, Yusuke Yanagiya , Masaru Sugimachi, and Kenji Sunagawa 1999. "Summation of dynamic transfer characteristics of left and right carotid sinus baroreflexes in rabbits." American Journal Physiology. 277 (Heart Circ. Physiol. 46): H857-H865.

7. Toru Kawada, Takayuki SATO, Masashi Inagaki, Toshiaki Shishido, Teiji TATEWAKI, Yusuke TANAGIYA, Can ZHENG, Masaru SUGIMACHI, and Kenji SUNAGAWA 2000.. "Closed –Loop identification of carotid sinus baroreflex transfer characteristics using electrical stimulation." Japanese Journal of Physiology, 50, 371-380.

8. Toru Kawada, Can Zheng, Yusuke Yanagiya, Kazunori Uemura, tadayoshi Miyamoto, masashi Inagaki, Toshiaki Shishido, Masaru Sugimachi, and Kenji Sunagawa 2002.."High –cut characteristics of the baroreflex neural arc preserve baroreflex gain against pulsatile pressure."American Journal of Physiology Heart Circ Physiology 282: H1149- H1156.

9.Tayayuki Sato, Toru Kawada, Hiroshi Miyano, Toshiaki Shishido, Masashi Inagaki, Ryoichi Yoshimura, Teiji Tatewaki, Masaru Sugumachi, Joe Alexander, Jr. and Kenji Sunagawa 1999. "New simple methods for isolating baroreceptor regions of carotid sinus and the aortic depressor nerves in rats."

10. J. T. Potts and T.G. Waldrop, " Discharge Patterns of Somatosensitive Neurons in the nucleus Tractus Solitarius of the Cats."2004

11. Jeffrey T. Potts .Annals New York Academy of Sciences. "Exercise and Sensory Integration Role of the Nucleus Tractus Solitarius."

12. Tayayuki Sato, Toru Kawada, Masashi Inagaki, Toshiaki Shishido, Masaru Sugumachi and Kenji Sunagawa 2003. "Dynamics of symapathrtic baroreflex control of arterial pressure in rats."Am J Physiol Regul Integr Comp Physiol 285 R262- 70.

13. Toru Kawada Yusuke Yanagiya, Kazunori Uemura, Tadayoshi Miyamoto, Can Zheng, Meihua Ali, , Masaru Sugumachi, and Kenji Sunagawa 2002. "Input-size dependence of the baroreflex neural arc transfer characteristics." Department of Cardiovascular Dynamics, National CardiovascularCenter Research Institute, Osaka 565-8565, Japan.

14. P.J Fadel, S.Ogoh, D. E. Watenpaugh, W. Wasmund, A. Olivencia-Yurvati, M. L. Smith, and P. B. Raven 2000. "Carotid baroreflex regulation of sympathetic nerve activity during dynamic exercise in humans." Department of Integrative Physiology and Cardiovascular Research Institute,University of North Texas Health Science Center, Fort Worth, Texas 76107 .

15. Jeffrey T. Potts, “Inhibitory neurotransmission in NTS: Implications for Baroreflex Resetting during Exercise”

16 Jeffery T.Potts and Jere H. Mitchell 1998. “Rapid resetting of carotid baroreceptor reflex by afferent input from skeletal muscle receptors” *Am. J. Physiol. 275*

17. Ljung L., “System Identification: Theory for the User”, 2nd Edition, Upper Saddle River, NJ: Prentice Hall PTR, 1999.

18. MATLAB User Manual (Release 13) ver. 6.5, 2002.

19. Bendat JS,Piersol AG, “ Random data : Analysis and measurement procedures” , 2nd Edition, Wiley-Interscience, 1986.

20. Proakis J.G., Manolakis D.G., Digital signal processing Principles , Algorithms, and Applications. Prentice Hall. New Jersey, 1996.

21. Marmarelis, P.Z and V.Z Marmarelis. Analysis of the physiological systems - The white noise approach. New York: Plenum, 1978.

22. Mimansa E “Transfer function analysis of a biological control system: Carotid sinus baroreflex function” ,Master thesis, Dept of Biomedical engineering , Univ. Texas at Southwestern ,Dallas.

BIOGRAPHICAL INFORMATION

Sheetal Deshmukh received her Bachelor of Engineering degree in Electronics from Pune University in 2003. She started her masters in Biomedical Engineering at The University of Texas at Arlington in 2004. Due to her interests in Physiological System Modeling and Identification and Biomedical Signal Processing, she started working on research project under Dr. Khosrow Behbehani. She has been working as a Graduate Research Assistant at the Department of Biomedical Engineering.